To the Graduate Council:

I am submitting herewith a thesis written by Ahmed A. Omar entitled "Pulsed Plasma-Pulsed GTA Arc: A Study of the Process Variables." I recommend that it be accepted in partial fulfillment of the requirements for the degree of Master of Science, with a major in Metallurgical Engineering.

Carl D. Lundin, Major Professor

We have read this thesis and recommend its acceptance:

J. E. Spinell

C R Brooks

Accepted for the Council:

Vice Chancellor
Graduate Studies and Research

PULSED PLASMA-PULSED GTA ARC: A STUDY OF THE PROCESS VARIABLES

A Thesis

Presented for the

Master of Science

Degree

The University of Tennessee

Ahmed A. Omar

December 1975

1266301

ACKNOWLEDGEMENTS

The author wishes to express his sincere gratitude and thanks to Dr. Carl D. Lundin for his guidance and patience through the course of this research program. The author would also like to extend his thanks to Mr. Ted A. Long of the Electronics Shop and his crew, to Mr. H. B. Thompson of the Machine Shop and his crew and to Mr. Art Freeborg and his men for their unlimited assistance and services. Special thanks are due to Mr. Arnold J. Beal of the Electronics Shop for installing and maintaining the welding power supplies used in this investigation and for assisting in taking the oscillograms shown in this thesis.

The author greatly appreciates the financial assistantship given to him by Dr. Homer F. Johnson, Head of the Chemical and Metallurgical Engineering Department of the University of Tennessee. The author would further like to extend his sincere appreciation and gratitude to TekTran Company (a Division of Air Products and Chemicals, Inc.) for their generous grant and for furnishing the plasma and GTA welding systems which made this research program possible. Last but not least, thanks are extended to Merrick Engineering, Inc. of Nashville for lending their TXR-200 welding power supply to assist in the progress of this research program.

ABSTRACT

A complete evaluation of the pulse parameters for the Plasma-Arc Welding (PAW) and Gas Tungsten-Arc Welding (GTAW) processes was conducted. The pulse parameters evaluated were: the background current (I_B), the peak current (I_p), the average current (I_{av}), the RMS current (I_{RMS}), the pulse time ratio (t_p/t_B), the pulse wave form and the pulse frequency (Hz). Both low (one-forty Hz) and high (two-twenty kHz) pulse frequencies were evaluated. High frequency was also superimposed on low frequency for the pulsed GTAW process. Comparisons of constant and pulsed current plasma welds were made for the melt-in, full penetration and keyhole modes of welding. For contrast, constant and pulsed current GTA welds were made under the same welding conditions of the plasma welds. Two plasma welding systems with different torch design and a GTA welding system were utilized and compared in this investigation. The material used was 0.109 inches thick Inconel 600 alloy sheets.

Optimum pulse welding conditions for both the PAW and GTAW processes were determined. The average current was found to be the controlling pulse welding parameter for both the PAW and GTAW processes. The background current was found to be optimum when it is the minimum melting current level for a given set of pulsed plasma-arc welding conditions. For this background current, the energy input was the lowest compared to all other pulse settings at the same average current. For the pulsed GTAW process with the given average current the lowest background current with the longest pulse duration (high pulse time

ratio (t_p/t_B) was found to be optimum. For contrast, the highest peak current at shortest pulse duration was found to be optimum for a given average current with the pulsed plasma process.

In general, it was found that for both the PAW and the GTAW processes, the lower the pulse frequency, the narrower the HAZ and the wider the fusion zone. At higher pulse frequencies, however, the HAZ became wider while the fusion zone became narrower, indicating a decrease in melting efficiency at higher pulse frequencies. Neither the high frequency pulsing of PAW or the GTAW processes, nor the superimposed high frequency on the low frequency pulsing resulted in any significant improvement in the weld bead configuration or microstructure.

The microstructural observations made in this study further illustrated an important aspect of the solidification process in welds. It was observed that the partially melting region (liquidus-solidus region) immediately adjacent to the fusion line often exhibited a grain size smaller than that of the HAZ region adjacent to it but slightly further away from the fusion line. A theory regarding the effect of the partially melted region on the weld fusion zone grain size and the possibility of influencing control over the grain size and shape by the pulsed current mode is postulated.

TABLE OF CONTENTS

CHAPTER		PAGE
I.	INTRODUCTION	1
II.	BASIC CONSIDERATIONS	4
	Gas Tungsten-Arc Welding Process (GTAW)	4
	Process Description (PAW)	4
	Plasma-Arc Welding Process	4
	Background	4
	Process Description	5
	Pulsed-Current Arc Welding Processes	9
	General	9
	Pulsed-Current Plasma Arc Welding	9
	Effect of Pulsed-Current on Arc Welds	11
	Metallurgical Effects	11
	Mechanical Effects	12
	Geometrical Effects	13
III.	EXPERIMENTAL PROCEDURES	15
	Equipment	15
	Power Supplies	15
	Torches	21
	Control and Monitoring Units	21
	Material	27
	Experimental Design	27
	Characterization of the Pulsed Plasma-Arc Welding Process	30

CHAPTER PAGE

Pulse Wave Form 38

Pulse Time Ratios (t_p/t_B) 38

Weld Current Control. 40

Pulse Frequency (Hz). 42

Measuring Techniques. 43

IV. RESULTS AND DISCUSSION. 44

Introduction. 44

Welding Power Supply Response Characteristics 44

General 44

Low Frequency Pulsing Power Supplies. 47

High Frequency Pulsing Power Supplies 56

High Frequency Superimposed on Low Frequency Pulsing Power Supplies. 60

Pulsed Plasma-Arc Welding Process 64

Results 64

Low Frequency Pulsed Plasma Welds (Melt-in Mode) 64

Low Frequency Pulsed Plasma Welds (Full Penetration and Keyhole Modes). 85

High Frequency Pulsed Plasma Welds (Melt-in Mode). 85

Pulsed GTA Welding Process. 86

Results 86

Low Frequency Pulsed GTA Welds 86

High Frequency Pulsed GTA Welds 95

CHAPTER PAGE

Superimposed Pulsed High Frequency on Pulsed Low Frequency GTA Welding Process 107
General. 107
Results. 108
Metallographic Observations. 111
General. 111
Results. 111
Pulsed Plasma-Arc Welds. 111
Pulsed GTA Welds 112
Dicussion. 113
V. CONCLUSIONS AND RECOMMENDATIONS. 122
LIST OF REFERENCES 126
VITA 131

LIST OF TABLES

TABLE		PAGE
I.	Power Input and Current Ratings of Welding Machines Used in This Investigation	17
II.	Chemical Analysis and Mechanical Properties of Inconel 600 Alloy.	28
III.	Non-Pulse Operating Parameters Held Constant Throughout This Investigation for Both the Pulsed Plasma and Pulsed Gas Tungsten-Arc Welding Processes.	31
IV.	Low Frequency Operating Pulse Welding Parameters for an Average Current of 50 and 60 Amperes.	32
V.	Low Frequency Operating Pulse Welding Parameters for an RMS Current of 50 and 60 Amperes.	34
VI.	High Frequency Operating Pulse Welding Parameters for an Average Current of 60 Amperes	36
VII.	Superimposed High Frequency on Low Frequency Pulse Parameters for a Composite Average Current of 60 Amperes for the GTAW Process	37
VIII.	Nominal and Actual Current Values and Measured Arc Voltage and the Associated Calculated Energy Inputs for the Welding Conditions Listed in Table IV for the Plasma Process	65
IX.	Nominal and Actual Current Values for the Pulsed High Frequency Welding Conditions Listed in Table VI . . .	99

LIST OF FIGURES

FIGURE		PAGE
1.	Comparison of Nonconstricted Arc Used for GTAW and a Constricted Arc Used for PAW, Showing the Effect of Constriction on Temperature and Heat Pattern	6
2.	Schematic Diagram of the Plasma-Arc Welding System and Torch Terminology	7
3.	Schematic Illustration of the Appearance of a Pulsed-Current Plasma-Arc Weld	10
4.	Welding Machines and Test Equipment Used in this Investigation. Left to Right: TekTran's LSC-300A Supply, Airco Plasma Control Unit (on Top of LSC-300 Supply), IONARC Plasma Control Unit (on Top of Welding Table), IONARC MPW 400 Torch and Welding Specimen Fixture, High Frequency Arc Starter (Under Table), Airco Torch Carriage and Speed Controller, Merrick Engineering TXR-200 Welding Power Supply, TekTran's TT-150A Supply, and TekTronix Type 547 Oscilloscope.	18
5.	High Frequency Pulsing Welding Machines: Merrick Engineering Supply (Left) and TekTran's Supply (TT-150A) in Center and TekTronix Oscilloscope (Right)	19
6.	A Complete Electrical Program for the GTAW Process, A Feature Furnished by TekTran's TT-150 Welding Power Supply . .	20
7.	IONARC (Model MPW-400) Machine Plasma Welding Torch and Hold Down Fixture	22

FIGURE PAGE

8. Schematic Illustration of the IONARC (MPW-400) Plasma Torch Structure 23

9. Schematic Illustration of Airco Sampac-200 Plasma Torch 24

10. Schematic Illustration of Airco-500 Amps (M50-A) TIG Torch 25

11. Elementary Illustration of an Ideal Pulsed-Current Square Wave Form and the Associated Pulse Parameters 29

12. Varying Time Ratio Versus Peak Current for a Constant Average Current of 50 Amperes 39

13. Schematic Pulse Wave Forms: (a) Ideal Rectangular, (b) Sloping Sides with Rise and Fall Times, (c) Overshoot, and (d) Rectangular Wave Form Showing Line Ripple Superimposed. 46

14. One Hz Pulsed Wave Forms: (a) GTAW and (b) PAW for Welding Conditions of I_p/I_B = 90/10 Amperes, t_p/t_B = 1/1 and I_{av} = 50 Amperes. 48

15. Two Hz Pulsed Wave Forms: (a) GTAW and (b) PAW for Welding Conditions of I_p/I_B = 90/10 Amperes, t_p/t_B = 1/1 and I_{av} = 50 Amperes. 49

16. Five Hz Pulsed Wave Forms: (a) GTAW and (b) PAW for Welding Conditions of I_p/I_B = 90/10 Amperes, t_p/t_B = 1/1, and I_{av} = 50 Amperes 50

17. Ten Hz Pulsed Wave Forms: (a) GTAW and (b) PAW

FIGURE PAGE

for Welding Conditions of I_p/I_B = 90/10 Amperes t_p/t_B = 1/1 and I_{av} = 50 Amperes 51

18. TekTran's LSC-300 Power Supply Response Characteristics, Pulse Amplitude Versus Pulse Frequency for t_p/t_B = 1/1. 53

19. Pulsed GTA Current Wave Forms Per TT-150 Welding Power Supply at I_p/I_B = 150/30 Amperes, t_p/t_B = 1/3 and I_{av} = 60 Amperes 54

20. High Frequency Pulsed GTA Current Wave Forms at t_p/t_B = 1/1 and I_{av} = 60 Amperes, I_B = 40 Amperes (TT-150 Supply) 57

21. High Frequency Pulsed GTA Arc Voltage Wave Forms: (a) Two KHz and (b) Ten KHz for I_{av} = 60 Amperes at t_p/t_B = 1/1 (TT-150 Supply) 59

22. High Frequency Pulsed GTA Current Wave Forms Per Merrick Engineering Supply (TXR-200) at I_{av} = 60 Amperes and t_p/t_B = 1/1 61

23. Superimposed High Frequency on Low Frequency GTA Current Wave Form; High Frequency = Two KHz, Low Frequency = Ten Hz; $\frac{I_{amp}/\text{Hi-Freq}}{I_{av}/\text{Lo-Freq}}$ = 10/50 and t_p/t_B = 1/1. 63

24. Effect of Low Frequency Pulsed PAW on (a) Weld Penetration and (b) Weld Fused Area for an Average Current of 50 Amperes at Varying I_{RMS}, I_p and t_p/t_B Values at I_B = 20 Amperes 67

FIGURE PAGE

25. Typical One Hz Pulse Weld Bead Spot Overlapping 70

26. Effect of Low Frequency Pulsed PAW on (a) Weld Penetration and (b) Weld Fused Area for an Average Current of 50 Amperes and a t_p/t_B = 1/1 Pulsed at Varying I_p, I_B and I_{RMS} Values. 73

27. Effect of Low Frequency Pulsed PAW on (a) Weld Penetration and (b) Weld Fused Area for an Average Current of 50 Amperes and a Pulse Frequency of One Hz at Varying I_p, I_{RMS}, I_B and t_p/t_B Values 75

28. Energy Input Per Unit Length for a Low Frequency Pulsed PAW of an Average Current of 50 Amperes at Varying I_p, I_B and t_p/t_B Values and a Pulse Frequency of One Hz. 77

29. Effect of Low Frequency Pulsed PAW on (a) Weld Penetration and (b) Weld Fused Area for an RMS Current of 50 Amperes and I_B = 10 Amperes at Varying I_p, t_p/t_B and I_{av} Values. 80

30. Effect of Low Frequency Pulsed PAW on (a) Weld Penetration and (b) Fused Area for an RMS Current of 50 Amperes at t_p/t_B = 1/1 and Varying I_p, I_B and I_{av} Current Values. 83

31. Effect of Low Frequency Pulsed GTA on (a) Weld Penetration and (b) Weld Bead Width for an Average Current of 60 Amperes and Varying I_{RMS}, I_p and t_p/t_B Values at I_B = 20 Amperes. 87

FIGURE PAGE

32. Effect of Low Frequency Pulsed GTAW on (a) Weld Penetration and (b) Weld Fused Area for an Average Current of 60 Amperes at t_p/t_B = 1/1 and Varying I_B and I_p Current Values 91

33. Effect of Low Frequency Pulsed PAW and GTAW Processes on (a) Weld Penetration and (b) Weld Fused Area (LSC-300 Supply) for the Welding Conditions of 50 Amperes Average Current at t_p/t_B = 1/1 and Varying I_B and I_p Current Values. 93

34. Effect of Varying Pulse Time Ratio (t_p/t_B), Peak and Background Currents on the Weld Bead Penetration for an Average Current of 50 Amperes at a Pulse Frequency of One Hz for the PAW and GTAW Processes. 96

35. Effect of Low Frequency Pulsed GTAW on the Weld Penetration for an RMS Current of 60 Amperes at Varying I_B, I_p, I_{av} and t_p/t_B Values 97

36. Effect of Low Frequency Pulsed PAW and GTAW on the Weld Penetration (LSC-300 Supply) Under the Same Conditions of an RMS Current of 50 Amperes at t_p/t_B = 1/1 and Varying I_B, I_p and I_{av} Current Values 98

37. Effect of High Frequency Pulsing on (a) Weld Penetration and (b) Weld Fused Area of the Pulsed GTAW Process for an Average Current of 60

FIGURE PAGE

Amperes at t_p/t_B = 1/1 and Varying Pulse Frequency and Background Current Values 101

38. Effect of High Frequency Pulsed GTAW on the Weld Penetration for an Average Current of 60 Amperes and Varying t_p/t_B and Pulse Frequency 104

39. Effect of High Frequency (10 KHz) Pulsed GTAW on the Weld Penetration for an Average Current of 60 Amperes at Varying I_B and t_p/t_B Values 105

40. Effect of High Frequency (2 KHz) Pulsed GTAW on the Weld Penetration for an Average Current of 60 Amperes at Varying I_B, I_p and t_p/t_B Values 106

41. Effect of Superimposed High Frequency (2 KHz) on Varying Low Frequency Pulsed GTAW on the Weld Penetration for a Composite Average Current of 60 Amperes 109

42. Effect of Superimposed High Frequency on Low Frequency Pulsed GTAW on the Weld Penetration for a Composite Average Current of 60 Amperes at t_p/t_B = 1/1 and Varying High and Low Pulse Frequency. 110

43. Fusion Zone Microstructure of a 60 Amperes Average Current Pulsed GTA Weld Bead at t_p/t_B = 1/1, I_B = 40 Amperes and I_p = 80 Amperes, Marble Reagent, 50X. 116

LIST OF SYMBOLS

Amps	=	amperes.
cm	=	centimeter.
CPS	=	cycle per second.
DC	=	direct current.
E	=	electrode.
E.I.	=	energy input.
f	=	pulse frequency.
g	=	grams.
GTAW	=	gas tungsten-arc welding.
HAZ	=	heat affected zone.
Hz	=	hertz.
Hi	=	high.
i	=	current.
I_{amp}	=	amplitude current.
I_{av}	=	average current.
I_{B}	=	background current.
I_{c}	=	constant current.
I_{eff}	=	effective current.
I_{p}	=	peak current.
IPM	=	inch per minute.
I_{rms}	=	root mean square current.
KHz	=	kilohertz.

KJ = kilojoules.

KW = kilowatt.

L = length of weld spot.

Lo = low.

LRC = inductance-resistance-capacitance network.

LSC = linear slope control.

ml = milliliter.

ms = millisecond.

PAW = plasma arc welding.

PPS = pulse per second.

RMS = root mean square.

S = welding travel speed.

SCR = silicon controlled rectifier.

t = time of one pulse cycle.

t_B = background duration time.

t_p = peak (pulse) duration time.

μs = microsecond.

vdc = volts direct current.

V = arc voltage.

V_B = background arc voltage.

V_p = peak arc voltage.

W = work.

Z = length of the weld spot minus the overlap distance.

CHAPTER I

INTRODUCTION

Developments of the past few years have shown that the welding current could be pulsed at varying frequencies ranging from a low of one half Hz to 30 KHz. Lundin (20) indicates that the idea behind pulsing the welding current is that such a process results in reduced heat inputs and rapid solidification compared to the continuous current operations. Reduced heat inputs and rapid solidification result in narrower heat-affected zone (HAZ) and finer substructure in the fused zone. This inhibits grain growth in both the HAZ and the fusion zone. According to Barabokhin (2), that because of the reduction of linear heat input in the pulsed-arc welding and the reduction of time of contact between the liquid and solid phases in the fusion zone, a much smaller quantity of brittle segregates is observed at the boundaries of the partially fused grains. This results in improved weld joint performance.

Rapid rate current pulsing, as indicated by Lenivkin and coworkers (18), introduces weld puddle vibration which increases the frequency of movement of the liquid metal in the weld pool. Thus when the liquid metal moves over the solidifying metal interface, portions of the solidified grains are dislodged and these in turn act as additional nuclei. This phenomena promotes reduction in the grain size.

Many researchers (1-46) have indicated that pulsing the welding current results in several advantages when applied to the GTA, GMA and

plasma arc processes. These advantages are:

1. Improved control of the welding heat inputs.

2. Improved weld quality and joint performance, due to reduced fusion zone and HAZ grain size.

3. Reduced distortion.

4. Control of the melting and solidification process will permit welding in other than the flat position.

5. Increased penetration and reduction in the extent of the HAZ.

These advantages may be achieved by controlling one or more of the pulsing variables:

1. Pulse amplitude or the peak current (I_p)

2. Pulse duration (t_p)

3. The background current (I_B)

4. The average current (I_{av})

5. The effective or the RMS current (I_{eff} or I_{rms})

6. The pulse frequency (Hz)

7. The pulse duration time ratio (t_p/t_B) where t_B is the background current duration time

8. The shape of the pulsed waveform

Coupled with the welding speed, these parameters will control the resultant weld configuration and possibly alter the microstructure and properties of the weld.

An up-to-date review of the open literature shows that no attempt to completely evaluate the pulsed arc mode utilizing the full range of pulse parameters has been made. Thus, the objective of this

research program is to evaluate the entire spectrum of pulse parameters for both low (1-40 Hz) and high (2-20 KHz) pulse frequencies in order to determine the controlling parameters. The basis for evaluation is the resulting metallurgical structure and geometrical configuration of the welds. Such an evaluation could lead to the optimum control of the process and further enhance its utility. Furthermore, it is anticipated that once such a determination is made, a relationship between the pulse parameters and the fundamental material properties may be possible.

CHAPTER II

BASIC CONSIDERATIONS

A. GAS TUNGSTEN-ARC WELDING PROCESS (GTAW)

Process Description

The Gas Tungsten-Arc is a welding process in which the heat is produced between a nonconsumable electrode and the work metal. The electrode, the weld puddle, the arc, and adjacent heated areas of the workpiece are protected from atmospheric contamination by a gaseous shield. This shield is provided by a stream of gas (usually an inert gas) or a mixture of gases (23).

The simplicity of the GTA process is important for mechanized welding because all of the parameters can be controlled easily. Very precise welds can be made in relatively thin sections at reasonable speeds, making the process advantageous for fabricating welded tubing (47).

B. PLASMA ARC WELDING PROCESS (PAW)

Background

A plasma is a gas which has been heated to a condition where it is at least partially ionized and is, therefore, capable of conducting electric current. Thus when an arc is established through the gaseous column separating two electrodes, some of the gas molecules become ionized. The ionized zone, or plasma stream, consists of positively charged atoms of the arc gas, an essentially equal number of electrons,

and neutral atoms or molecules. The electrical conductivity of a plasma stream varies with the degree of ionization (28).

The expression "plasma arc" has recently become associated with those processes employing a constricted arc. Arc constriction is brought about by forcing the arc to pass through a small nozzle or opening as it passes from the electrode to the workpiece.

Plasma arc jet was first introduced to industry in 1955 for the cutting of aluminum plates. Commercial equipment for plasma arc surfacing was brought out in 1961, and plasma arc welding was introduced in 1963 (28).

Process Description

Plasma arc welding is a gas-shielded nonconsumable electrode welding process that utilizes a constricted arc. It is an extension of gas tungsten arc welding (GTAW). Both low current (0.1-75 amps) and high current (above 75 amps) plasma arc welding are practiced; but the equipment and areas of application of the two versions are different (28).

Constricting the arc increases the arc voltage for a given arc current and thus when compared to GTAW, produces a higher temperature columnar-shaped plasma arc. This constriction is the primary difference between GTAW and PAW as shown in Figure 1.

Since the stream of plasma gas is constricted and very narrow, it does not provide adequate shielding of the molten weld metal and, consequently, a larger diameter concentric stream of shielding gas is necessary to protect the weld from contamination. PAW process is illustrated schematically in Figure 2.

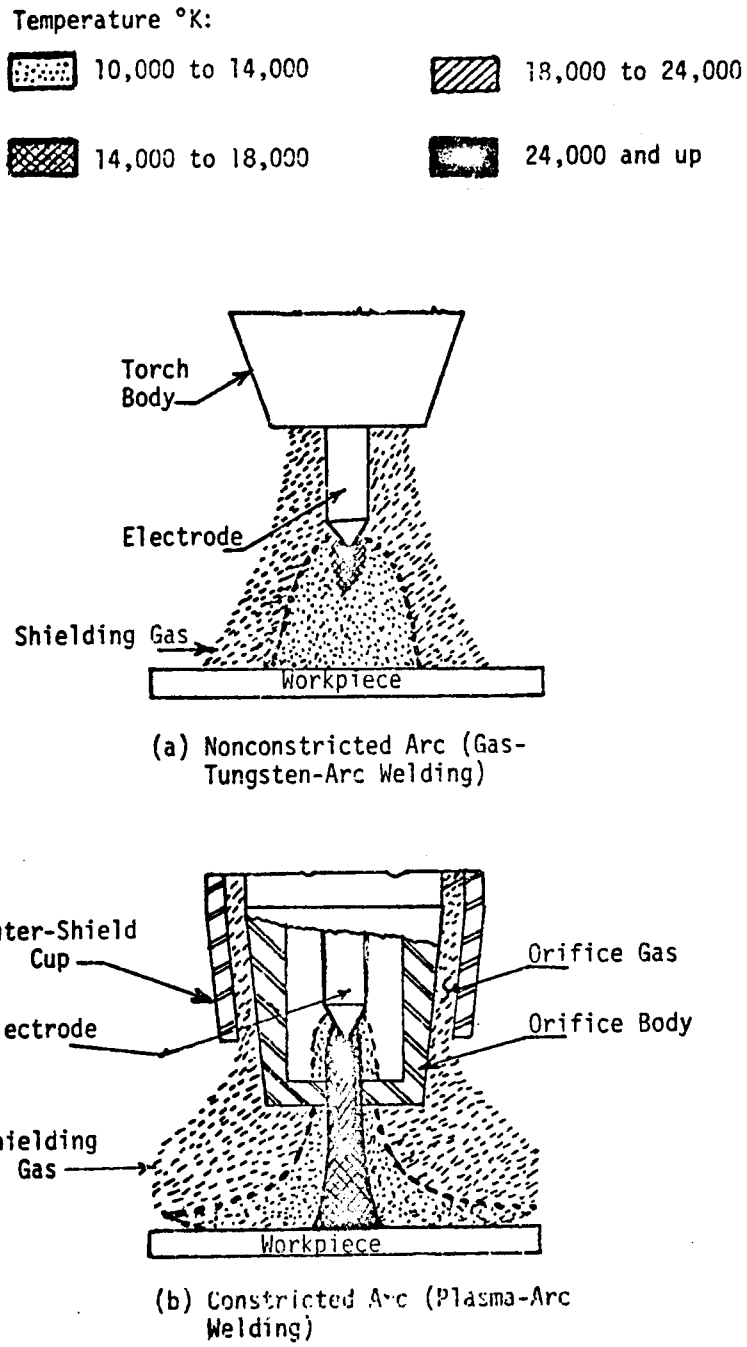


Figure 1. Comparison of a Nonconstricted Arc Used for GTAW and a Constricted Arc Used for PAW, Showing the Effect of Constriction on Temperature and Heat Pattern

Source: Metals Handbook, Vol. 6, Welding and Brazing, American Society for Metals (ASM), Metals Park, Ohio (1971), pp. 113-140.

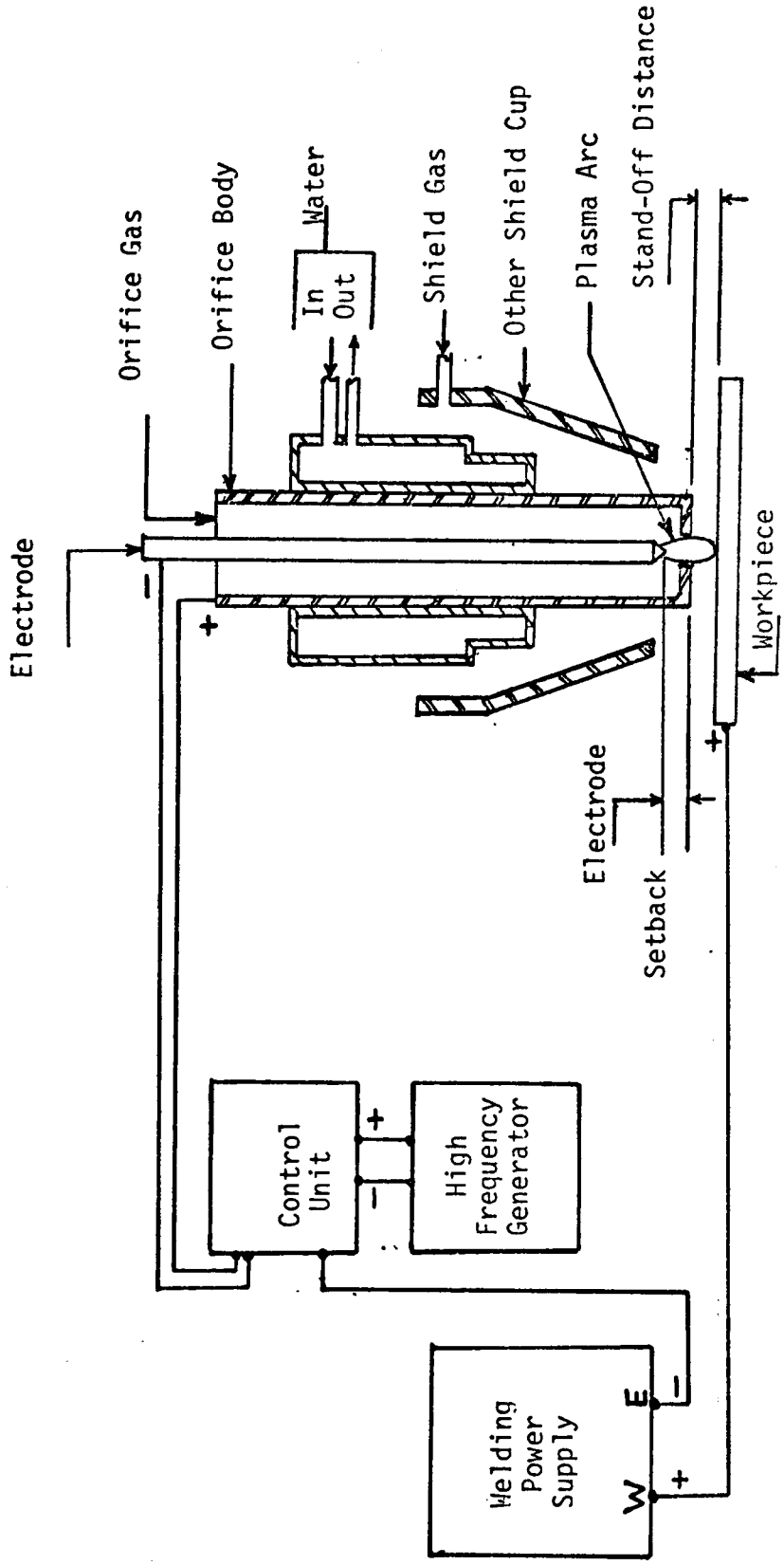


Figure 2. Schematic Diagram of the Plasma-Arc Welding System and Torch Terminology

There are two types of welding that can be performed with the plasma process (41). The first is the "puddle type" or "melt-in" mode of welding in which a low flow of plasma gas is used that will not deform the weld puddle. The second type is referred to as "keyhole" mode of welding. In this type, a higher velocity plasma gas pierces the plate and forms a small hole at the bottom of the crater. As the weld progresses, molten metal from the leading edge of the pool flows around both sides of the keyhole and is brought together by surface tension to form the weld. This mode of welding produces a full penetration weld with a narrow HAZ.

In PAW two primary variables must be selected for optimum performance; first, the choice of nozzle size suitable for a given current capability and thus a given material thickness. Second, plasma gas flow rate. In general:

1. Low plasma gas flow rates with increasing current lead to nozzle burnout.

2. At relatively high current and increasing plasma gas flow rate, the additional pressure acting on the weld metal by the gas stream flow and arc plasma jet leads to gouging (41).

3. Low currents and high plasma gas flow rates result in low heat input and poor efficiency (41).

Plasma arc welding process has several advantages over the standard GTAW process (41).

1. Improved arc direction and stiffness lead to improved control of heat input to the work without arc wander or jump.

2. Greater welding stand-off distances allow greater tolerance

for arc length variation by the operator; less sensitivity of puddle size to arc length changes.

3. Higher welding speed for plasma welding with a narrower heat-affected zone.

4. Less sensitivity to mismatch or poor joint fitup.

5. Controlled penetration by using a keyhole welding technique

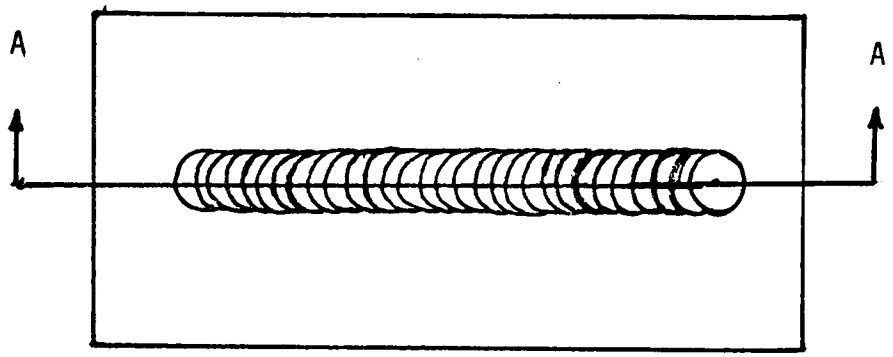
C. PULSED-CURRENT ARC WELDING PROCESSES

General

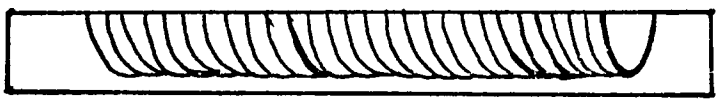
Pulsed-current has been successfully used with GTA and GMA welding processes. The pulsed-current arc welding processes employ two levels of welding current instead of the single level that is used conventionally. Welding current is, in effect, switched between a high and a low level to produce a pulsating welding arc. When used with GTA welding, pulsed current produces a continuously welded seam consisting of overlapping arc-spot welds as illustrated in Figure 3. Each of these arc-spot welds is produced with the high level welding current, after which the current is switched to the lower level (42). The lower level current maintains the arc so that arc reignition problems can be avoided. When used with gas metal-arc welding, pulsed current offers an improved method for controlling metal transfer from the welding wire to the weld joint.

Pulsed-Current Plasma Arc Welding

Lundin and Ruprecht (19) studied the effect of pulsed current on the penetration characteristics of the plasma and the GTA welding processes and reported that pulsed current operation has a more significant



(a) Top View



(b) Section AA

Figure 3. Schematic Illustration of the Appearance of a Pulsed-Current Plasma-Arc Weld

influence on penetration with the plasma process than with the GTAW process. Ashauer and Goodman (1) investigated continuous-current and pulsed-current plasma arc welding for the automatic welding of square-butt joints in piping of schedule 40 carbon steel, stainless steel, and copper-nickel. They cited the following beneficial effects of the pulsed-current welding mode compared to that of the steady state mode welds:

1. Slightly lower average current could be used.

2. The pulsed welding process appeared to be more immune to slight parametric changes and thus more practical and reproducible.

3. Pulsed-current produced welds with improved root-bead contour.

4. Pulsed-current provided deeper penetration capability for an average current level.

Ashauer and Goodman further indicated that the optimum pulse frequency was found to be six pulses per second. Similar investigation was conducted by Smart and Pinfold (36) who used pulsed plasma arc to butt weld one-fourth inch thick stainless steel plates and found that welds produced by the modulated plasma process had better consistency of the under bead than those produced by the unmodulated current. They also indicated that for the range of parameters examined, a pulse duration of 0.25 second and a frequency of two Hz produced the best welds.

D. EFFECT OF PULSED-CURRENT ON ARC WELDS

Metallurgical Effects

Petrov and Slavin (29) studied the effects of welding parameters of the pulsed-current gas tungsten-arc on the quality of welds and

indicated that the pulsed-current process produces welds having heat-affected zones narrower than those produced with continuous current. They also indicated that under appropriate pulsed-current welding conditions, the weld metal solidified and cooled much more rapidly than with continuous current. The shorter times at elevated temperatures offer some important advantages in that:

1. There is less time available for contamination of weld metal from gases in the surrounding atmosphere or gases that diffuse from the base metal into the weld metal.

2. High solidification rates are accompanied by the formation of "fine-grained" structures in the weld metal.

3. The metal remains in the brittle temperature reanges for shorter periods of time, thus reducing the rish of hot cracking.

Petrov and Slavin further indicated that under some conditions of the pulsed-current welding porosity was reduced considerably compared with that obtained by continuous current. They observed that the weld metal takes on a randomly oriented structure which provides greater resistance to crack propagation.

Mechanical Effects

A survey of the published literature revealed little material on how the mechanical properties of a weld arc affected by the weld bead microstructure. Tret'yakov and co-workers (40) studied the pulsed argon arc welding of thin titanium alloys and reported that the strength of the welded joint was 85 to 90 percent of the parent metal for all the thicknesses examined. Vilkas (44) reported that pulsed-current produced higher strength Ti-6Al-4V welds than did continuous

current. Shnayder (32) studied the use of pulsed-current gas tungsten arc butt welding of copper strip for fabrication of coaxial cables and reported that a thermal severity of (interpulse time/pulse time or t_B/t_p) value of three or (3/1) gave the maximum weld strength. Lundin and Ruprecht (19) studied the pulsed-current plasma arc welds in Inconel sheets and reported that the tensile yield strength of both partial and full penetration welds was 10 to 15 percent higher than the as-received base metal while the ultimate tensile strength was lower by about 10 percent. They further observed that the transverse ductility, in terms of elongation, was about 50 percent less than the longitudinal ductility.

Geometrical Effects

In analyzing welds resistance to hot cracking, Prokhorov and Mastryukova (30) found that the shape and dimensions of the primary grains determine the following hot cracking parameters:

1. The position of the upper boundary of the brittle temperature range
2. The ductility in the brittle temperature range
3. The strength of the deformed metal in that range

Lundin (20) indicated that while the primary structure in arc welds on the majority of metals and alloys is columnar, and since the pulsed-current mode of operation produces a weld seam consisting of overlapping spot welds where solidification in each spot proceeds from the periphery toward the center, a variety of growth direction exist around the weld circumference and thus pulsed-current welds may exhibit unique properties.

Slavin and co-workers (34) reported that the extent to which welded spots overlap one another has a great effect on the penetrating power of pulsed arc. Petrov and Slavin reported that the amount of overlap is determined by the size and spacing of the solidified weld pools.

Matthews (22) reported that weld depth-to-width ratio was improved when rapid pulse rates (2 to 22 KHz) were used. Edmonds (8) indicated that under the same welding conditions and for low pulse rates (1-10 pps), pulsing the arc had increased the weld depth by 12 percent and the melting efficiency by 20 percent.

CHAPTER III

EXPERIMENTAL PROCEDURES

All welds made for this study were bead-on-plate type. The experimental procedures used in this investigation are divided into the following areas in order of discussion:

1. Equipment
2. Materials
3. Experimental Design
4. Measuring Techniques

A. EQUIPMENT

Power Supplies

A combination of three commercially available transistorized GTA and plasma arc welding power supplies were used. Each power supply is optionally equipped with either a low frequency or a high frequency pulser or a combination of both. The optional pulser is designed to furnish a signal to the welding machine control circuit which creates a pulsing output. A brief description of the operating characteristics and design features of each power supply is given below.

TekTran's LSC-300 Amps Power Supply. This is a three phase, 60 Hz, solid state, direct current welding machine. It is designed to serve as the power source for both the GTA and GMA welding processes. It also is being used as a power source for the plasma-arc welding process (PAW). It is equipped with an optional low frequency pulser

capable of pulsing the arc current from a low of 0.5 Hz to a high of 50 Hz. Its power input, current and voltage ratings are listed in Table I. The machine is show in Figure 4 first on the left.

TekTran's 150 Amps Transistor Power Supply (TT-150A). This is a transistorized, three phase 60 Hz direct current welding machine. It is designed to primarily serve as the power source for the GTA welding process. Its power input, current and voltage ratings are listed in Table I. The machine is shown in Figure 5.

The TT-150 welding power supply is equipped with an electronic weld programmer that automatically controls all weld input parameters of the welding cycle. Figure 6 shows an electronically controlled welding cycle for the GTA welding process.

The TT-150 welding power supply is also equipped with two fast response optional pulsers, a low frequency pulser which has a pulsing capability of 0.5 to 50 Hz and a high frequency pulser with pulsing capability of 2 to 20 KHz. The high and low pulsers could be operated separately or simultaneously.

Merrick Engineering Welding Power Supply (TXR-200). This is a three phase, 50/60 Hz, programmable direct current welding machine. It is primarily designed to serve as a power source for the GTA welding process, but could be utilized for the plasma-arc welding process. Its power input, current and voltage ratings are listed in Table I. It is equipped with a high frequency pulser with a pulse repetition rate capability of 2 to 30 KHz. The machine is shown in Figure 5.

TABLE I

POWER INPUT AND CURRENT RATINGS OF WELDING MACHINES USED IN THIS INVESTIGATION

Welding Machine	Weld Current Range (Amps)	Rated Welding Current at 15 vdc	Duty Cycle	Maximum Open Circuit Voltage DC	Power Input at the Rated Load Three Phase 60 Hz	
					KW	KVA
TekTran's (LSC-300A)	4-400	300	100%	75	7.4	17
TekTran's (TT-150A)	1.5-150	150	100%	45	4.9	5.5
Merrick Engineering (TXR-200)	5-200	200	100%	50	9.8	10.7



Figure 4. Welding Machines and Test Equipment Used in this Investigation. Left to Right: Tektran's LSC-300A Supply, Airco Plasma Control Unit (on Top of LSC-300 Supply), IONARC Plasma Control Unit (on Top of Welding Table), IONARC MPW-400 Torch and Welding Specimen Fixture, High Frequency Arc-Starter (Under Table), Airco Torch Carriage and Speed Controller, Merrick Engineer TXR-200 Welding Power Supply, TekTran's TT-150A Supply, and TekTronix Type 547 Oscilloscope

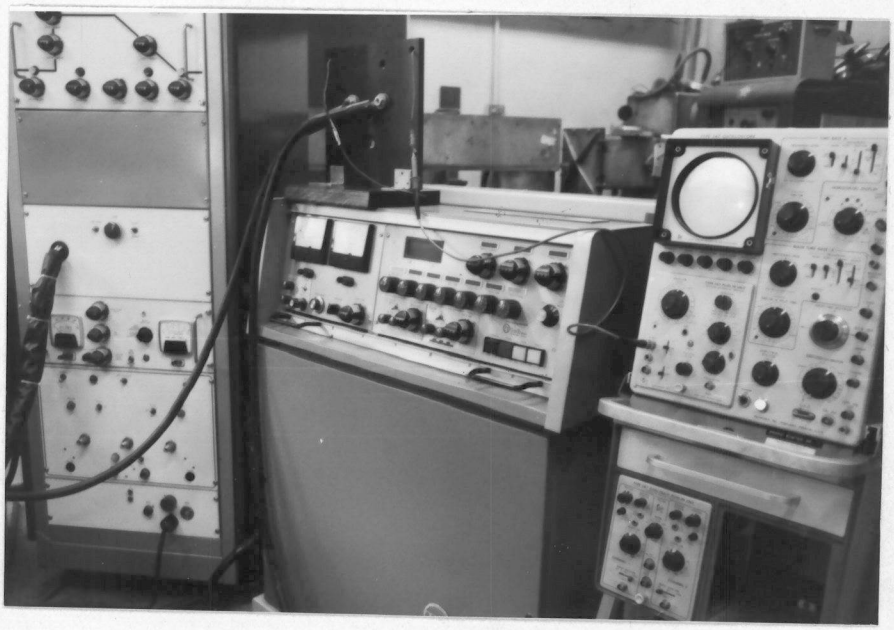


Figure 5. High Frequency Pulsing Welding Machines: Merrick Engineering Supply (Left) and TekTran's Supply (TT-150A) in Center and TekTronix Oscilloscope (Right)

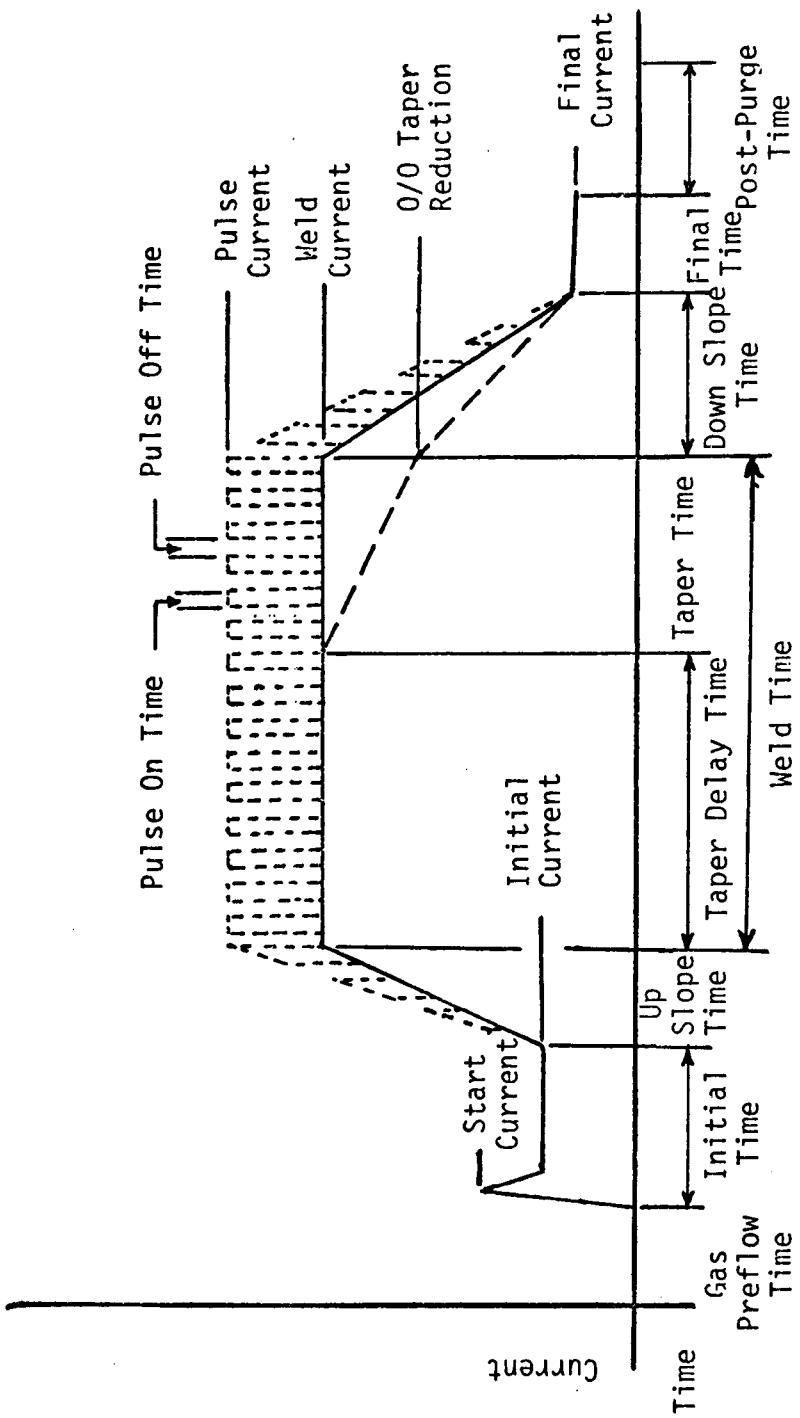


Figure 6. A Complete Electrical Program for the GTAW Process, a Feature Furnished by TekTran's TT-150 Welding Power Supply.

Torches

Three water-cooled welding torches were used in this investigation. A 500 ampere capacity Airco Model M50-A GTA torch, a 200 ampere Airco plasma welding torch and a 400 ampere Ionarc plasma torch (MPW-400). The Ionarc MPW-400 plasma torch is shown in Figure 7 along with the weld specimen hold down fixture.

The hold down fixture consisted of a one-inch thick copper plate and two aluminum hold down plates. The copper plate had a half-inch square groove machined in it so that a backing gas could be used when full penetration welds were made.

A 3/32 inch diameter, 2 percent thoriated tungsten electrode ground to a conical tip with a 60 degree included angle was used throughout this investigation. A torch carriage with electronic governor was used to hold the torch and control the travel speed. Fifteen feet of 4/0 copper welding cables were used.

It should be noted that while the basic plasma welding torch structure is the same as shown in Figure 2, the copper orifice design, size and shape, varies from one torch to another depending on the manufacturer's design philosophy. Figures 8 and 9 are schematic illustration of the plasma torches used in this investigation. Figure 10 is an illustration of the GTA torch used. Nozzle size and configuration could affect the thermal and thus the melting efficiency of the process.

Control and Monitoring Units

In addition to the welding power supplies and torches, the plasma

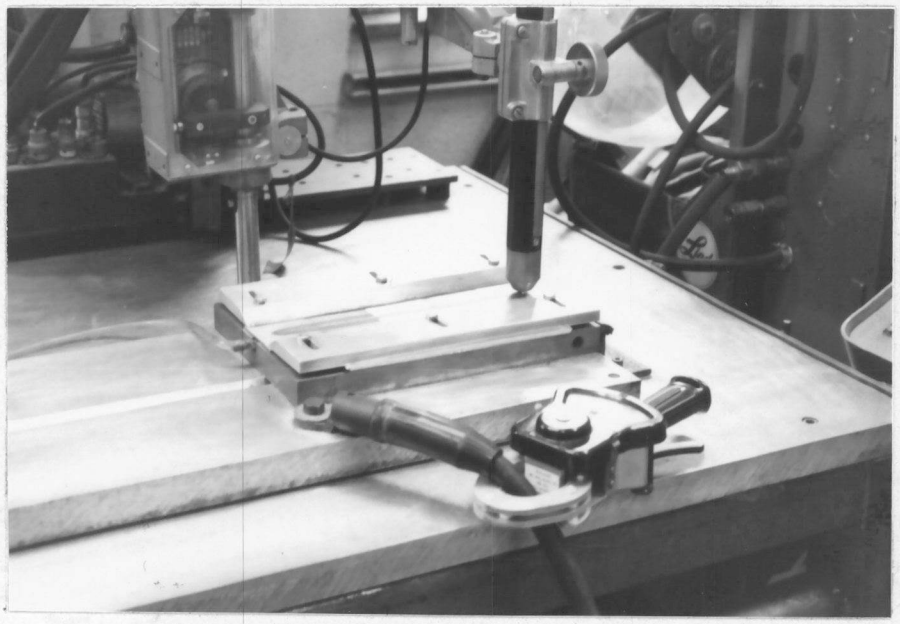


Figure 7. IONARC (Model MPW-400) Machine Plasma Welding Torch and Hold Down Fixture

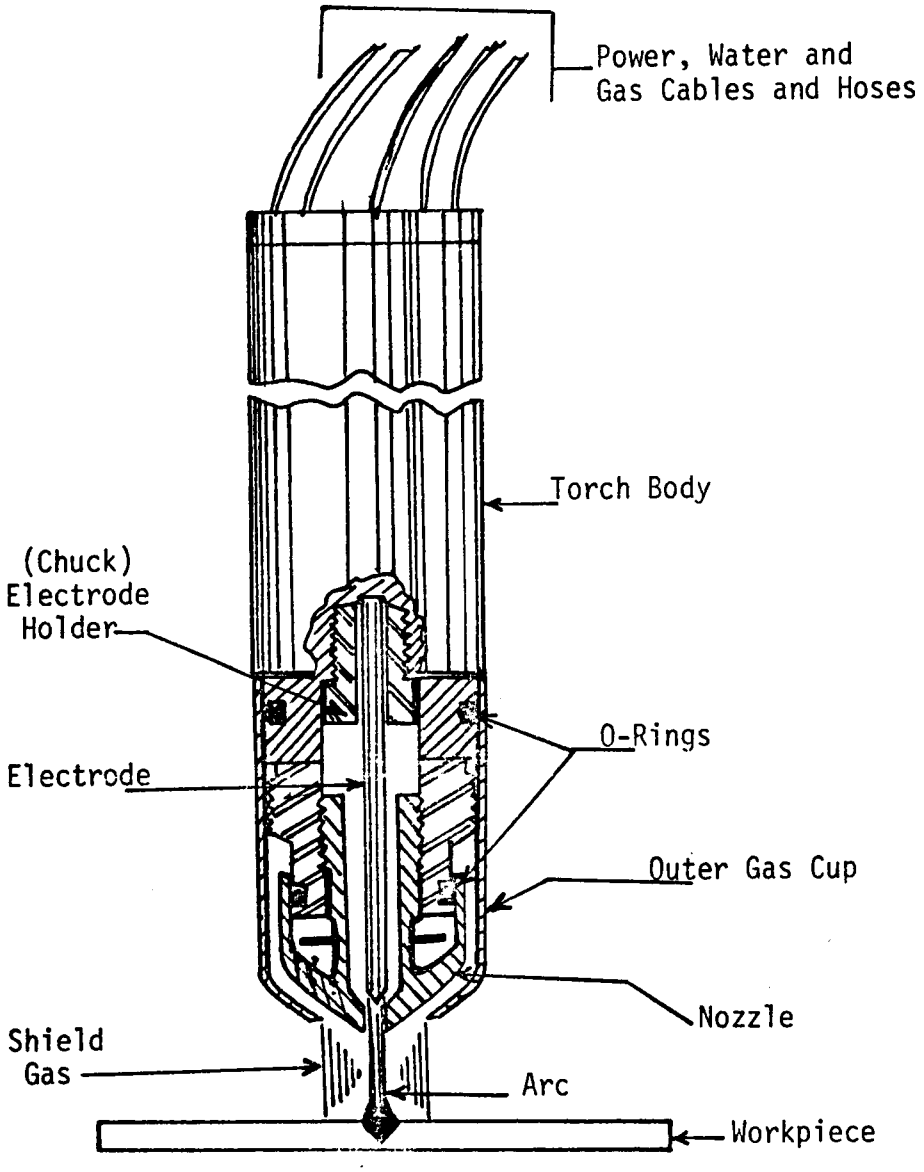


Figure 8. Schematic Illustration of the IONARC (MPW-400) Plasma Torch Structure

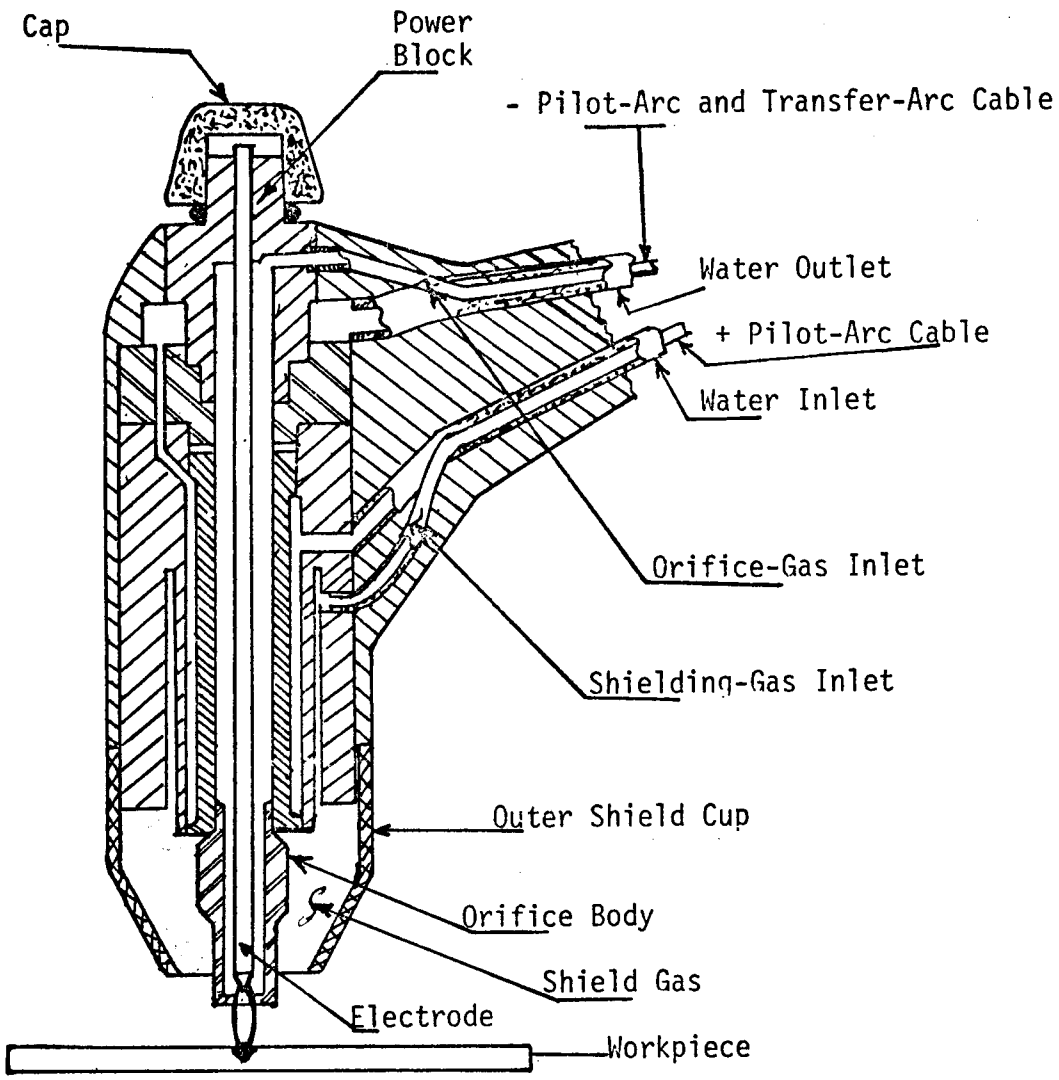


Figure 9. Schematic Illustration of Airco Sampac-200 Plasma Torch

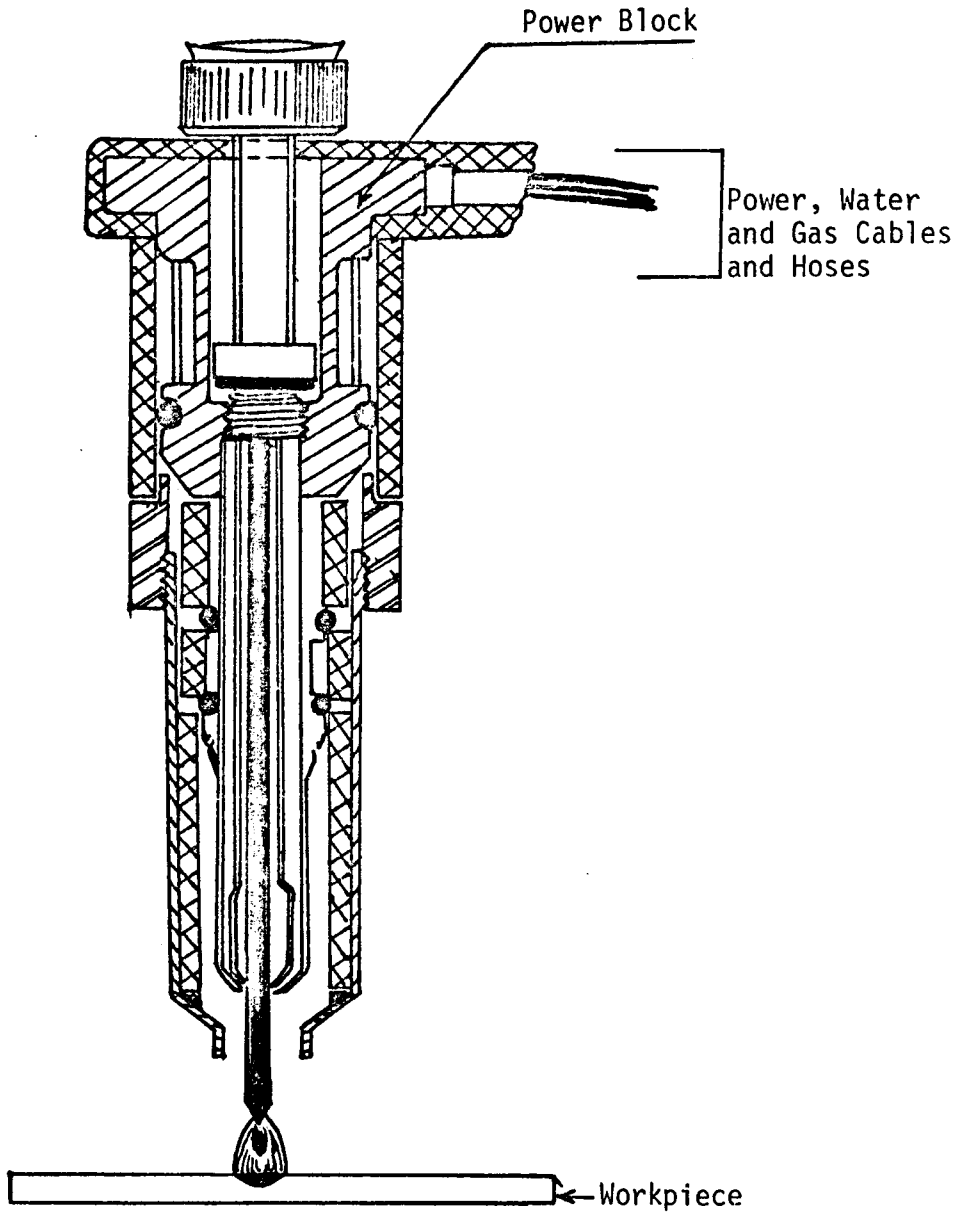


Figure 10. Schematic Illustration of Airco-500 Amps (M50-A) TIG Torch

welding systems included control units. The control units, shown in Figure 4 served as the control center providing pilot current regulation, metering of AC and DC weld current and DC pilot current, adjustment and regulation of gases and safety shutdown due to water failure or input current overload.

The control units contain three gas flow meters each; one meter regulates the orifice gas flow rate and the other two are used for regulation and mixing of the shield gas. The gas pre-purge and post-purge times are regulated by two time delay relays incorporated in the control units.

The constant and pulsed current and voltage waveforms of the arc were monitored on a TekTronix type 547 oscilloscope and photographed with a poloroid camera. The oscilloscope, shown in Figure 5, features two identical time-base generators used singly or electronically alternated for viewing a single signal or multiple signals at two sweep rates. Its sweep rates (at 1X magnification) range from 0.1 micro-second per centimeter to five seconds per centimeter in 24 calibrated steps.

Along with the oscilloscope, two high gain plug-in amplifier units were separately used to produce a signal display.Type 1A1 Dual-Trace plug-in amplifier contained two identical high gain fast rise calibrated channels. And type 1A7 amplifier, which is a high-gain low noise adjustable band width DC-coupled differential amplifier. Its minimum deflection factor is ten microvolts per centimeter and its maximum band width is DC to 500 KHz at all deflection factors.

B. MATERIAL

The material used for this study was Inconel 600 alloy. The chemical analysis and mechanical properties for this heat of Inconel 600 are shown in Table II. The sheets used in this investigation were in the cold rolled and annealed condition. The size of the sheets was 12 inches long by two and one half inches wide and 0.109 inches thick each. The sheets were degreased with methanol and ground clean with fine aluminum oxide abrasive discs. The gas used for this investigation was welding grade bottled argon.

C. EXPERIMENTAL DESIGN

Figure 11 shows an ideal pulsed-current square wave form and the associated pulse parameters that were investigated. For the square wave shown in Figure 11, the average current (I_{av}) is equal to

$$I_{av} = \frac{I_B t_B + I_p t_p}{t_B + t_p} \qquad (1)$$

and the effective current (I_{eff}) or the root-mean-square value (I_{rms}) is given by

$$I_{eff} = I_{rms} = \left(\frac{1}{t}\int_0^t i^2 dt\right)^{1/2} \qquad (2)$$

Thus the effective current as shown in Figure 11 is equal to:

TABLE II

CHEMICAL ANALYSIS AND MECHANICAL PROPERTIES OF INCONEL 600 ALLOY

Element	Weight Percent
C	0.04
Mn	0.26
Fe	7.47
S	0.007
Si	0.24
Cu	0.22
Ni	76.14
Cr	15.60

0.2 percent offset yield strength - 37,400 psi

Ultimate strength - 92,985 psi

Fracture strength - 178,225 psi

Percent elongation - 42.50 percent for two inch gage length

Heat number - NX203

Condition - cold rolled and annealed (CRA)

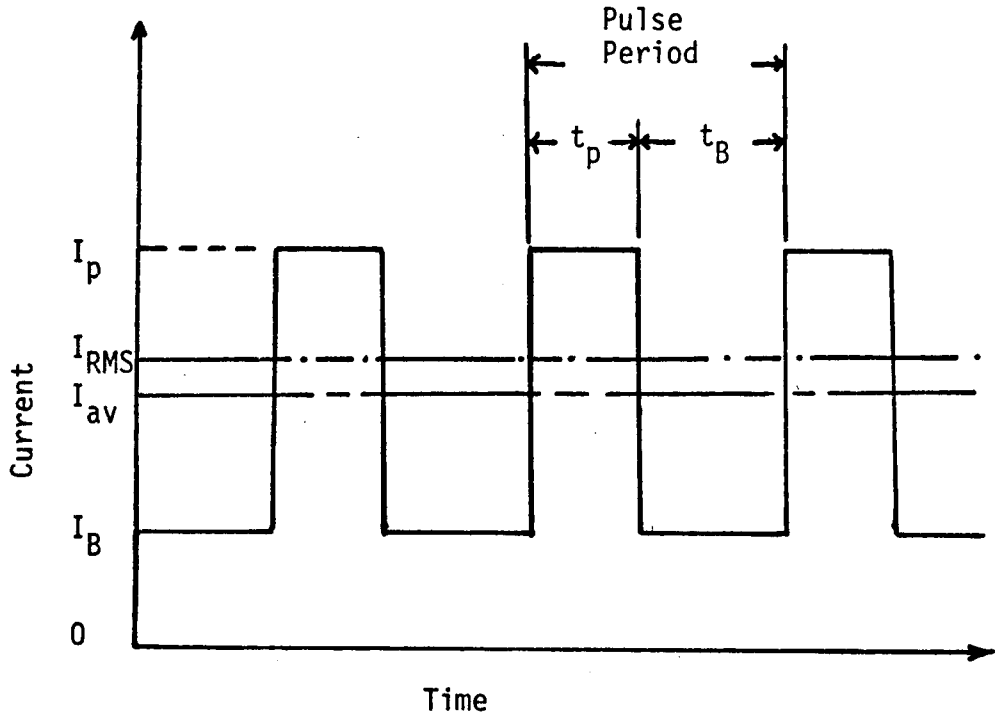


Figure 11. Elementary Illustration of an Ideal Pulsed-Current Square Wave Form and the Associated Pulse Parameters

$$I_{eff} = I_{rms} = \left(\frac{I_B^2 t_B + I_p^2 t_p}{t}\right)^{1/2} \quad (3)$$

where (t) is the time of one pulse cycle or

$$t = t_B + t_p \quad (4)$$

The pulse frequency (f) is defined as:

$$f = \frac{1}{t} = \frac{1}{t_B + t_p} \quad (5)$$

Thus, since the primary objective of this investigation was to evaluate the optimum condition and importance of each of the process pulse parameters, a welding program that enabled the complete evaluation of those parameters had been established. This welding program is represented by the data shown in Tables III through VII. The operating parameters listed in those tables are combination of set and calculated values. Equations (1) through (5) were used to calculate those parameters with consideration given to the material thickness and the rated output of the welding equipment used. Both plasma and gas tungsten-arc welding processes were evaluated under the same operating parameters.

Characterization of the Pulsed Plasma-Arc Welding Process

In order to properly study the importance and determine the optimum condition of each of the process pulse parameters, all non-pulse parameters of the process were held constant throughout this

TABLE III

NONE-PULSE OPERATING PARAMETERS HELD CONSTANT THROUGHOUT THIS INVESTIGATION FOR BOTH THE PULSED PLASMA AND PULSED GAS TUNGSTEN-ARC WELDING PROCESSES

Parameter	Value
Arc Length/GTA	3/32 Inch
Electrode, Size and Material	3/32 Inch Diameter, 2% Thoriated Tungsten
Electrode Stand-Off Distance/PAW	3/32 Inch
Electrode Setback Distance/PAW	0.120 Inch
Electrode Vertex Angle	60 Degrees
Copper Orifice Diameter	0.093 Inch
Orifice Gas Flow Rate/PAW	2 1/2 CFH Argon
Shield Gas Flow Rate/PAW	25 CFH Argon
Shield Gas Flow Rate/GTA	30 CFH Argon
Travel Speed	4 IPM
Material	Inconel 600
Plate Size	2 1/2 x 12 x 0.109 Inch Thick
Hold Down Plate Separation	1 1/2 Inch
Initial Plate Temperature	100 $\pm$ 25°F

TABLE IV

LOW FREQUENCY OPERATING PULSE WELDING PARAMETERS FOR AN AVERAGE CURRENT OF 50 AND 60 AMPERES

I_{av} (Amps)	I_{rms} (Amps)	I_B (Amps)	I_p (Amps)	Pulse Period (ms)		t_p/t_B	I_p/I_B	Frequency (Hz)[a]
				t_p	t_B			
50	55.07	10	63.33	750	250	3/1	6.33	A
50	57.48	10	70.08	666	333	2/1	7.01	A
50	64.03	10	90	500	500	1/1	9	A
50	75.55	10	130.15	333	666	1/2	13.01	A
50	85.44	10	170	250	750	1/3	17	A
50	52.92	20	60	750	250	3/1	3	A
50	54.35	20	65.08	666	333	2/1	3.25	A
50	58.31	20	80	500	500	1/1	4	A
50	65.53	20	110.15	333	666	1/2	5.51	A
50	72.11	20	140	250	750	1/3	7	A
50	51.32	30	56.67	750	250	3/1	1.89	A & B
50	52.0	30	60.08	666	333	2/1	2	A & B
50	53.85	30	70	500	500	1/1	2.33	A & B
50	57.50	30	90.15	333	666	1/2	3	A & B
50	61.44	30	110	250	750	1/3	3.67	A & B
60	64.26	20	73.3	750	250	3/1	3.67	C & B
60	72.11	20	100	500	500	1/1	5	C & B
60	91.65	20	180	250	750	1/3	9	C & B

TABLE IV (continued)

I_{av} (Amps)	I_{rms} (Amps)	I_B (Amps)	I_p (Amps)	Pulse Period (ms)		t_p/t_B	I_p/I_B	Frequency (Hz)[a]
				t_p	t_B			
60	62.45	30	70	750	250	3/1	2.33	C & B
60	67.08	30	90	500	500	1/1	3	C & B
60	79.37	30	150	250	750	1/3	5	C & B
60	61.13	40	66.7	750	250	3/1	1.67	C & B
60	63.25	40	80	500	500	1/1	2	C & B
60	69.28	40	120	250	750	1/3	3	C & B

[a]A = 1, 2, 5 and 10 Hz for plasma and GTA per TekTran's LSC-300 Supply.

B = 1, 2, 10, 20, 30 and 40 Hz for GTA only per TT-150 Supply.

C = 1, 2, 5, and 10 Hz for plasma only per TekTran's LSC-300 Supply.

D = 1, 2, 5, 10, 20, 30 and 40 Hz for GTA only per TT-150 Supply.

TABLE V

LOW FREQUENCY OPERATING PULSE WELDING PARAMETERS FOR AN RMS CURRENT OF 50 AND 60 AMPERES

I_{av} (Amps)	I_{rms} (Amps)	I_B (Amps)	I_p (Amps)	Pulse Period (ms)		t_p/t_B	I_p/I_B	Frequency (Hz)[a]
				t_p	t_B			
45.6	50	10	57.45	750	250	3/1	5.745	D & E
43.86	50	10	60.86	666	333	2/1	6.086	D
40.0	50	10	70	500	500	1/1	7	D & E
35.13	50	10	85.48	333	666	1/2	8.548	D
32.13	50	10	98.5	250	750	1/3	9.85	D & E
47.42	50	20	56.56	750	250	3/1	2.828	D & E
46.35	50	20	59.6	666	333	2/1	2.874	D
43.91	50	20	67.82	500	500	1/1	3.202	D & E
40.59	50	20	81.9	333	666	1/2	4.095	D
38.45	50	20	93.8	250	750	1/3	4.690	D & E
48.81	50	30	55.08	750	250	3/1	1.836	D & E
48.27	50	30	57.48	666	333	3/1	1.916	D
47.02	50	30	64.03	500	500	1/1	2.134	D & E
45.14	50	30	75.55	333	666	1/2	2.518	D
43.86	50	30	85.44	250	750	1/3	2.848	D & E
42.74	50	10	63.33	614	386	1.59	6.33	A
31.04	50	10	90	263	737	.36	9	A
23.28	50	10	170	83	917	.09	17	A

TABLE V (continued)

I_{av} (Amps)	I_{rms} (Amps)	I_B (Amps)	I_p (Amps)	Pulse Period (ms) t_p	Pulse Period (ms) t_B	t_p/t_B	I_p/I_B	Frequency (Hz)[a]
46.24	50	20	60	656	344	1.91	3	A
41.0	50	20	80	350	650	.56	4	A
33.08	50	20	140	109	981	.12	7	A
48.46	50	30	56.67	692	308	2.25	1.89	A & B
46.0	50	30	70	400	600	.67	2.33	A & B
41.44	50	30	110	143	857	.17	3.67	A & B
54.3	60	20	73.3	644	356	1.81	3.67	C & B
46.6	60	20	100	333	666	.50	5.0	C & B
36.0	60	20	180	100	900	.11	9.0	C & B
57.0	60	30	70	675	325	2.08	2.33	C & B
52.5	60	30	90	375	625	.60	3.0	C & B
45.0	60	30	150	125	875	.14	5.0	C & B
58.7	60	40	66.7	702	298	2.36	1.67	C & B
56.7	60	40	80	417	583	.72	2.0	C & B
52.5	60	40	120	156	844	.19	3.0	C & B

[a]A = 1, 2, 5, and 10 Hz for Plasma & GTA per TekTran's LSC-300 Supply.

B = 1, 2, 5, 10, 20, 30 and 40 for GTA only per TT-150 Supply.

C = 1, 2, 5, and 10 Hz for Plasma per TekTran's LSC-300 Supply.

D = 1, 2, 5 and 10 Hz for Plasma per TekTran's LSC-300 Supply.

TABLE VI

HIGH FREQUENCY OPERATING PULSE WELDING PARAMETERS FOR AN AVERAGE CURRENT OF 60 AMPERES

I_{av} (Amps)	I_B (Amps)[a]	Frequency (KHz)	Pulse Period (μs)		t_p/t_B	Process[b]
			t_p	t_B		
60	H	2	333.3	166.7	2/1	P & G
60	H	2	250	250	1/1	P & G
60	H	2	166.7	333.3	1/2	P & G
60	H	10	66.7	33.3	2/1	P & G
60	H	10	50	50	1/1	P & G
60	H	10	33.3	66.7	1/2	P & G
60	H	20	33.38	16.67	2/1	P & G
60	H	20	25	25	1/1	P & G
60	H	20	16.67	33.33	1/2	P & G

[a]H = Initial weld level current or the background current level set at 20, 30, and 40 amperes. These were the nominal values for the actual values seen in Table IX.

[b]P = PAW process.

G = GTAW process.

TABLE VII

SUPERIMPOSED HIGH FREQUENCY ON LOW FREQUENCY PULSE PARAMETERS FOR A COMPOSITE AVERAGE CURRENT OF 60 AMPERES FOR THE GTAW PROCESS

Low Frequency				High Frequency			
I_B (Amps)	I_p (Amps)	Frequency (Hz)[a]	t_p/t_B	Amplitude (Amps)	Frequency (KHz)	t_p/t_B	Composite Av. Current (Amps)
20	40	F	1/1	30	2	1/1	60
20	40	F	1/1	30	10	1/1	60
20	40	F	1/1	30	20	1/1	60
20	60	F	1/1	20	2	1/1	60
20	60	F	1/1	20	10	1/1	60
20	60	F	1/1	20	20	1/1	60
20	80	F	1/1	10	2	1/1	60
20	80	F	1/1	10	10	1/1	60
20	80	F	1/1	10	20	1/1	60

[a]F = 1, 2, 5, 10 and 20 Hz for the GTAW process only.

investigation. The fixed parameters and their values are listed in Table III. The following pulse parameters were investigated:

Pulse Waveform. The square wave mode of pulse operation was selected for use in this study since it provides the simplest analysis of the influence of pulse variables. The pulse amplitudes and duration can be readily compared on the basis of both a pulse severity (I_p/I_B) and the energy input per pulse. The average current value is easily calculated as is the RMS and energy input. As the pulse shape varies from the square waveform, the direct comparison of pulse parameters becomes more difficult especially if a contrast between GTAW and PAW is attempted. It is recognized that the ability to pulse in the square wave mode is related to the amplitude and frequency of the waveform and the power supply type. The square response degenerates as the pulse amplitude and frequency increase. The characteristics of the wave form will be discussed in relation to the oscillograms obtained for each operational mode as the discussion of response and effect is developed later.

Pulse Time Ratios (t_p/t_B). Some authors have referred to the term (t_B/t_p = G) as "thermal severity" (40, 32) and others (7, 34, 36) referred to t_p/t_B as the "mark space ratio." In this discussion, the term t_p/t_B is referred to as the pulse time ratio. The pulse time ratios evaluated in this investigation were selected to span the range of the maximum and minimum values attainable within the welding power supply time and current response capability. The ratios used are listed in the data tables of IV through VII. Figure 12 represents

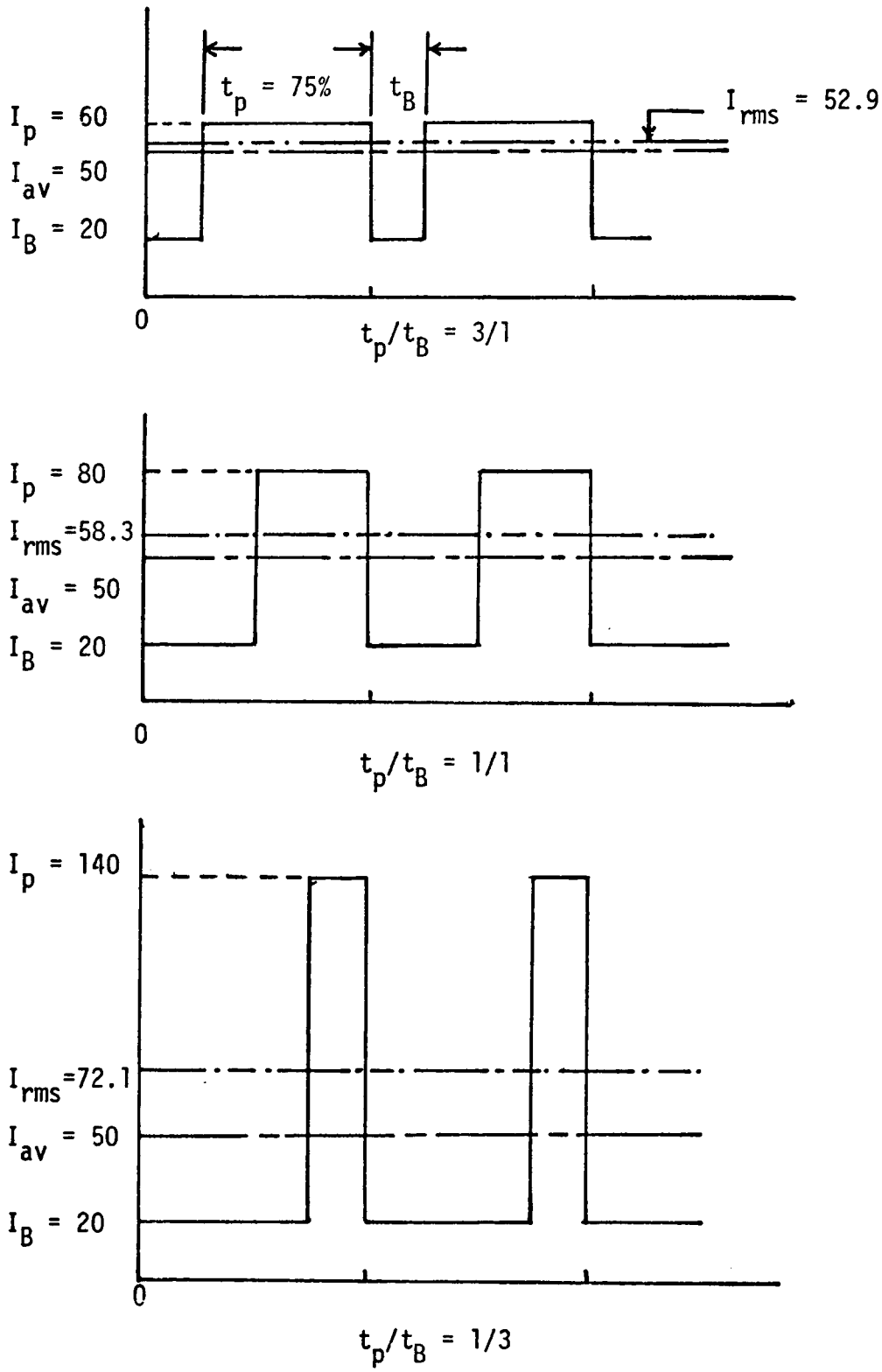


Figure 12. Varying Time Ratio Versus Peak Current for a Constant Average Current of 50 Amperes

a typical arrangement of the current-pulse time ratio used in this investigation for an average current of 50 amperes. Similar arrangements were used for the RMS pulsed current mode.

Weld Current Control. The approach taken in this investigation to evaluate the effect of varying weld current modes was as follows:

The constant current mode (I_c). Two values of 50 and 60 amperes of constant current mode of welding were chosen. Taken into consideration in arriving at these levels, was the material thickness and alloy type. The 50 amperes value was used for the melt-in mode and the 60 amperes were used for the full penetration mode of the plasma welding process. The same values were used with the GTAW process for comparison purposes. It should be noted that for the constant current mode of welding, the average current is equal to the RMS current and is also equal to the constant current.

The average pulsed current mode (I_{av}). The same current values of 50 and 60 amperes used for the constant current mode, were used for the average pulsed current mode. By using Equation (1), page 27, the peak currents were calculated for the given pulse time ratios and background currents as shown in Tables IV through VII. The corresponding values of the RMS current (I_{rms}) shown in Table IV were calculated by using Equation (3), page 30.

The RMS pulsed current mode (I_{rms}). The same current values of 50 and 60 amperes used for the constant current and average current modes were used for the RMS pulsed current mode also. Equation (3) was

used to calculate either the peak current values for the given pulse time ratios and background currents, or the pulse time ratios for the given peak and background currents. In this study both methods were considered and the calculated values of the peak currents and pulse time ratios are shown in Table V. The corresponding values of the average current shown in Table V were calculated by using Equation (1).

The pulse amplitude or the peak current (I_p). The pulse amplitudes or the peak current values used in this investigation were calculated for the given average current, RMS current and pulse time ratios to span the welding power supply rated output. Equations (1) and (3) were used. These values which ranged from a low of 57 amperes for the long duration pulse time ratio to 180 amperes for the short duration pulse time ratio are shown in Tables IV through VII.

The background current (I_B). In pulsed current welding processes, the principle is to keep the background current as low as possible for the maximum cooling effect. In this study, however, three values of background current, characterized as low, medium, and high relative to the average current, were used. Background currents of 10, 20, and 30 amperes were used with the 50 amperes average pulsed current and currents of 20, 30 and 40 amperes were used with the 60 amperes average pulsed current. The same background current settings were used for the RMS pulsed current mode of welding also.

The peak to background current ratio (I_p/I_B). Lundin and

Ruprecht (19), Smart and Pinfold (36) indicate that the process melting efficiency and the weld bead depth-to-width ratio for the pulsed current plasma welding process were enhanced at higher I_p/I_B current ratios for a given average current. Jackson (14) and Leitner and coworkers (17), on the other hand, have shown that an increased I_p/I_B current ratio for the GTAW process resulted in a decrease in the "process efficiency" with no tangible increase in the weld bead penetration. In this study, the influence of varying I_p/I_B current ratio was evaluated for both the GTAW and PAW processes under the results and discussion chapter of this thesis.

Pulse Frequency (Hz). Two ranges of pulse frequency were evaluated in this study--a low frequency range of one to forty Hz and a high frequency range of two to twenty kHz. In addition, a combined operation was evaluated where high frequency pulsing was superimposed on the low freqnecy wave form.

The low frequency pulsing of the plasma process was limited to one, two, five and ten Hz due to the plasma power supply response limitations. This will further be discussed in Chapter IV under power supply response characteristics section. For the GTAW process, however, frequencies of one, two, five, ten, twenty, thirty and forty Hz were evaluated since the power supply (TT-150 supply) used for making the appropriate welds has a faster response capability than does the plasma power supply (TekTran's LSC-300 supply). It should be noted that the TT-150 power supply used for making the GTA welds could not be used with the plasma welding system since the plasma arc voltage

is equal to and sometimes exceeds the open circuit voltage of the TT-150 power supply.

Welding conditions are shown in Tables IV and V for the low frequency pulsing and in Tables VI and VII for the high frequency pulsing and the superimposed high frequency on low frequency, respectively.

D. MEASURING TECHNIQUES

Longitudinal and transverse sections of the weld beads were cut, mounted, polished and etched to reveal the fusion and heat-affected zone microstructure. Marble's reagent (4g $CuSO_4$, 20ml HCl, 20ml H_2O) or cupric sulphate etchant was used. A calibrated filar eyepiece and a microscope were used to measure the dimensions of the fusion zone. A Lietz Orthoplan microscope with camera attachment was used to examine and record the fusion zone and HAZ microstructure.

CHAPTER IV

RESULTS AND DISCUSSION

A. INTRODUCTION

The majority of the work published on the pulsed-current GTA and plasma welding processes is descriptive in nature and fails to establish the optimum conditions for the pulse parameters investigated. This leaves many fundamental questions regarding the pulsed-current welding operation unanswered.

Unfortunately, the specific behavior of the welding power supply and that of the welding system in general is often neglected in assessing the importance of the various pulse parameters and the generalizations drawn are quite often relevant only to the system under study. This investigation seeks to completely document the process characteristics and to utilize the simplest pulse wave form available to enable straight forward analysis of the pulsed current mode of operation. To provide a basis for understanding, Section B gives a complete description of the response characteristics of the power supplies utilized.

B. WELDING POWER SUPPLY RESPONSE CHARACTERISTICS

General

The reported advantages of pulsing the welding current and the need for more repeatability and reliability in control of such welding processes as GMA, GTA and PAW has resulted in the introduction of a new

breed of fully transistorized welding power supplies. These supplies have the added capability of being programmable together with the ability to provide high pulse repetition rate response.

Generally, the square wave pulsed output is the most widely offered. Ideally, a power supply which is to provide a square wave should have minimum rise time. The voltage and current should rise with an infinite slope and the "sides" of the pulse should thus be vertical. No overshoot should be evident in the ideal form (Figures 11 and 13). In practice, however, the pulses will have "sloping sides" because of the finite rise time and fall time which is related to the LRC characteristics of the welding system. Figure 13 illustrates three typical pulse shapes exhibited by the power supplies used in this investigation and an ideal rectangular wave form as shown in Figure 13a. Figure 13b illustrates a typical rise and fall time phenomena. The 90 percent criteria has been applied in the electronics field to provide a basis for rise time and fall time measurements. The rise is normally faster than the fall time because the output is being driven during the on-time interval. When the pulse is terminated, the fall time is a primary characterization of the welding circuit behavior. Figure 13c shows a wave form with overshoot on both the leading and trailing edges. Overshoot often accompanies a pulse with a rapid rise time. All AC rectified power supplies have a ripple component indicative of the time frequency. In the case of three phase supplies, the ripple frequency is 360 Hz. The ripple is superimposed on the output wave form regardless of whether the supply is pulsed or not. Figure 13d shows the combined square pulse and ripple.

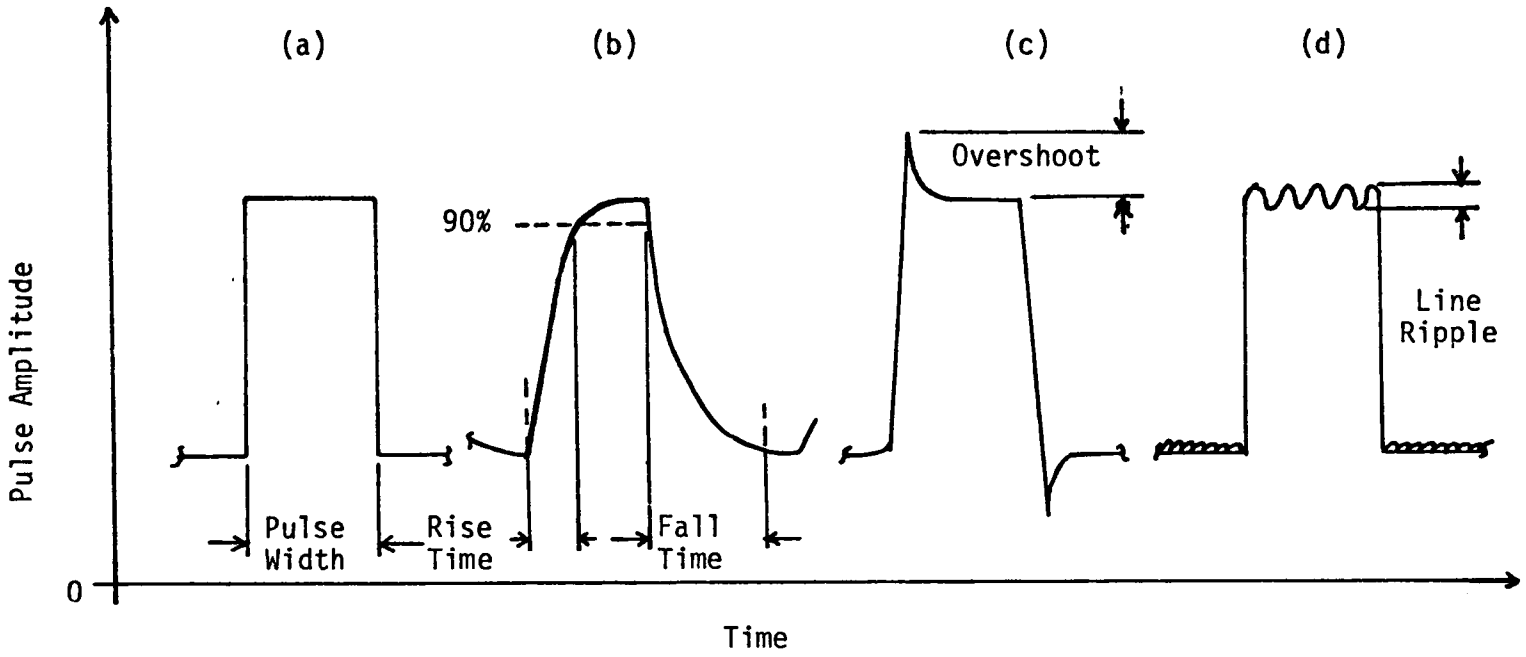


Figure 13. Schematic Pulse Wave Forms: (a) Ideal Rectangular, (b) Sloping Sides with Rise and Fall Times, (c) Overshoot, and (d) Rectangular Wave Form Showing Line Ripples Superimposed

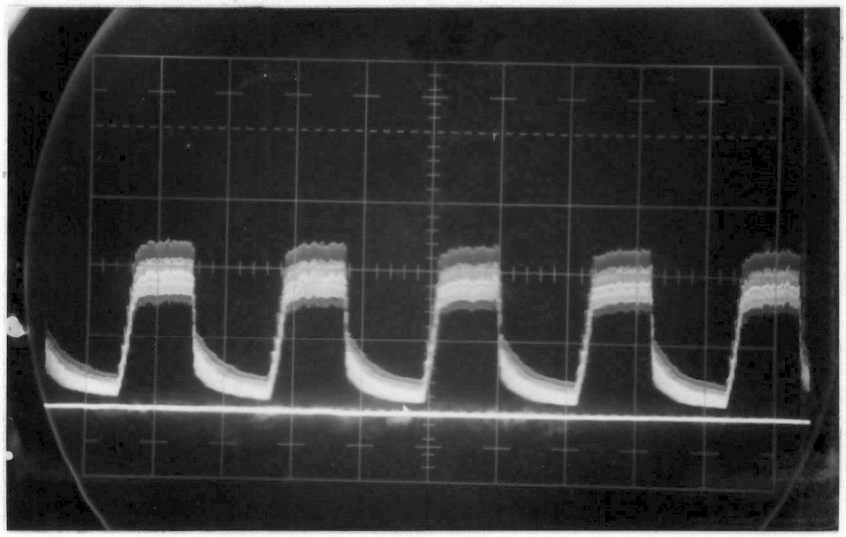
The pulse shape characteristics illustrated in Figure 13 are discussed for each power supply used in this investigation. It should be noted that all pulse wave forms for all weld settings evaluated were monitored and documented and were used to measure the actual values of the peak, background and average currents and voltage thus the energy input for each pulse. The actual and nominal values of such pulse parameters were documented and are shown on pages 65 and 99.

Low Frequency Pulsing Power Supplies

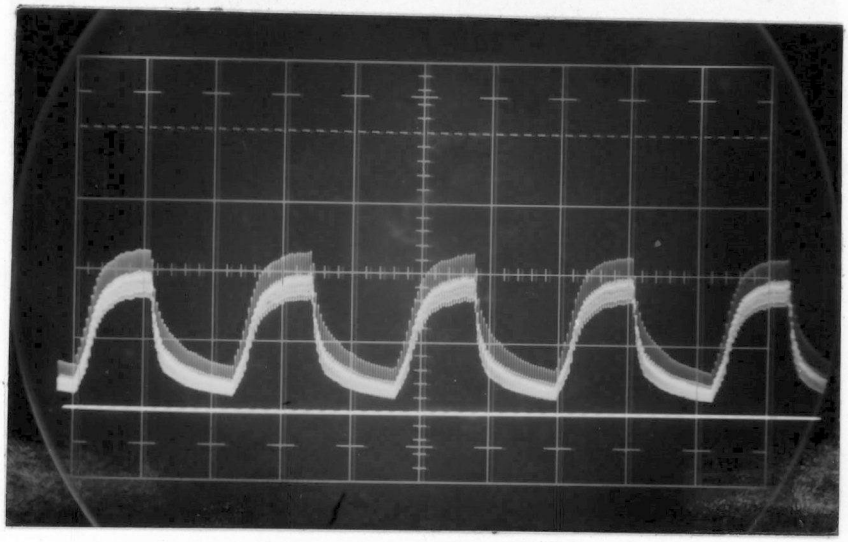
TekTran's LSC-300 Power Supply. This supply was used to produce all of the low frequency pulsed plasma welds and a portion of the GTA welds. The response characteristics varied slightly when operated in the plasma mode as compared to the GTA mode of operation. Figures 14a and 14b through 17a and 17b show oscillograms for the GTAW and PAW current wave forms pulsed at one, two, five and ten Hz respectively under the following conditions: I_p = 90 amperes, I_B = 10 amperes, t_p/t_B = 1/1 for an average current of 50 amperes. An inspection of these oscillograms shows the following:

1. The 360 Hz line ripple is readily seen superimposed on the pulsed current output wave form. It is also observed that the amplitude of the ripples is a function of the current level (Cf I_p and I_B).

2. In all of the oscillograms shown it is seen that the pulse rise and fall times constitute an appreciable part of the total pulse time. This becomes more apparent at pulse frequencies of five Hz which causes the square pulse wave form to degenerate into a saw-tooth wave form.

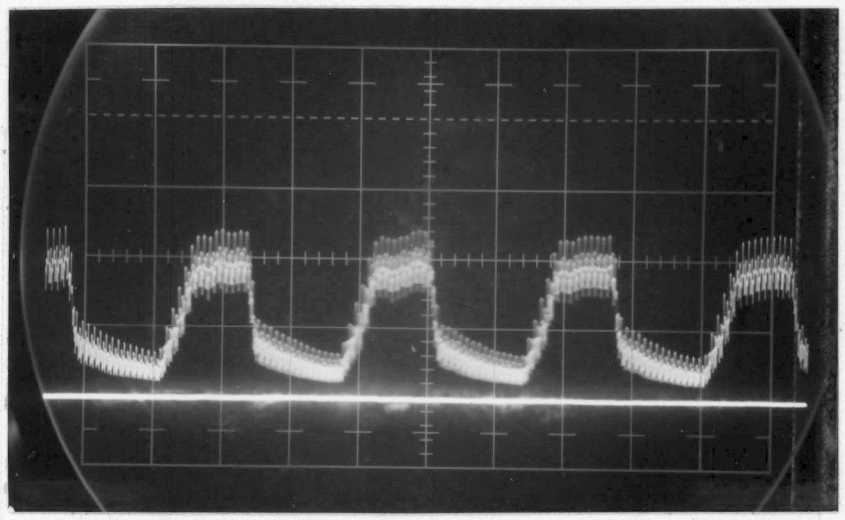


(a) One Hz GTA Pulse

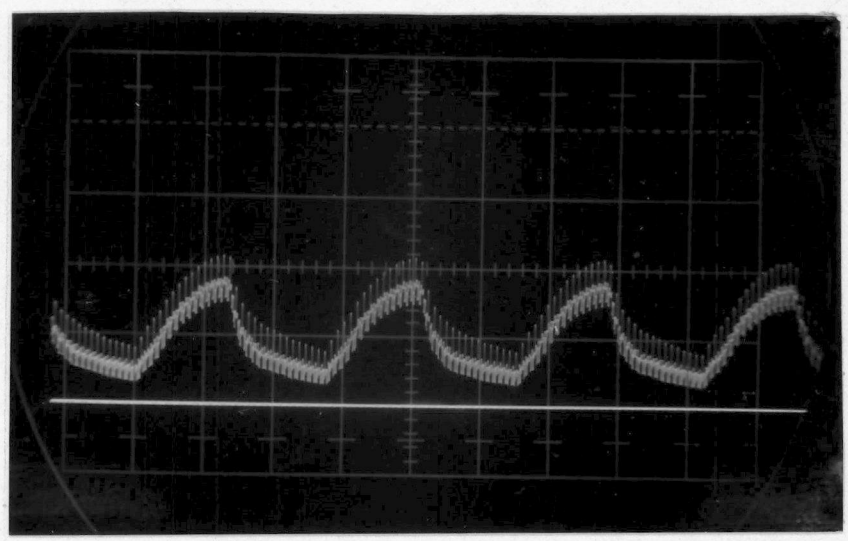


(b) One Hz Plasma Pulse

Figure 14. One Hz Pulsed Wave Forms: (a) GTAW and (b) PAW for Welding Conditions of I_p/I_B = 90/10 Amperes, t_p/t_B = 1/1 and I_{av} = 50 Amperes

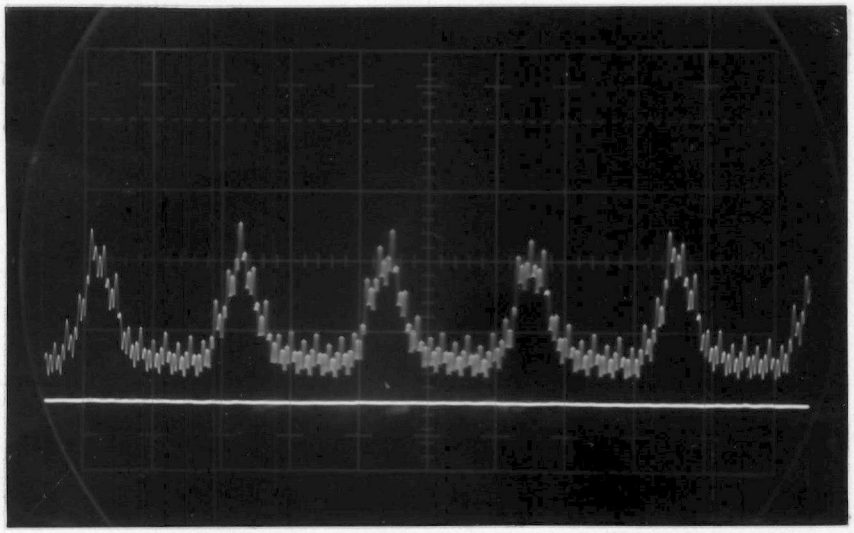


(a) Two Hz GTA Pulse

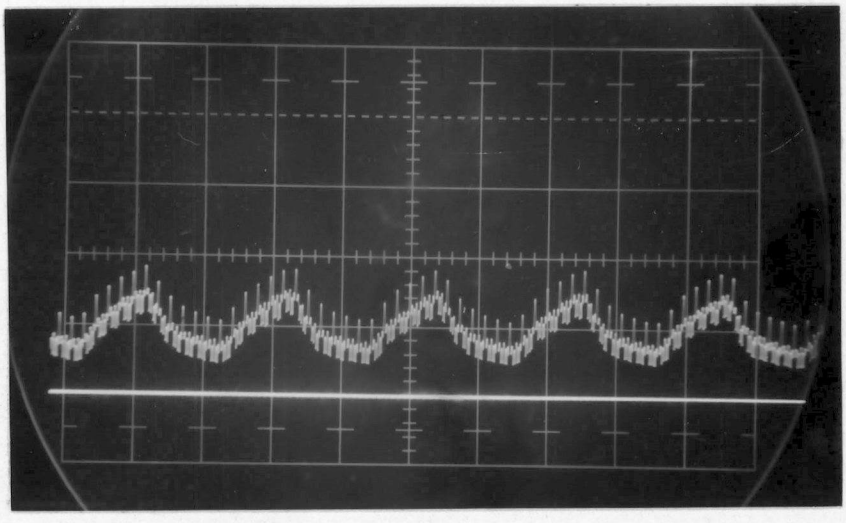


(b) Two Hz Plasma Pulse

Figure 15. Two Hz Pulsed Wave Forms: (a) GTAW and (b) PAW for Welding Conditions of I_p/I_B = 90/10 Amperes, t_p/t_B = 1/1 and I_{av} = 50 Amperes

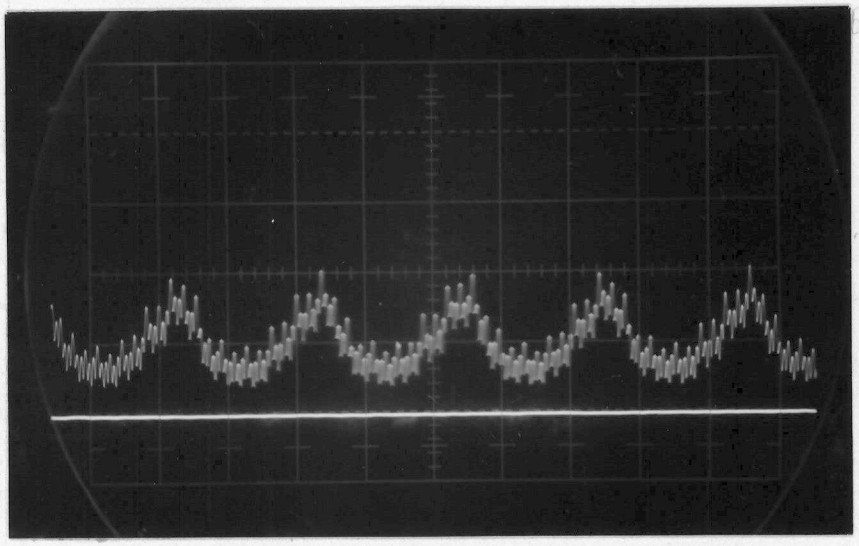


(a) Five Hz GTA Pulse

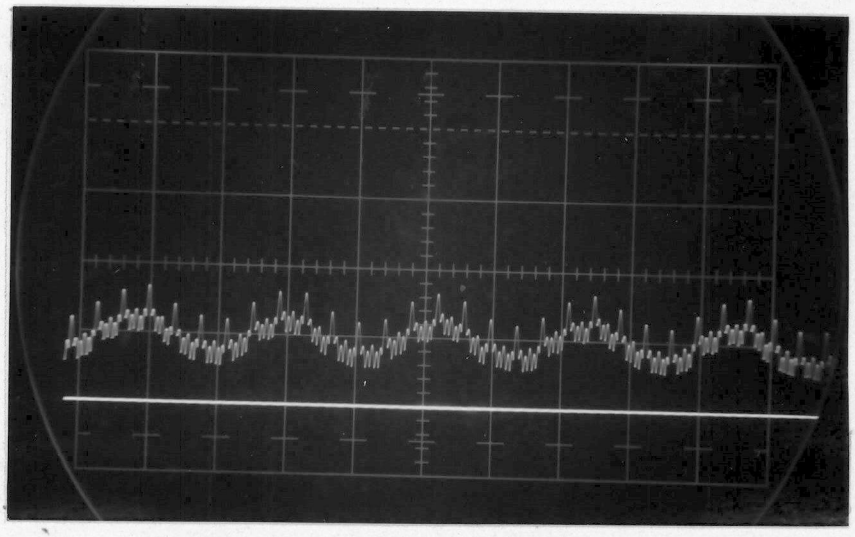


(b) Five Hz Plasma Pulse

Figure 16. Five Hz Pulsed Wave Forms (a) GTAW and (b) PAW for Welding Conditions of I_p/I_B = 90/10 Amperes, t_p/t_B = 1/1 and I_{av} = 50 Amperes



(a) Ten Hz GTA Pulse



(b) Ten Hz Plasma Pulse

Figure 17. Ten Hz Pulsed Wave Forms (a) GTAW and (b) PAW for Welding Conditions of I_p/I_B = 90/10 Amperes, t_p/t_B = 1/1 and I_{av} = 50 Amperes

3. Furthermore, in comparing the plasma wave forms to those of the GTA, it is easily seen that the plasma arc response is far more sluggish and degenerates at a lower frequency than does the GTA arc.

4. In spite of the wave form degeneration, the average current was maintained within $\pm$ 3 percent of its nominal value. It should be noted that the arc voltage wave form was identical to that of the current wave form variation and was in phase with the current wave form.

5. In general, the response characteristics of the LSC-300 supply as exhibited by the oscillograms shown can be schematically represented in Figure 18. At the lower frequency end the pulse is square and reaches the desired amplitudes; but as the frequency rises, the pulse amplitudes are not maintained and the wave form degenerates into a saw-tooth. However, the average current level is maintained.

TekTran's TT-150 Power Supply. Unlike the response of the LSC-300 supply which is controlled by a number of SCR's, the TT-150 supply is a fully transistorized supply and is equipped with fast response high and low frequency pulsers. An almost ideal square wave could be produced for a maximum pulse amplitude of 200 amperes at a 25 percent duty cucle or t_p/t_B = 1/3 and at pulse frequencies of up to 30 Hz. Above 30 Hz, however, and for high pulse amplitudes (above 100 amperes), the pulse became rounded in shape. Figure 19 shows four GTA current waveforms pulsed at five, ten, twenty and thirty Hz respectively for the welding conditions of I_p = 150 amperes, I_B = 30 amperes, t_p/t_B = 1/3 and I_{av} = 60 amperes. (It should be remembered that this power supply cannot be used with the plasma system since the plasma arc voltage is normally equal and sometimes exceeds the open circuit voltage of the

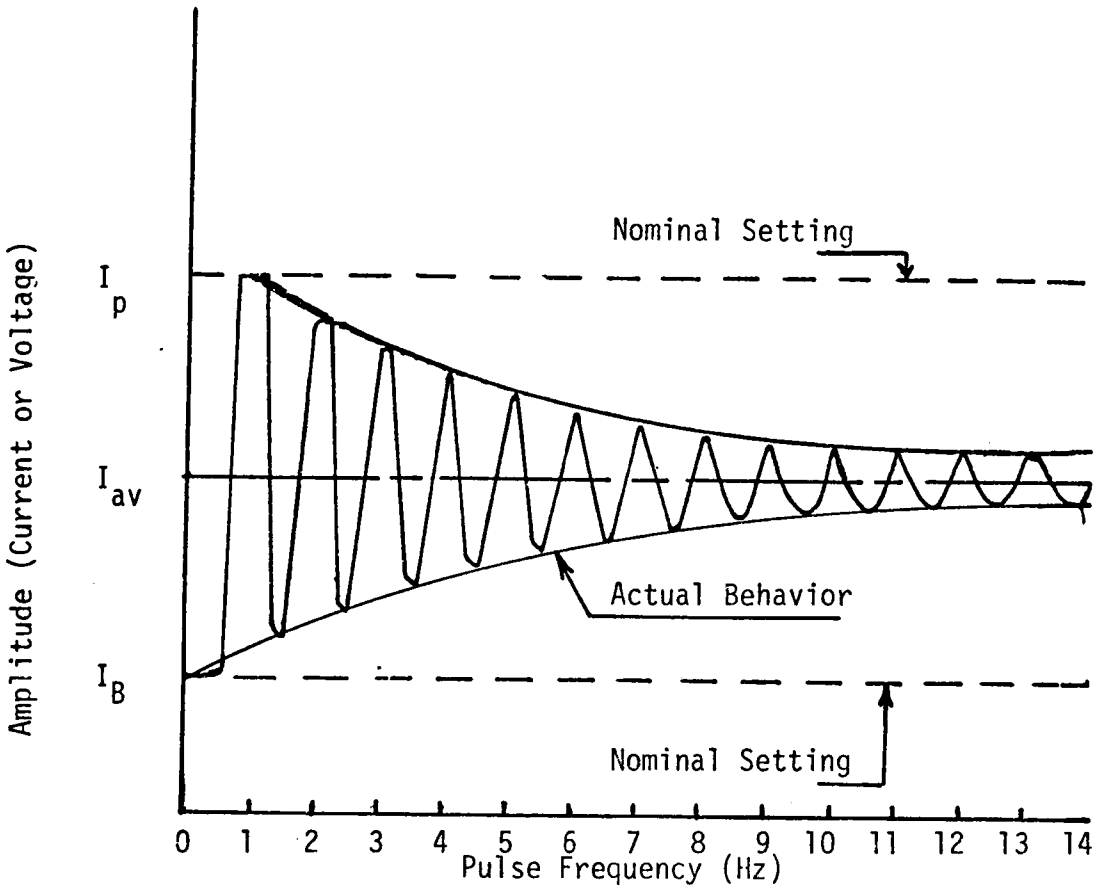
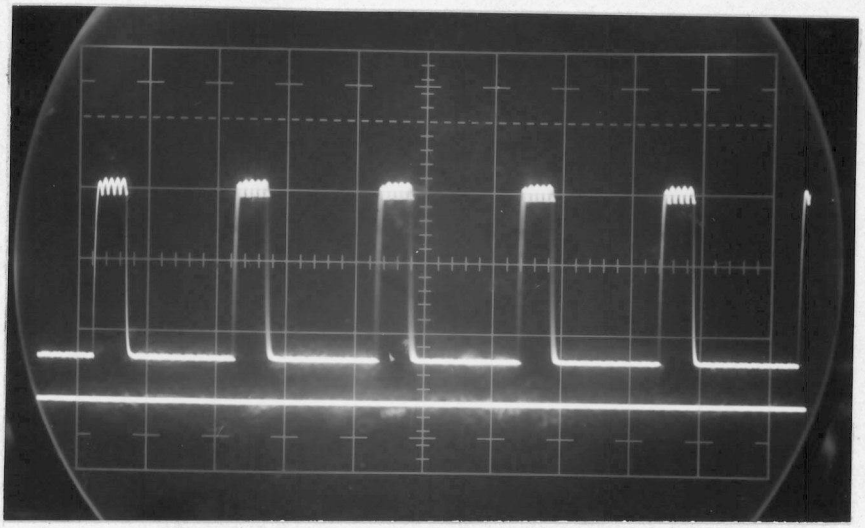
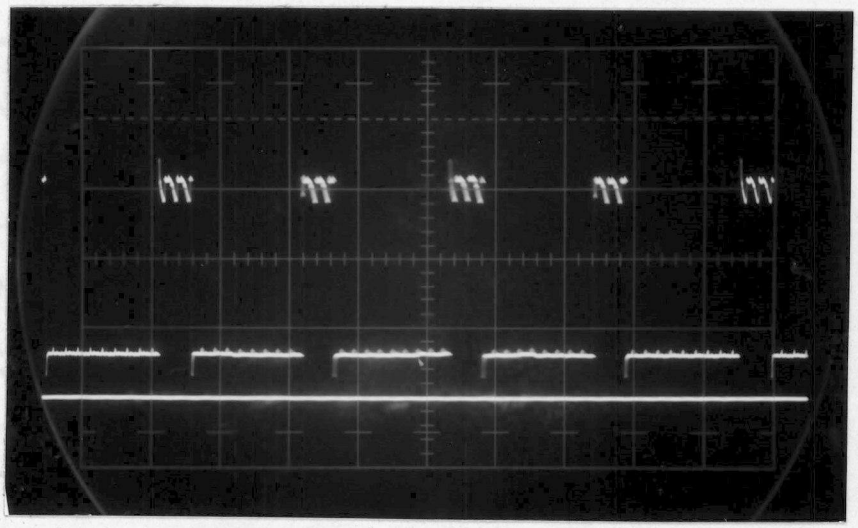


Figure 18. TekTran's LSC-300 Power Supply Response Characteristics, Pulse Amplitude Versus Pulse Frequency for t_p/t_B = 1/1

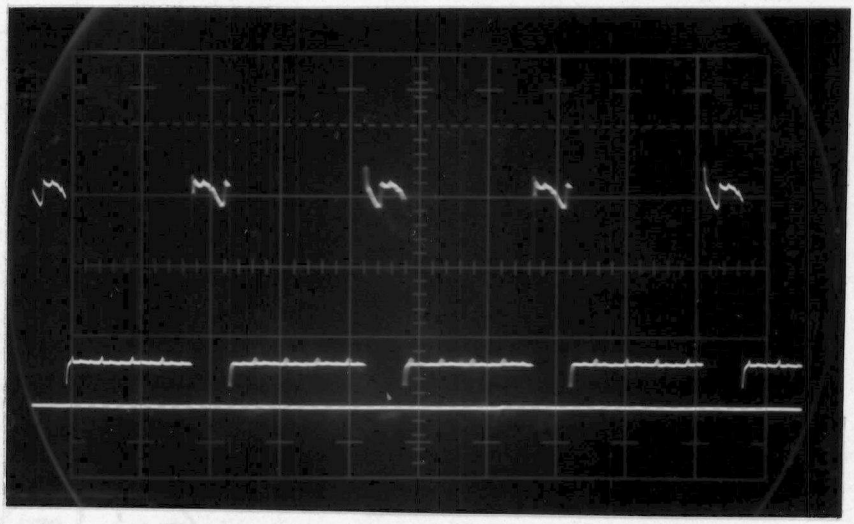


(a) Five Hz at .01 sec/cm

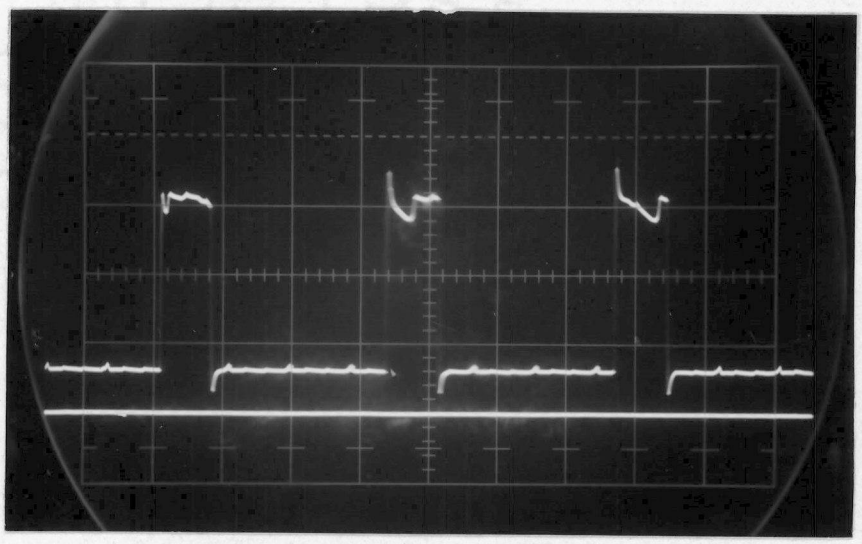


(b) Ten Hz at 50 ms/cm

Figure 19. Pulsed GTA Current Wave Forms Per TT-150 Welding Power Supply at I_P/I_B = 150/30 Amperes, t_p/t_B = 1/3 and I_{av} = 60 Amperes



(c) 20 Hz at 20 ms/cm



(d) 30 Hz at 10 ms/cm

Figure 19. (continued)

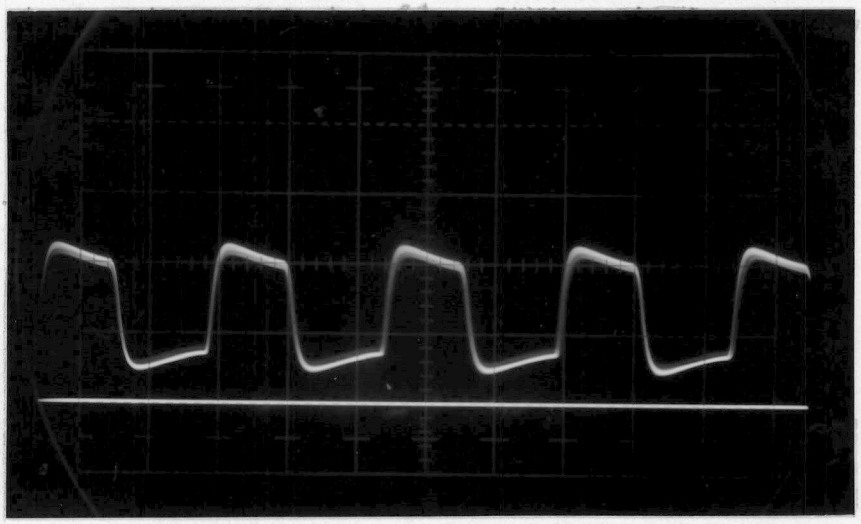
TT-150 supply which is 25 VDC).

It is noteworthy that the line ripples seen superimposed on the wave forms of the output of this supply are much smaller than those in the LSC-300 supply wave forms especially the background pulse ripples. The current wave form overshoot phenomena is readily seen for pulse frequencies of ten Hz and above.

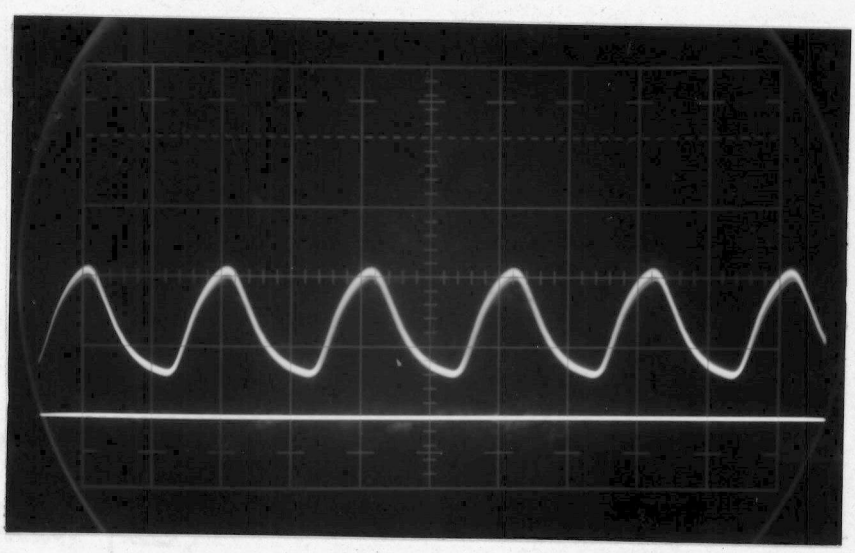
High Frequency Pulsing Power Supplies

TekTran's TT-150 Power Supply. This power supply has the capability of pulsing the welding arc at high frequencies of two to twenty kHz. Frequencies evaluated in this study were two, ten and twenty kHz for pulse time ratios of t_p/t_B = 2/1, 1/1, and 1/2 and for an average current of 60 amperes. Figure 20 shows three current wave forms pulsed at two, ten and twenty kHz for the pulse time ratio of t_p/t_B=1/1. As seen from the oscillograms, the response characteristics of this supply for the high frequency pulsing resembles to some degree that of TekTran's LSC-300 low frequency power supply. At two kHz the wave form is essentially square. At ten kHz the wave form has a saw-tooth appearance but still maintains the amplitude. At 20 kHz the saw-tooth wave form is degraded to the point where the amplitude reached is significantly different than that desired. Similar behavior is experienced by the arc voltage as seen in Figure 21 which shows voltage oscillographs of two and ten kHz for an average current of 60 amperes pulsed at t_p/t_B = 1/1.

Merrick Engineering (TXR-200) Power Supply. This unit has a high frequency pulsing capability of two to thirty kHz. Many calibration problems were encountered that made it extremely difficult to analyze

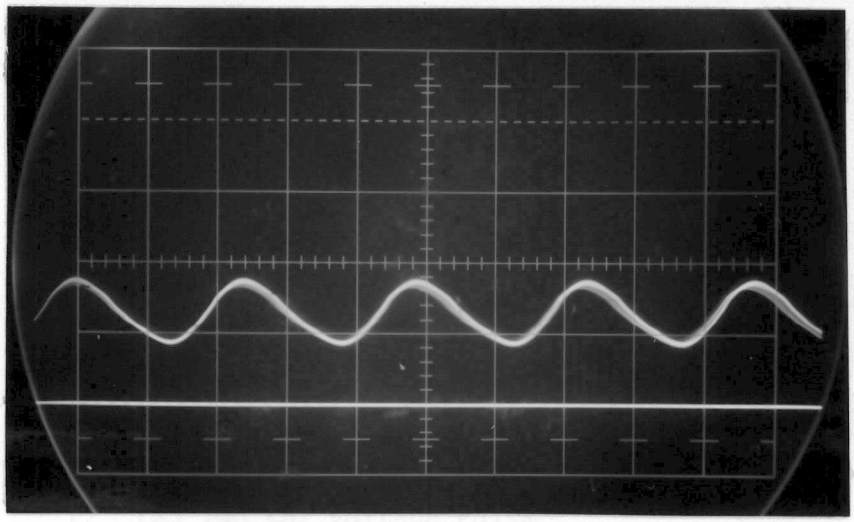


(a) Two KHz Current Pulse



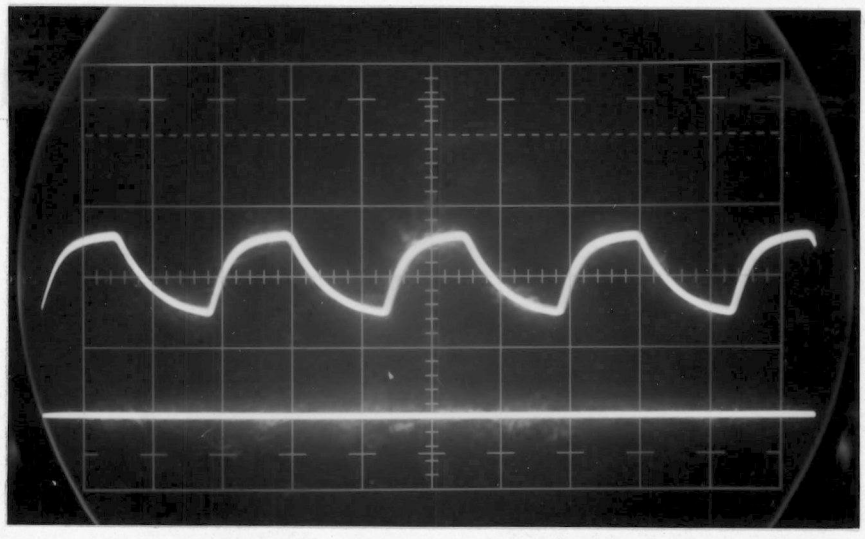
(b) Ten KHz Current Pulse

Figure 20. High Frequency Pulsed GTA Current Wave Forms at t_p/t_B = 1/1 and I_{av} = 60 Amperes, I_B = 40 Amperes (TT-150 Supply)

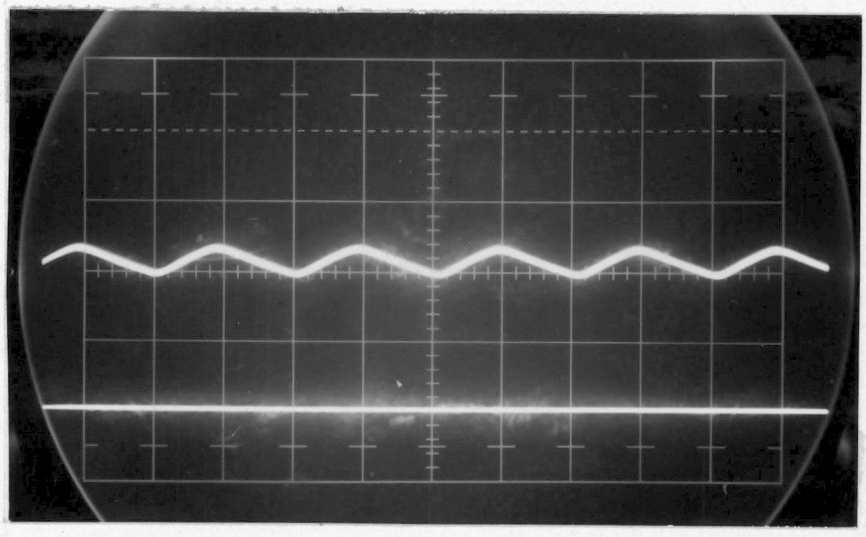


(c) Twenty KHz Current Pulse

Figure 20. (continued)



(a) Two KHz Voltage Pulse



(b) Ten KHz Voltage Pulse

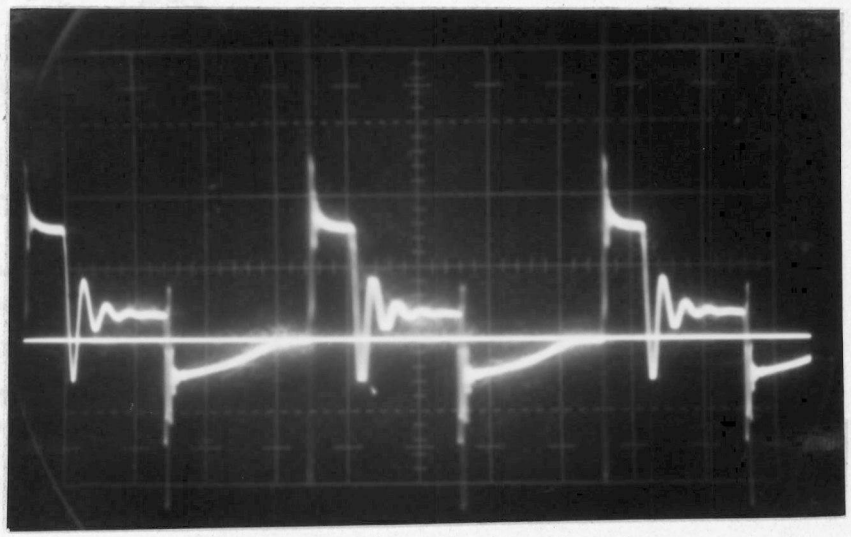
Figure 21. High Frequency Pulsed GTA Arc Voltage Wave Forms (a) Two KHz and (b) Ten KHz for I_{av} = 60 Amperes at t_p/t_B = 1/1 (TT-150 Supply)

the response characteristics of this supply. Neither the pulse time ratios nor the pulse peak and background levels could be adequately monitored. Unexplained sharp current reversals were experienced for all pulsing conditions evaluated in this study. Figure 22a, b, and c shows three typical oscillograms of GTA current wave forms pulsed at two, ten and twenty kHz respectively for a t_p/t_B = 1/1 and an average current of 60 amperes. In comparing these oscillograms with those shown in Figure 20 for the TT-150 supply pulsed under the same conditions, it is seen that while the pulse time ratios of t_p/t_B = 1/1 was not achieved by the Merrick Supply, its output wave forms have a faster response time than that of the TT-150 supply. Thus the Merrick Supply displayed a squarer wave form and did not degenerate to a saw-tooth as did the TT-150 wave form at pulse frequencies above ten kHz.

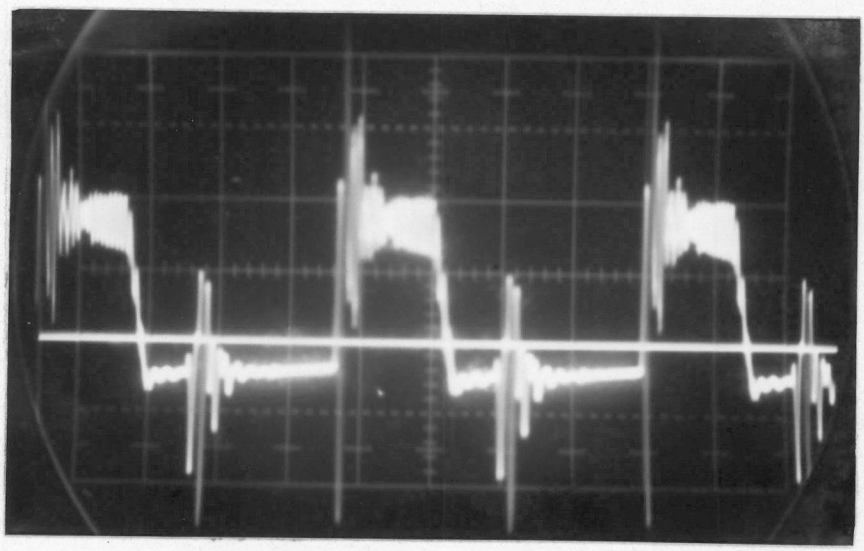
The average current for all welds made with the Merrick Supply was monitored on the machine ammeter as well as with a clip-on ammeter surrounding the welding cable.

High Frequency Superimposed on Low Frequency Pulsing Power Supplies

Tektran's TT-150 Power Supply. The TT-150 power supply features the capability of producing both the high and low frequency pulsing simultaneously. This capability was utilized and Figure 23 shows a representative GTA oscillogram for a pulse frequency of two kHz superimposed on a low frequency of ten Hz (t_p/t_B = 1/1) for an average current of 60 amperes.

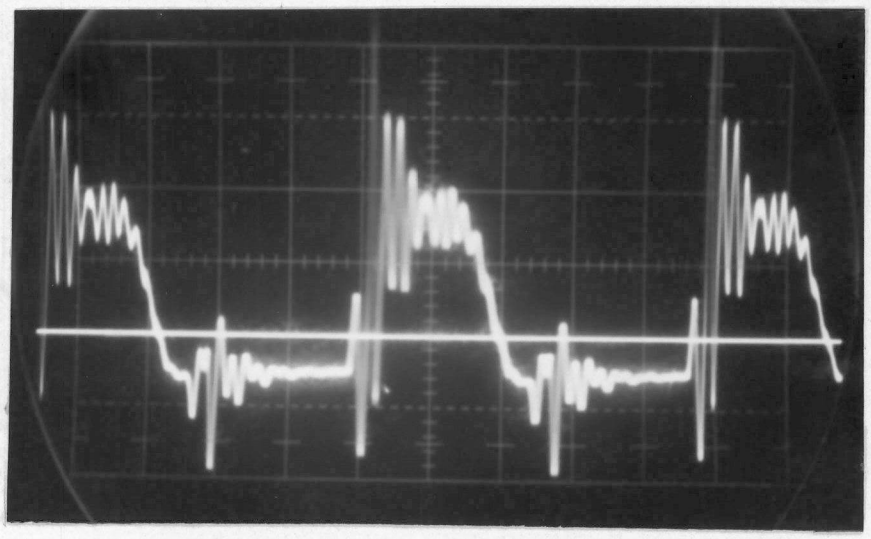


(a) Two KHz Current Pulse at 0.1 ms/cm



(b) Ten KHz Current Pulse at 20 ms/cm

Figure 22. High Frequency Pulsed GTA Current Wave Forms Per Merrick Engineering Supply (TXR-200) at I_{av} = 60 Amperes and t_p/t_B = 1/1



(c) Twenty KHz Current Pulse at 10μ sec/cm

Figure 22. (continued)

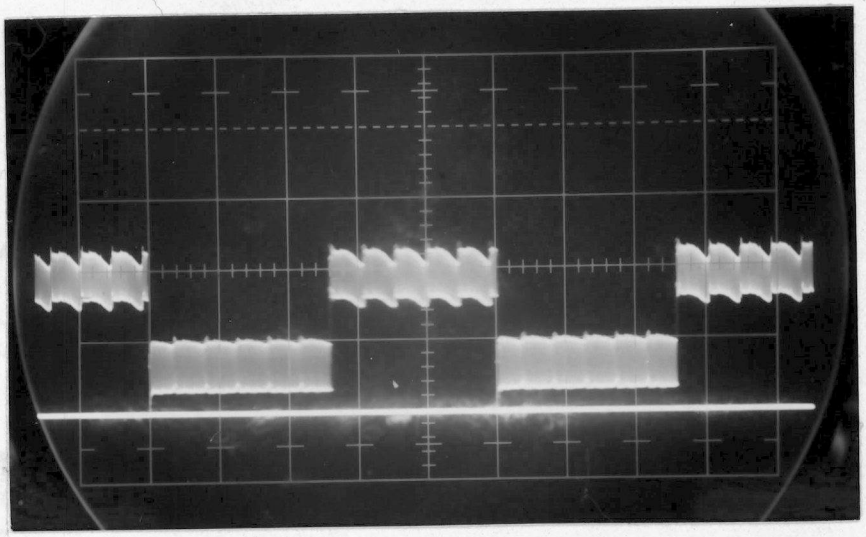


Figure 23. Superimposed High Frequency on Low Frequency GTA Current Wave Form; High Frequency = Two KHz, Low Frequency = Ten Hz; $\frac{I_{amp}/\text{Hi-Freq}}{I_{av}/\text{Lo-Freq.}} = \frac{10}{50}$; and $t_p/t_B = 1/1$

C. PULSED PLASMA ARC WELDING PROCESS

Results

Low Frequency Pulsed Plasma Welds (Melt-In Mode). In analyzing the macroscopic features of each of the welds made, primary considerations were given to the effect of the different pulse settings on the weld bead geometry such as depth, width, the transverse cross-sectional area, depth-to-width ratio and the root uniformity. Equal considerations were given to the overall macroscopic quality and appearance of each weld. A good quality weld bead is one that is free of undercuts, sagging, crater cracks and exhibits uniform penetration.

Due to the response characteristics of the power supply used in this investigation, it should be noted that all values of I_B, I_p and I_{rms} shown in the following six figures are the nominal set values which are valid only for the pulse setting of one Hz. The actual values of the current levels were measured from the oscillograms and are listed in Table VIII for each pulse frequency. It should also be noted, however, that the average current remained essentially the same regardless of the variations experienced in the pulse amplitude and background current levels.

Figure 24 shows the effect of varying the RMS current, the peak current, and the pulse time ratio (t_p/t_B) on the weld bead depth and cross-sectional area for an average current of 50 amperes and a background current of 20 amperes. It is easily seen that the increase in the weld bead depth and cross-sectional area is a function of an increase in the peak current, I_p, and concurrently the increase in the

TABLE VIII

NOMINAL AND ACTUAL CURRENT VALUES AND MEASURED ARC VOLTAGE AND THE ASSOCIATED CALCULATED ENERGY INPUTS FOR THE WELDING CONDITIONS LISTED IN TABLE IV FOR THE PLASMA PROCESS

Pulse Frequency (Hz)	Time Ratio (t_p/t_B)	I_B (Amps)		I_p (Amps)		I_{av} (Amps)		I_{RMS} (Amps)		Arc Voltage		Energy Input
		Nominal	Actual	Nominal	Actual	Nominal	Actual	Nominal	Actual	Lo	Hi	$(kJ/in)^m$
1	3/1	10	20	63.33	65	50	51	55	57	17	22	17.363
2	3/1	10	25	63.33	62	50	50	55	55	18.5	21	16.382
5	3/1	10	30	63.33	60	50	50	55	54	18.5	21	16.256
10	3/1	10	40	63.33	55	50	50	55	51.7	20	21	15.994
1	1/1	10	20	90	90	50	51	64	65.2	17	24	18.750
2	1/1	10	25	90	85	50	50	64	62.2	18	22.5	17.719
5	1/1	10	30	90	72	50	50	64	55.2	19	21.5	15.563
10	1/1	10	40	90	60	50	50	64	51.0	19.5	20.5	15.075
1	1/3	10	20	170	165	50	53	85.4	84.4	16.5	26	20.288
2	1/3	10	25	170	135	50	51	85.4	70.9	17.5	24	17.072
5	1/3	10	30	170	100	50	50	85.4	56.4	18.5	21.5	14.723
10	1/3	10	40	170	80	50	50	85.4	53.0	19.5	20.5	14.925
1	3/1	20	30	60	60	50	51	52.9	54	18	22	16.875
2	3/1	20	35	60	58	50	51	52.9	53.2	19	21.5	16.523
5	3/1	20	40	60	55	50	50	52.9	51.7	19.5	20.5	14.456
10	3/1	20	45	60	55	50	51	52.9	52.7	19.5	20.5	15.975

TABLE VIII (continued)

Pulse Frequency (Hz)	Time Ratio (t_p/t_B)	I_B (Amps)		I_p (Amps)		I_{av} (Amps)		I_{RMS} (Amps)		Arc Voltage		Energy Input (kJ/in)[m]
		Nominal	Actual	Nominal	Actual	Nominal	Actual	Nominal	Actual	Lo	Hi	
1	1/1	20	30	80	80	50	52	58.3	60.4	17.5	22.5	17.438
2	1/1	20	35	80	75	50	52	58.3	58.5	18	22	17.100
5	1/1	20	38	80	65	50	52	58.3	53.2	18.5	21	15.510
10	1/1	20	40	80	60	50	50	58.3	51	19	20.5	14.925
1	1/3	20	25	140	140	50	52	72.1	73.3	17	25	17.906
2	1/3	20	30	140	120	50	51	72.1	65.4	17.5	23.5	16.481
5	1/3	20	38	140	85	50	50	72.1	54	18	21.5	14.548
10	1/3	20	42	140	70	50	49	72.1	50.5	18.5	20.5	14.123
1	3/1	30	35	56.67	57	50	51	51.3	52.4	17.5	20.5	15.443
2	3/1	30	42	56.67	55	50	52	51.3	52.1	18.5	20	15,289
5	3/1	30	45	56.67	55	50	52	51.3	52.7	19	19.5	15.272
10	3/1	30	48	56.67	52	50	51	51.3	51	19.5	19.5	14.918
1	1/1	30	35	70	70	50	51	53.85	55.3	17.5	21.5	15.881
2	1/1	30	38	70	70	50	51	53.85	56.3	18	21	16.155
5	1/1	30	42	70	65	50	50	53.85	54.7	18.5	20.5	15.821
10	1/1	30	45	70	55	50	50	53.85	56	19	20	14.663
1	1/3	30	30	110	110	50	50	61	61	19	24.5	16.519
2	1/3	30	35	110	100	50	50	61	58.5	19.5	23.5	16.491
5	1/3	30	40	110	75	50	50	61	51.1	19.8	22.0	15.098
10	1/3	30	45	110	65	50	48	61	50.7	20.0	21.5	15.124

[m] kJ/in = kilojoules per inch.

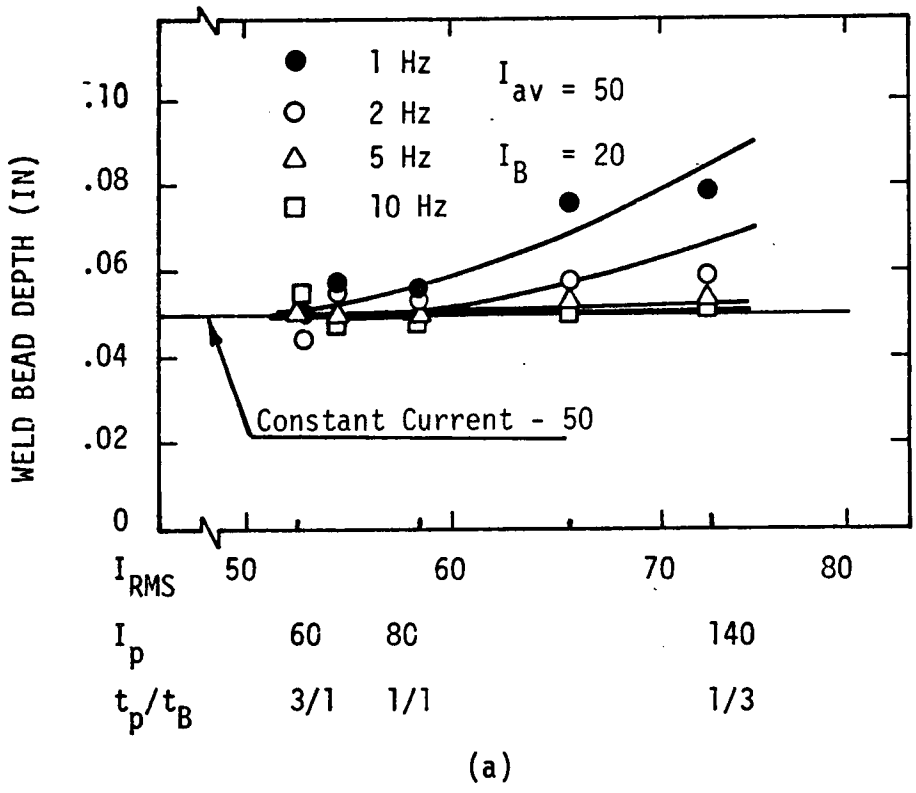
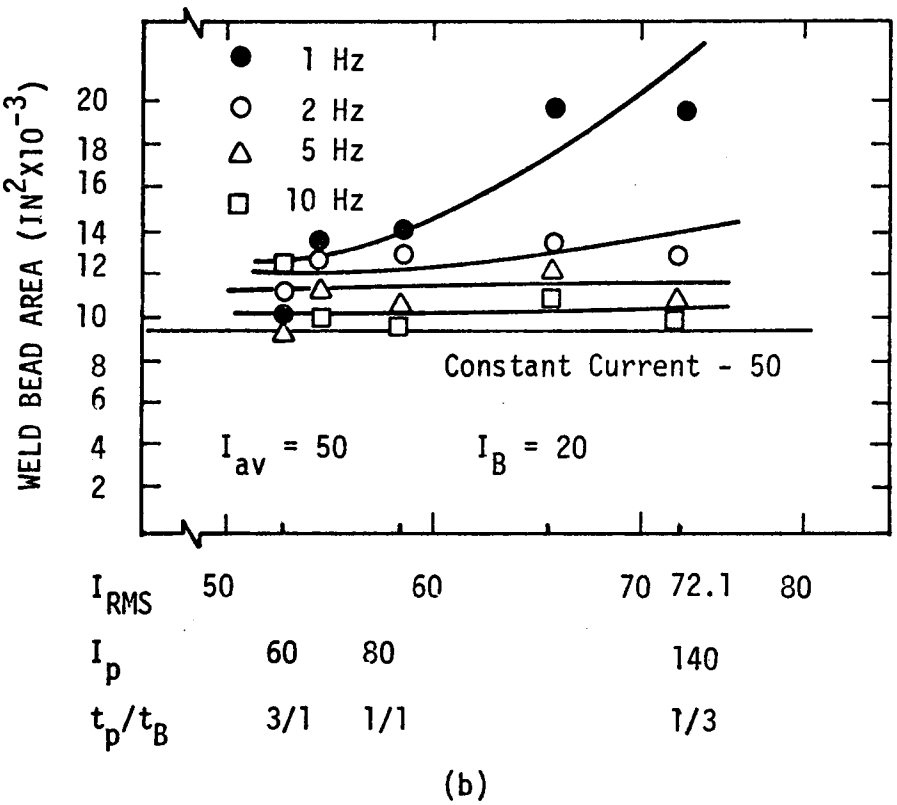


Figure 24. Effect of Low Frequency Pulsed PAW on (a) Weld Penetration and (b) Weld Fused Area for an Average Current of 50 Amperes at Varying I_{RMS}, I_p and t_p/t_B Values at I_B = 20 Amperes



(b)

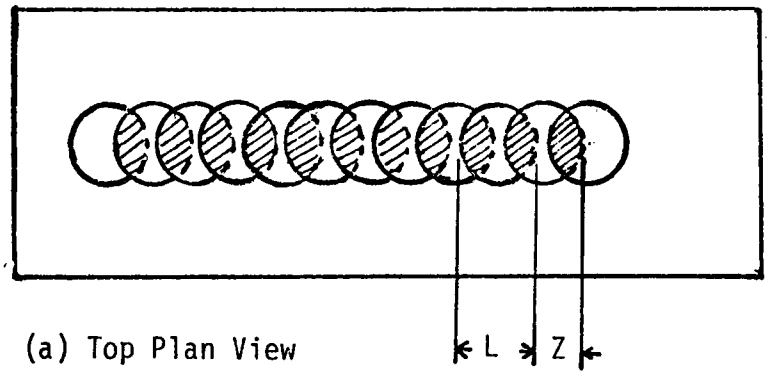
Figure 24. (continued)

RMS current. For the pulse frequencies of five and ten Hz, however, the peak current never reached its nominal value and thus the increase in either the weld bead depth or cross-sectional area is not observed. This observation testifies to the importance of the peak current in the pulsed welding operation of the plasma arc. One has to expect, however, that even if the peak current reaches its nominal value at all settings of pulse frequency, a decrease in the weld bead penetration and cross-sectional area will be experienced as the pulse frequency is increased. This fact is not attested to the plasma data presented, but is evident in the pulsed GTA operation where the peak currents were attained and the square wave response was maintained (the plasma operation has an inherent interia effect as compared to GTA). (See pages 87-88, 91-92, 96, and 97.)

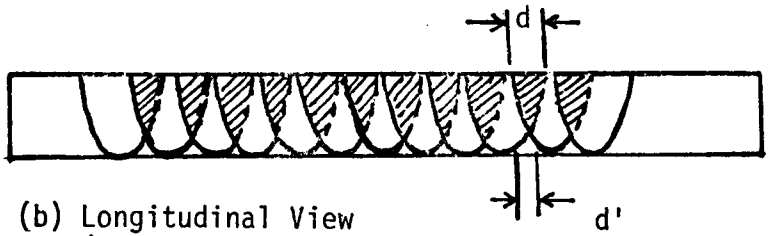
From the results shown in Figure 24 it is evident that the maximum weld penetration and melting efficiency (as reflected by the weld bead area) are obtained at a pulse frequency of one Hz. However, a major disadvantage of pulsing the welding arc at low rates is the tendency to lose overlap in the individual spots produced (see Figure 25). The minimum weld spot overlap distance producing a uniform root appears to be the most desirable from the solidification control standpoint and will also tend to produce the narrowest HAZ.

The degree of the weld bead spot overlapping is controlled by four parameters. These parameters are:

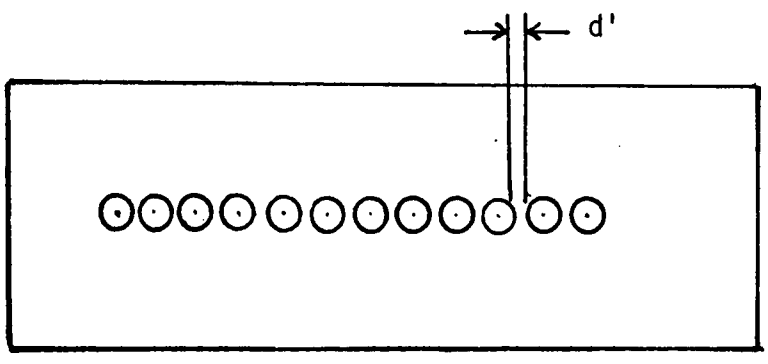
1. The pulse duration t_p or the pulse time ratio t_p/t_B--the longer the pulse duration, the greater is the degree of the weld spot overlapping.



(a) Top Plan View



(b) Longitudinal View
(Side Cross-Section)



(c) Underbead View

Figure 25. Typical One Hz Pulse Weld Bead Spot Overlapping

2. The pulse amplitude or the peak current (I_p)--an increase in the pulse amplitude, or the peak current, leads to an increase in the weld spot overlapping distance d. This is due to the increase in energy input per unit length which increases the size of the weld pool thus increasing the degree of overlapping.

3. The pulse frequency--The higher the pulse frequency, the greater the degree of weld spot overlapping. This, however, may result in a more extensive HAZ and enhanced grain growth.

4. The welding speed (S)--with other parameters held constant, the higher the welding speed, the smaller the degree of weld spot overlapping becomes and the lower the welding speed, the greater is the degree of the weld spot overlapping. This is due to a direct decrease or increase of the energy input per unit length upon varying the welding speed. By definition the energy input (E.I.) per unit length for a constant current welding operation is given as:

$$E.I. = \frac{V \times I_c \times 60}{S} \quad \text{Joules/In.} \qquad (6)$$

where V is the arc voltage and I_c is the arc current. When pulsing the arc, however, the above equation becomes:

$$E.I. = \frac{(V_B I_B t_B + V_p I_p t_p) \times 60}{St} \quad \text{Joules/In.} \qquad (7)$$

where V_B, I_B and t_B are the background voltage, current and duration time, and V_p, I_p and t_p are the peak voltage, current and pulse duration time respectively. "t" is the time of one pulse cycle.

Thus by reducing the welding speed, the energy input per unit length will increase which leads to the growth of the weld pool thus increasing the degree of the weld spot overlapping. Here again, excessive energy input could lead to heat build up which causes weld burn through, undercuts, sagging and cracking.

Figure 26 shows the effect of varying peak and background currents on the weld bead depth and cross-sectional area for an average current of 50 amperes and a pulse time ratio of t_p/t_B = 1/1. A potentially important result is easily observed in this figure; where at a background current setting of 30 amperes an increases of 75% in the weld bead penetration and area is experienced when comapred to those welds made with a background current setting of ten amperes. It should be further noted that as the background current level is increased, the peak current level is decreased for the same average current. Similar results are also observed in Figure 27 where the peak current, the background current and the pulse time ratio were varied for a pulse frequency of one Hz and an average current of 50 amperes.

By direct measurement of the pulsed arc voltages and currents and by using Equation (7), page 71, the energy input for each weld was calculated and plotted as shown in Figure 28. Carefully note that the energy input for the background current level of 30 amperes is significantly less than that at lower background current for the same average current of 50 amperes. Thus the optimum weld macroscopic properties and optimum utilization of the energy input appears to be achieved at a background current of a melting magnitude for the given welding conditions. This is not to suggest that by increasing

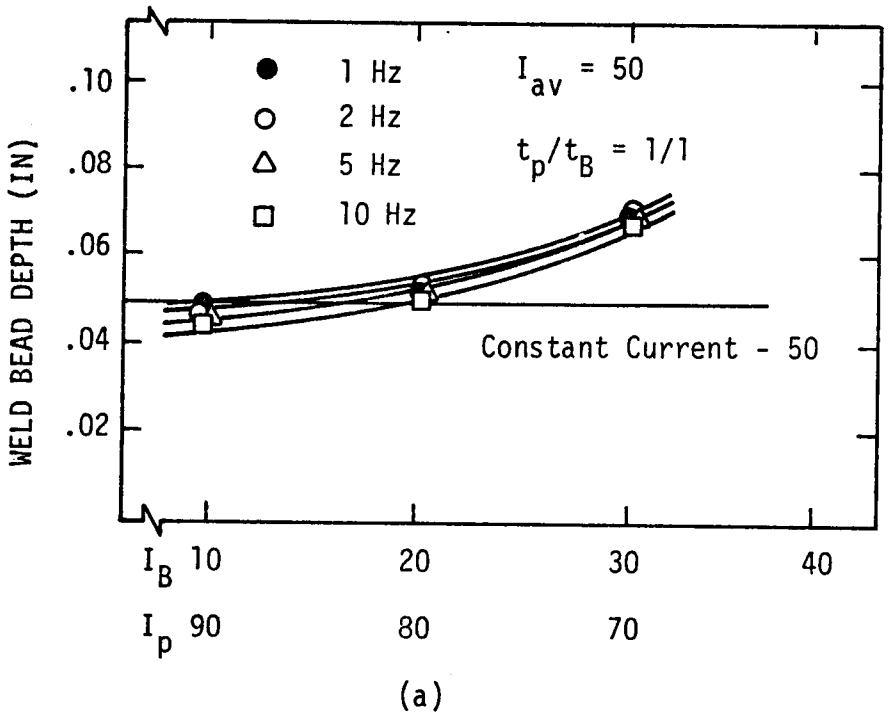
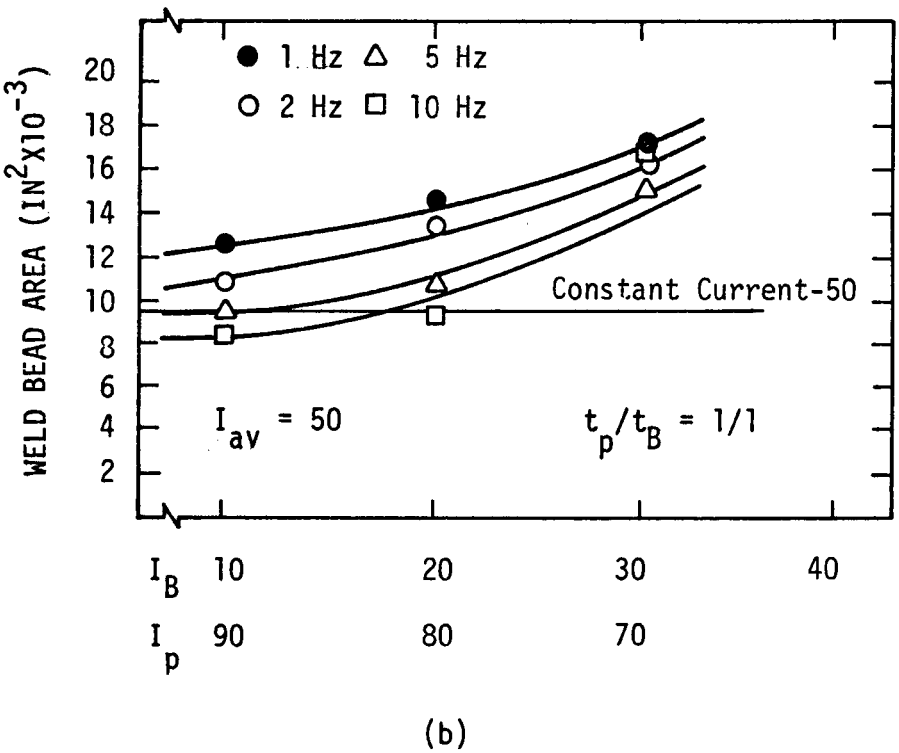


Figure 26. Effect of Low Frequency Pulsed PAW on (a) Weld Penetration and (b) Weld Fused Area for an Average Current of 50 Amperes and a t_p/t_B = 1/1 Pulsed at Varying I_p, I_B and I_{RMS} Values



(b)

Figure 26. (continued)

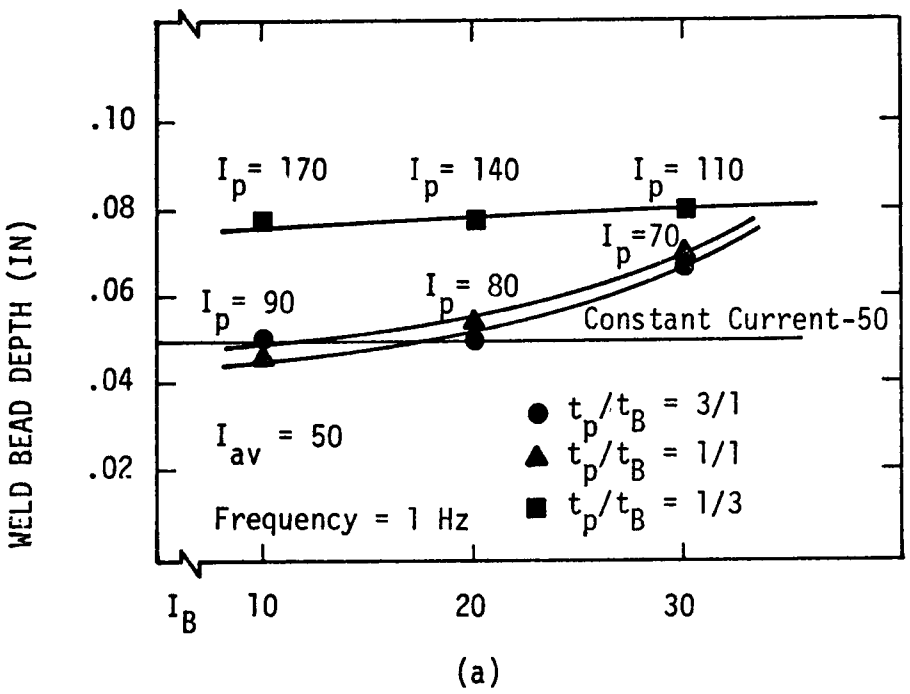
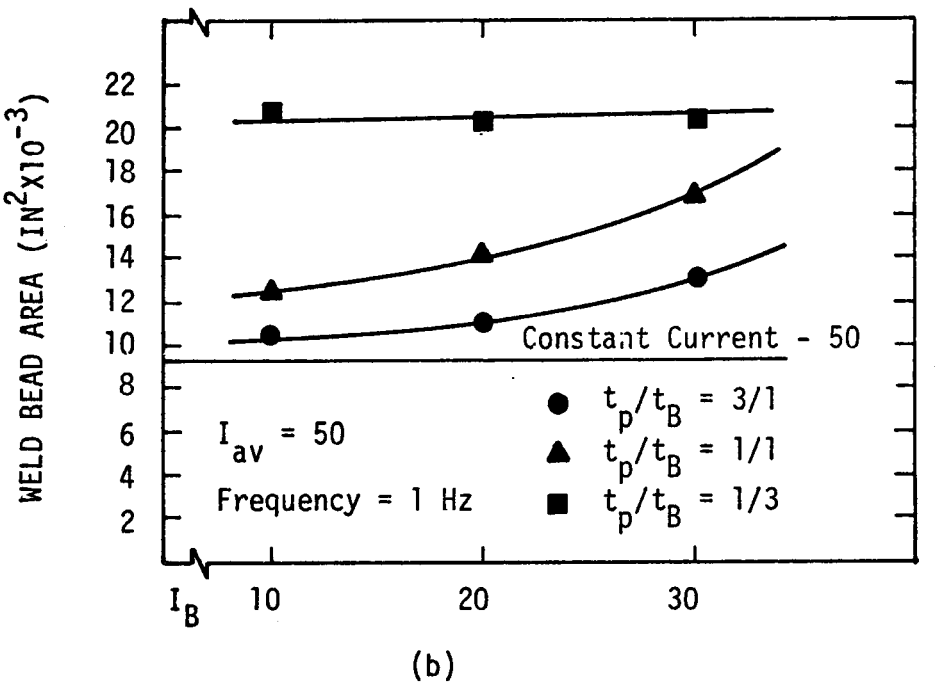
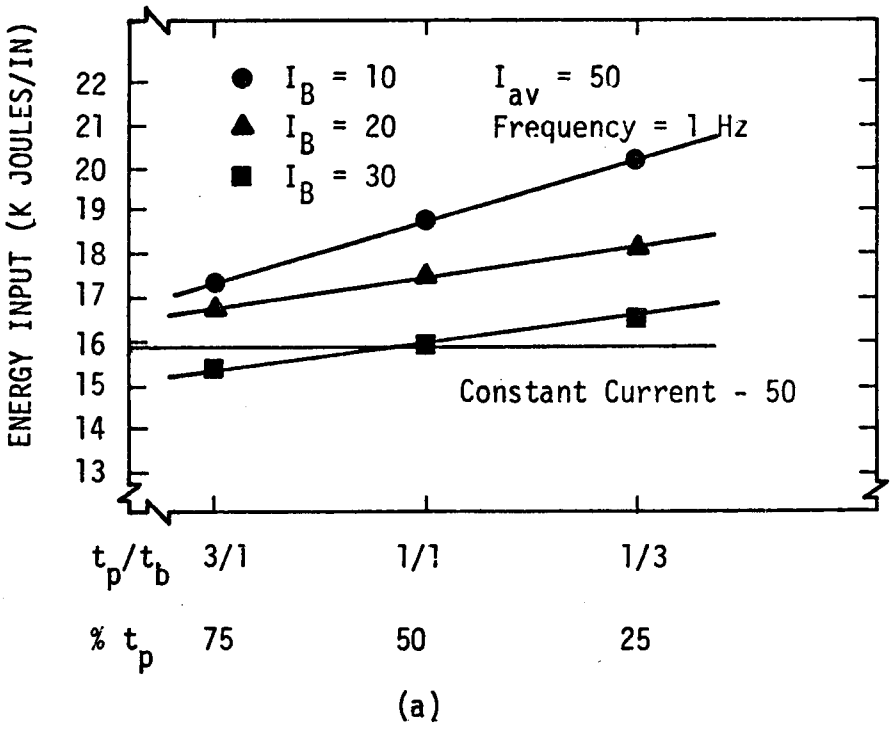


Figure 27. Effect of Low Frequency Pulsed PAW on (a) Weld Penetration and (b) Weld Fused Area for an Average Current of 50 Amperes and a Pulse Frequency of One Hz at Varying I_p, I_{RMS}, I_B and t_p/t_B Values



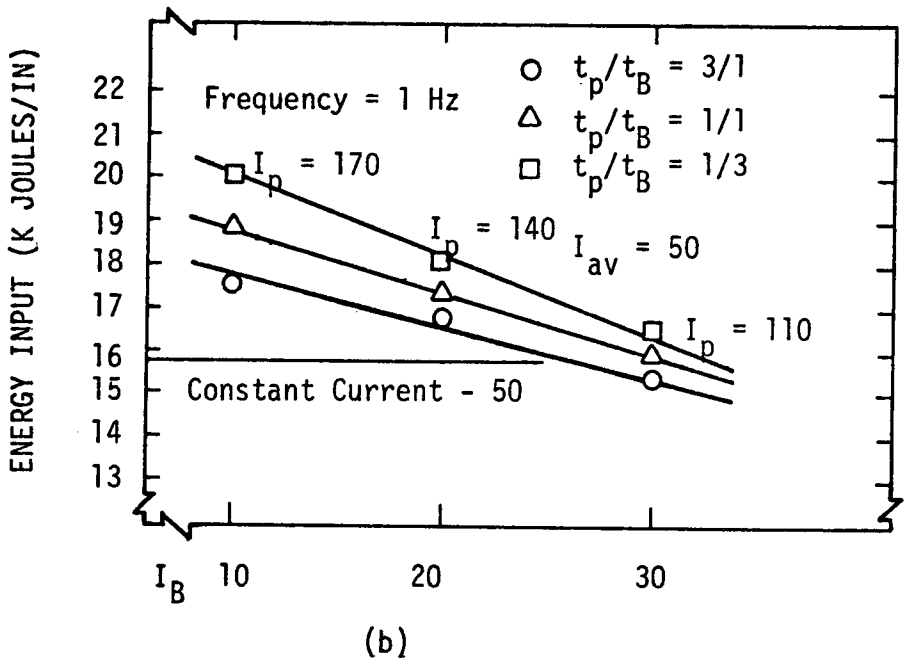
(b)

Figure 27. (continued)



(a)

Figure 28. Energy Input Per Unit Length for Low Frequency Pulsed PAW of an Average Current of 50 Amperes at Varying I_p, I_B and t_p/t_B Values and a Pulse Frequency of One Hz



(b)

Figure 28. (continued)

the background current level to a value equal to the peak current (i.e., constant current) would lead to further optimization of the weld penetration. Thus, the optimum background current setting is one that achieves minimum melting for the welding conditions used.

The increase in the weld bead depth and cross-sectional area as well as the reduction in energy input per unit length experienced as the background current became a melting current current could be explained as follows: A melting background current will maintain a molten weld pool upon which the peak current impinges. The increased arc pressure of peak current could possibly lead to greater weld pool depression, thus enhancing the weld bead penetration and the melting efficiency.

It should be noted that in Figure 27, the largest increase in the weld bead depth and area occurred at a pulse time ratio of t_p/t_B = 1/3. This is to be expected since at that time ratio the peak current and the associated energy input per unit length were the highest as shown in Figure 28.

Figure 29 shows the effect of varying the average current, the peak current and the pulse time ratio on the weld bead depth and area for an RMS current of 50 amperes and a background current level setting of ten amperes. It is clearly seen that the increase in the weld bead depth and area is proportional to the increase in the average current. It is also seen that in this arrangement, neither the increasing peak current nor the RMS current had any controlling effect on the weld bead depth and area. It should further be noted that while the peak current assumes its highest values at the lowest average current, thus

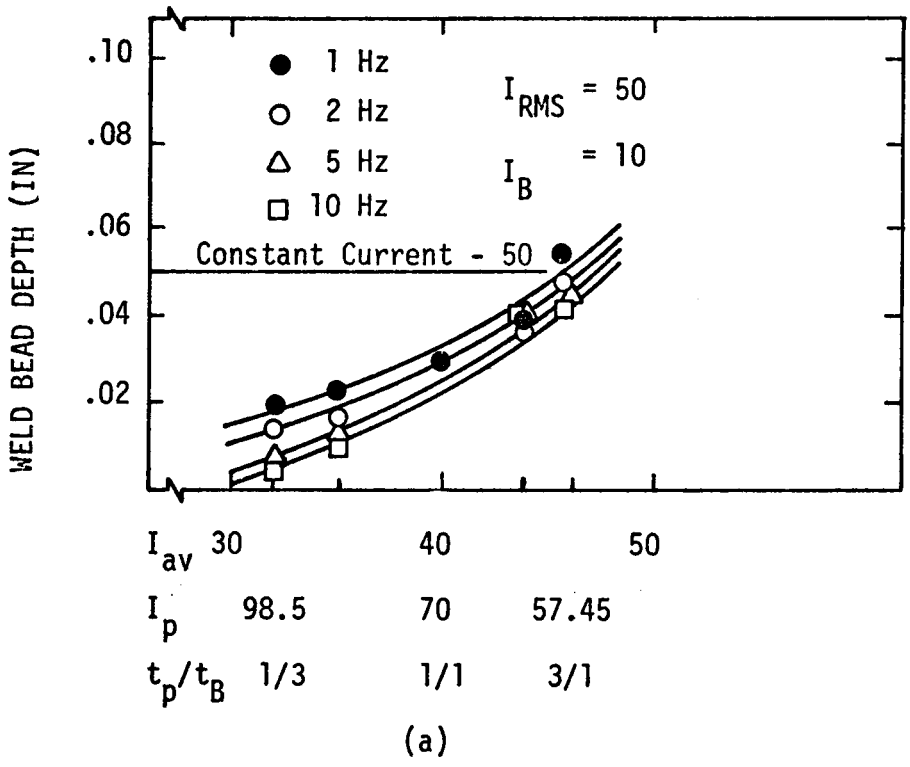
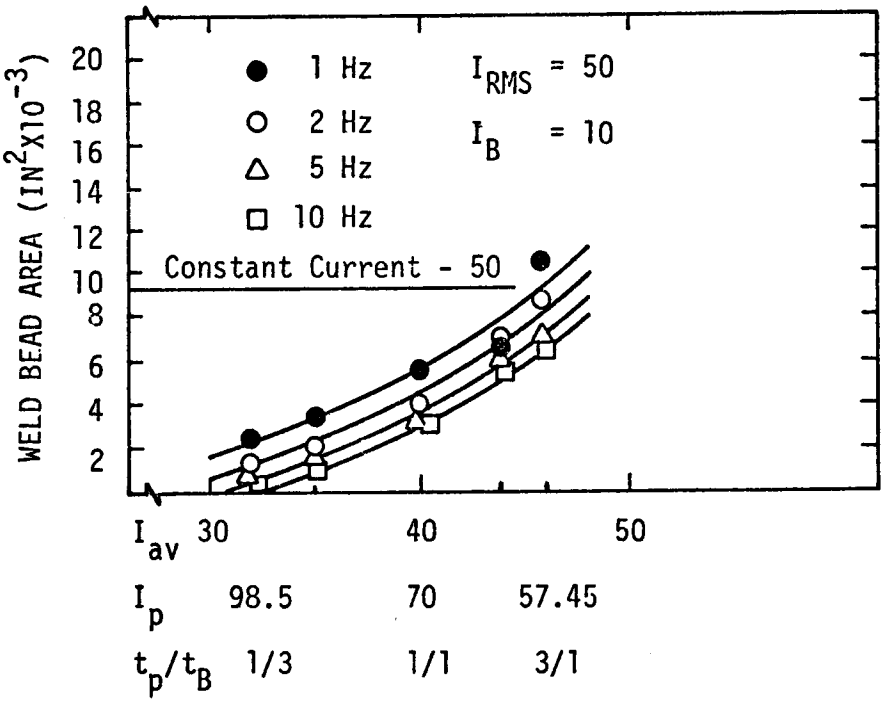


Figure 29. Effect of Low Frequency Pulsed PAW on (a) Weld Penetration and (b) Weld Fused Area for an RMS Current of 50 Amperes and I_B = 10 Amperes at Varying I_p, t_p/t_B and I_{av} Values



(b)

Figure 29. (continued)

increasing the I_p/I_B ratio, the weld penetration and melt area are the smallest. This is not to suggest, however, that an increase in the I_p/I_B ratio has no influence on the weld penetration. It is seen in Figures 24 and 27 that for a given average current, the highest weld penetration and area resulted at the highest I_p/I_B ratio.

Figure 30 is another example that illustrates the importance of the average current and its influence on the weld bead depth and area when varried due to varying peak and background currents for a constant RMS current of 50 amperes and a pulse time ratio of t_p/t_B = 1/1. Here again it is shown that the controlling weld parameter is the average current.

While the response of the power supply used in this investigation was not sufficient to enable the peak current and concurrently the RMS current to reach their nominal values for pulse frequencies beyond one or two Hz, many fundamental conclusions could be derived from the results obtained. Such conclusions are:

1. In general, the average current is the controlling pulse welding parameter that determines the degree of melting efficiency.

2. There is an optimum background current setting which when used in the pulsed plasma arc welding process leads to an enhanced weld penetration and melting efficiency coupled with a tangible reduction in energy consumption. It was found that the background current is optimized when it is chosen to produce and maintain a molten pool at all times.

3. For a given average current at a constant background current and constant pulse frequency, the higher the peak current and

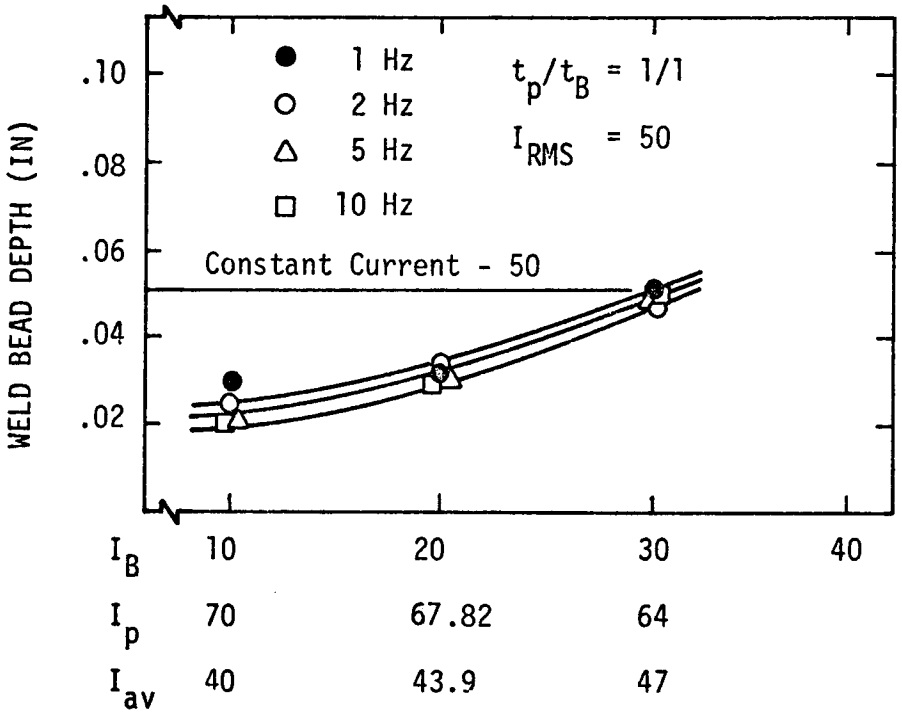
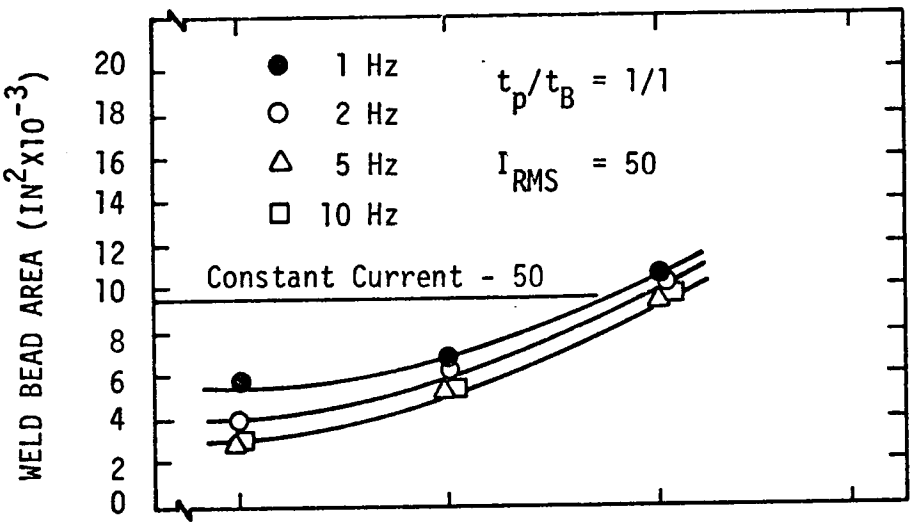


Figure 30. Effect of Low Frequency Pulsed PAW on the (a) Weld Penetration and (b) Fused Area for an RMS Current of 50 Amperes at t_p/t_B = 1/1 and Varying I_p, I_B and I_{av} Current Values



I_B	10	20	30	40
I_p	70	67.82	64	
I_{av}	40	43.9	47	

(b)

Figure 30. (continued)

concurrently the higher the effective current and the I_p/I_B ratio, the deeper and wider the weld bead becomes. Thus, an optimum weld setting for a given constant average current would be at high peak current and short pulse duration.

4. The optimum low pulse frequency appears to lie between one and five Hz.

5. Low frequency pulsing of the plasma arc does enhance the weld bead penetration and area when the proper or the optimum pulse parameters settings are used.

6. No reduction in the energy consumption of the pulsed plasma arc welding was experienced when compared to that of the constant current mode.

Low Frequency Pulsed Plasma Welds (Full Penetration and Keyhole Modes). A constant current of 60 amperes produced full penetration welds when applied to the plasma system for the welding conditions listed in Table III, page 32. When an RMS pulsed current of 60 amperes was used under the same conditions of Table III and for the pulse welding parameters listed in Table V, page 37, full penetration and keyhole mode welds were achieved at lower average currents. The keyhole mode welds were achieved at lower average current of 57 amperes and the full penetration welds were achieved at an average current of 54 amperes at the low frequency pulsing of one, two, five and ten Hz. An argon backing gas was used at a flow rate of 20 cubic feet per hour (20 CFH) to protect the weld underbead from oxidation.

High Frequency Pulsed Plasma Welds (Melt-in Mode). High frequency

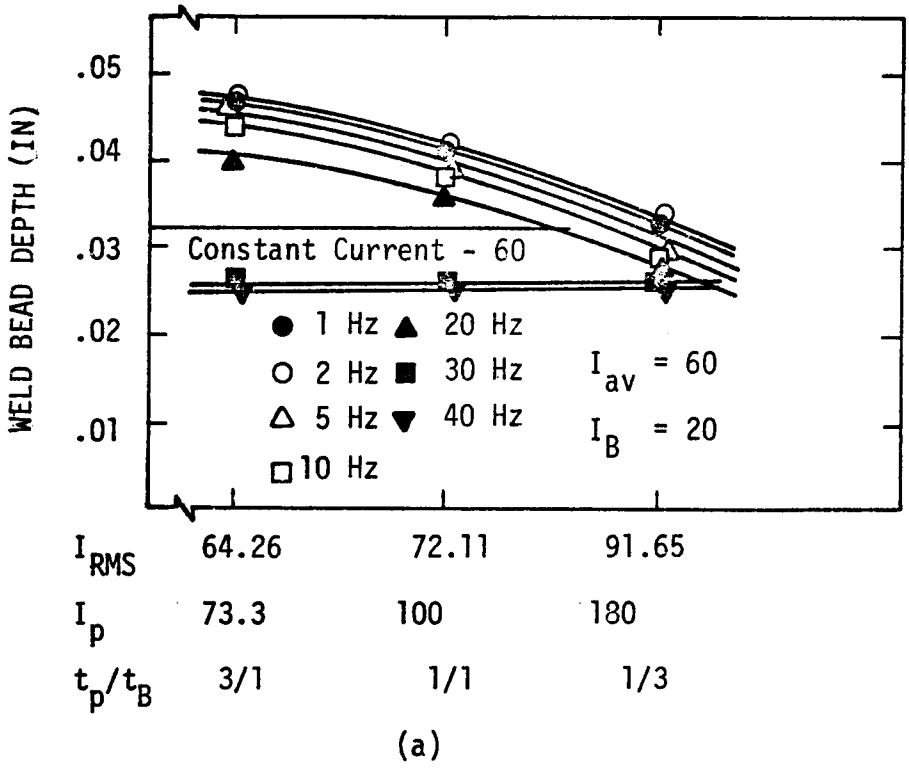
pulsing of the plasma arc was attempted utilizing the Merrick Engineering power supply. No advantages were observed when an average current of 50 amperes was pulsed at two, ten, and twenty kHz and the resulting weld configuration and microstructure were compared to those of a 50 ampere constant current welds made with the same supply. In fact, the weld bead penetration and area of the high frequency pulsing operation was less than one half that of the constant current welding mode. This was not the case, however, in the low frequency pulsing mode of operation where weld bead penetration and area were enhanced when the optimum pulse welding conditions were used.

D. PULSED GTA WELDING PROCESS

Results

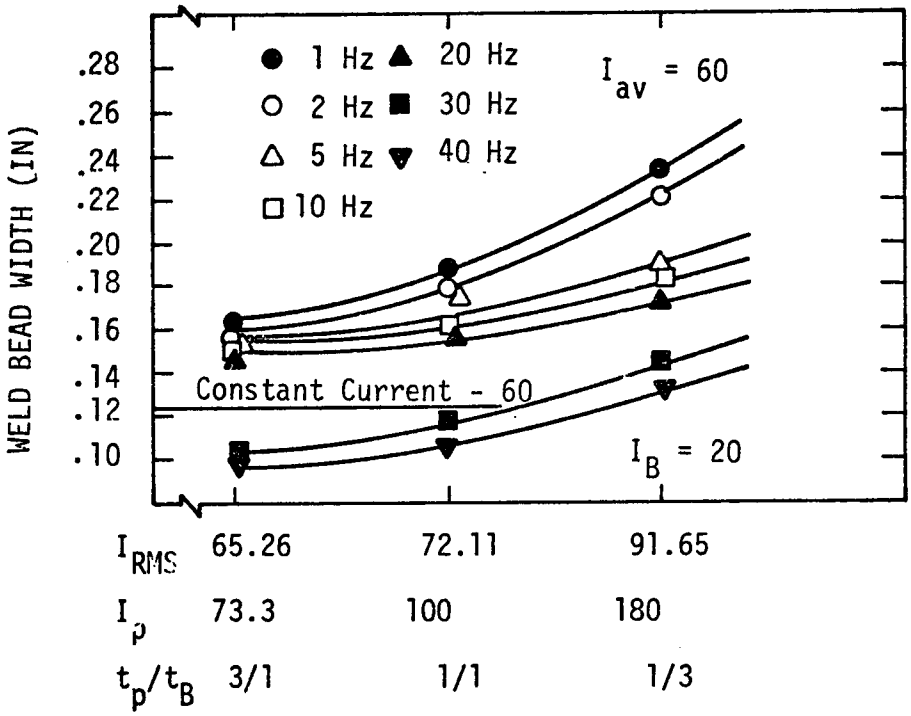
Low Frequency Pulsed GTA Welds. In order to contrast the influence of each of the pulse parameters between two similar processes, the same parameters used for the pulsed plasma arc welds were analyzed for the pulsed GTA welds. This evaluation provided useful information on the pulsed GTA operation in its own right and permitted the interpretation of power supply response characteristics between processes. (It should be noted that all GTA welds of 60 amperes average and RMS currents were made with TekTran's TT-150A power supply and those of 50 amperes average and RMS currents were made with TekTran's LSC-300A power supply.)

Figure 31 shows the effect of increasing peak and RMS currents on the weld bead depth and width for an average current of 60 amperes and a background current of 20 amperes with varying pulse time ratios. It



(a)

Figure 31. Effect of Low Frequency Pulsed GTA on (a) Weld Penetration and (b) Weld Bead Width for an Average Current of 60 Amperes and Varying I_{RMS}, I_p and t_p/t_B Values at I_B = 20 Amperes



(b)

Figure 31. (continued)

is seen that unlike the effect in the plasma process, increasing the peak current decreases the weld bead depth, but both the GTA and plasma operations resulted in an increase in weld bead width over the same range of variables. Thus while welding with high peak currents at short pulse duration for a given average current was found to be the optimum condition in the pulsed plasma process as shown in Figure 24, page 67, the opposite was experienced in the pulsed GTA process. Similar observations on the effect of increasing peak current in the pulsed GTA process was made by Leitner and co-workers (17). Since the electrode vertex angle of 60 degrees was maintained for all the GRA and plasma welds, the observation made on the influence of increasing peak current could be interpreted by examining the arc profile for both processes of pulsed GTA and pulsed plasma. Arc profiles are shown in Figure 1, page 6. As shown in Figure 1, the arc for the GTA process is not constricted and is conical in nature. Thus, when pulsed at higher peak currents, it expands and grows radially. This expansion and growth of the GTA arc result in a wider weld bead since the arc impinges on a wider area of the weld specimen. Savage (31) and Jackson (14) indicate that an increase in the GTAW current causes the arc plasma to climb the surface of the conical tip of the electrode. The amount of climb was found to be approximately proportional to the increase in current, thus the current density of the emitting surface remained essentially constant.

In contrast, the plasma arc is constricted and thus is columnar in shape. While it expands when pulsed, the constriction by the orifice and the flow of the plasma gas help to maintain the pulsed arc cylindrical in shape, thus impinging on a smaller area of the workpiece compared

to a similarly pulsed GTA arc.

The influence of varying peak and background currents on the weld bead depth and area for a given average current of 60 amperes and a constant pulse time ratio of t_p/t_B = 1/1 is shown in Figure 32. As seen in that figure, there is an apparent separation between the weld made at 30 and 40 Hz and those of lower frequencies, in that the 30 and 40 Hz pulsed weld data fall in a straight line with no increase in depth as the peak and RMS currents are increased with a 60 ampere average current.

For the lower pulse frequencies, however, an increase in the background current results in a decrease in the weld penetration. This is in contrast to the pulsed plasma (see Figure 26, page 73; Figure 27, page 75; and Figure 33) where the higher background currents give improved penetration. However, the fused area data does not exhibit any such deviation between the one-twenty Hz and 30 and 40 Hz data. In this instance also the pulsed plasma weld bead area increases over the same peak and background current variations (see Figures 26 and 33). As shown in Figure 33, this behavior is not consistent as the power source is changed and the same pulse parameters are utilized. (The Figure 33 data was derived from the LSC-300 power supply.)

It should be noted that the total energy input per unit length for the pulsed GTA process stayed within 10 percent of that of the constant current mode of operation (see Figure 32). It is also to be noted that the energy input was slightly higher for the lower background current levels than it was for the higher background current settings. This is primarily due to the influence of the arc voltage changes and the peak current level as the background current was varied from 20 to 40 amperes.

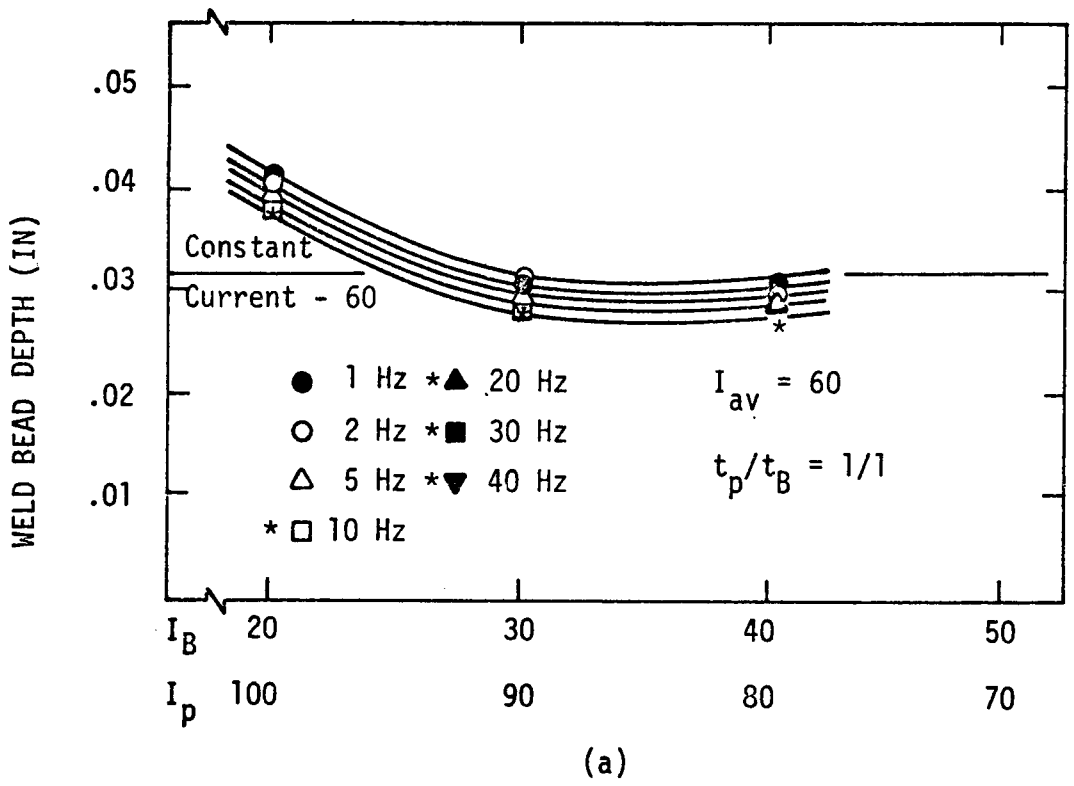


Figure 32. Effect of Low Frequency Pulsed GTAW on (a) Weld Penetration and (b) Weld Fused Area for an Average Current of 60 Amperes at t_p/t_B = 1/1 and Varying I_B and I_p Current Values

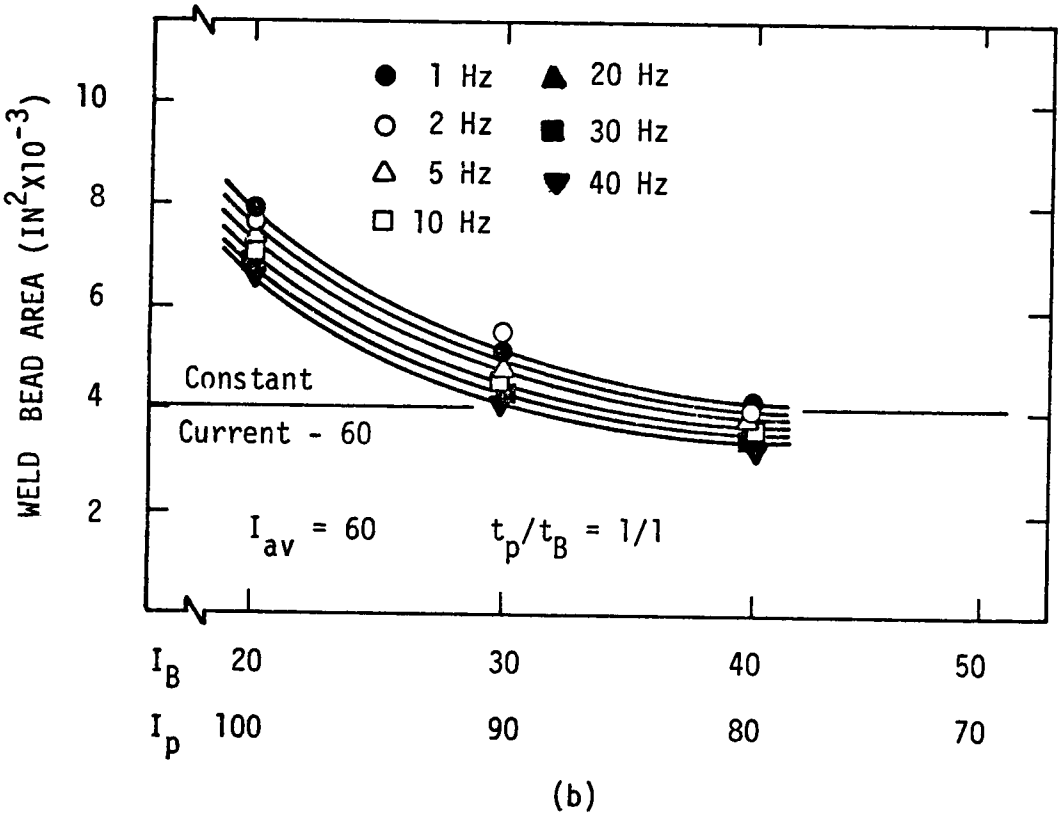
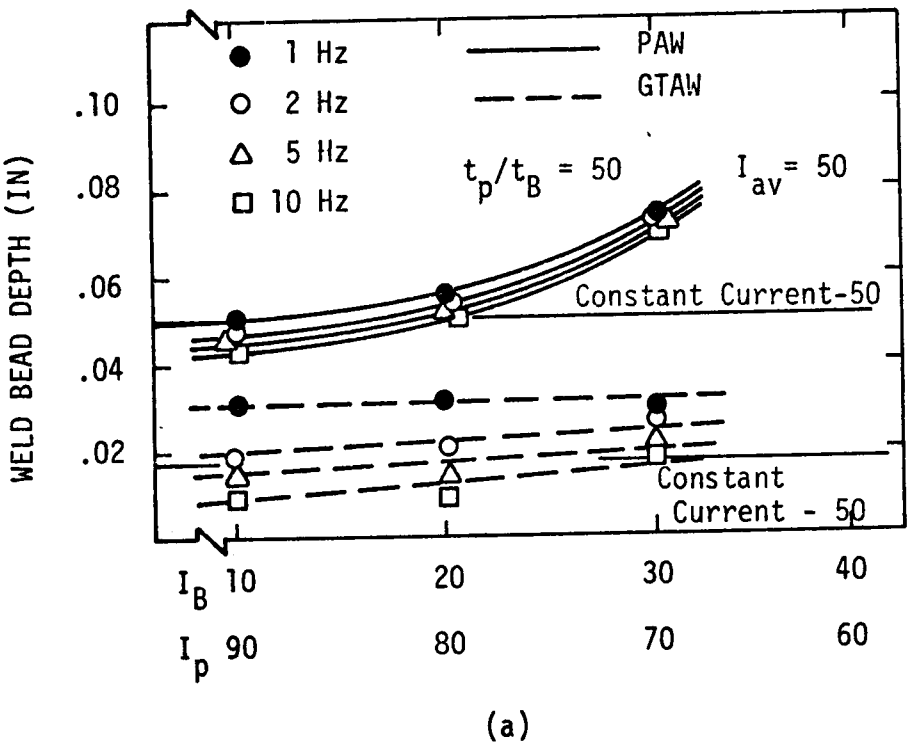


Figure 32. (continued)



(a)

Figure 33. Effect of Low Frequency Pulsed PAW and GTAW Processes on (a) Weld Penetration and (b) Weld Fused Area (LSC-300 Supply) for the Welding Conditions of 50 Amperes Average Current at t_p/t_B = 1/1 and Varying I_B and I_p Current Values

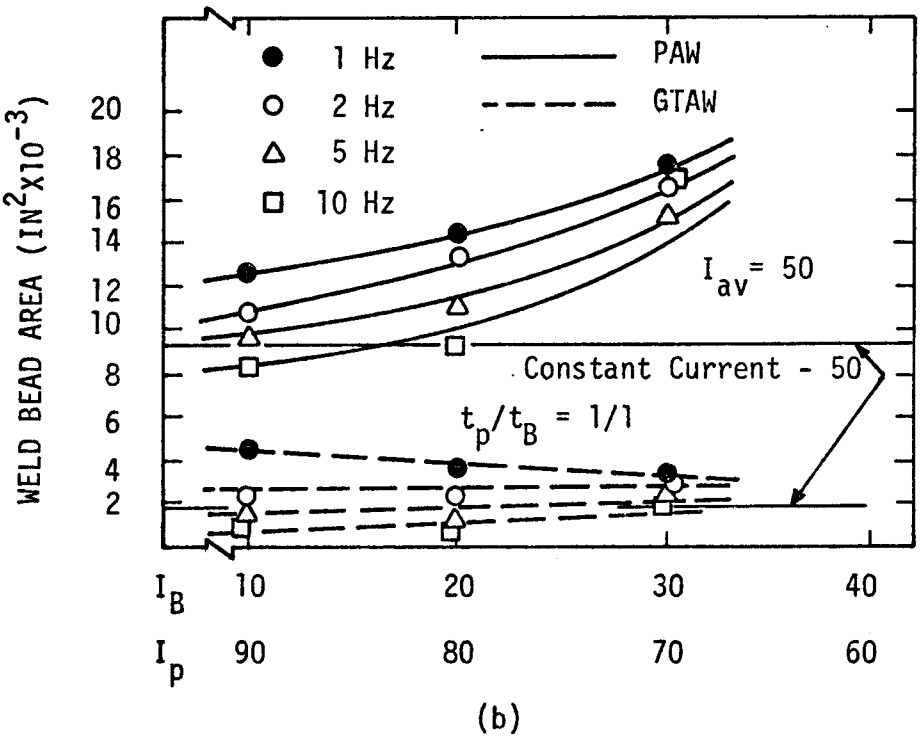


Figure 33. (continued)

In general, while it is seen that the pulsed plasma arc achieves its optimum conditions at a short duration pulse time ratio (t_p/t_B = 1/3) and high peak currents, the pulsed GTA welds are not significantly affected by variations in the time ratio. These data are illustrated in Figure 34.

The influence of the varying average current on the weld bead depth for an RMS current of 60 amperes at varying peak current, background current and pulse time ratio settings is shown in Figure 35. As it was seen in the low frequency pulsed plasma process (Figure 30) and as shown in Figure 36, the average current is the controlling pulse weld parameter for the GTA process as well as the plasma arc process. It should be noted that for both the pulsed plasma and pulsed GTA the weld penetration data approaches the constant current penetration as the average current approaches the constant current value.

High Frequency Pulsed GTA Welds. The same high frequencies of two, ten, and twenty KHz investigated in the pulsed plasma process were studied in the pulsed GTA welding process. These frequencies were evaluated for an average current of 60 amperes at varying background currents and pulse time ratios. The nominal and actual values of the currents evaluated are shown in Table IX.

The effect of high frequency pulsing on the weld bead depth and area for an average current of 60 amperes at constant pulse time ratio of t_p/t_B = 1/1 and different background current settings is shown in Figure 37. It is observed that the weld bead depth and area were increased at higher background current settings when compared to the

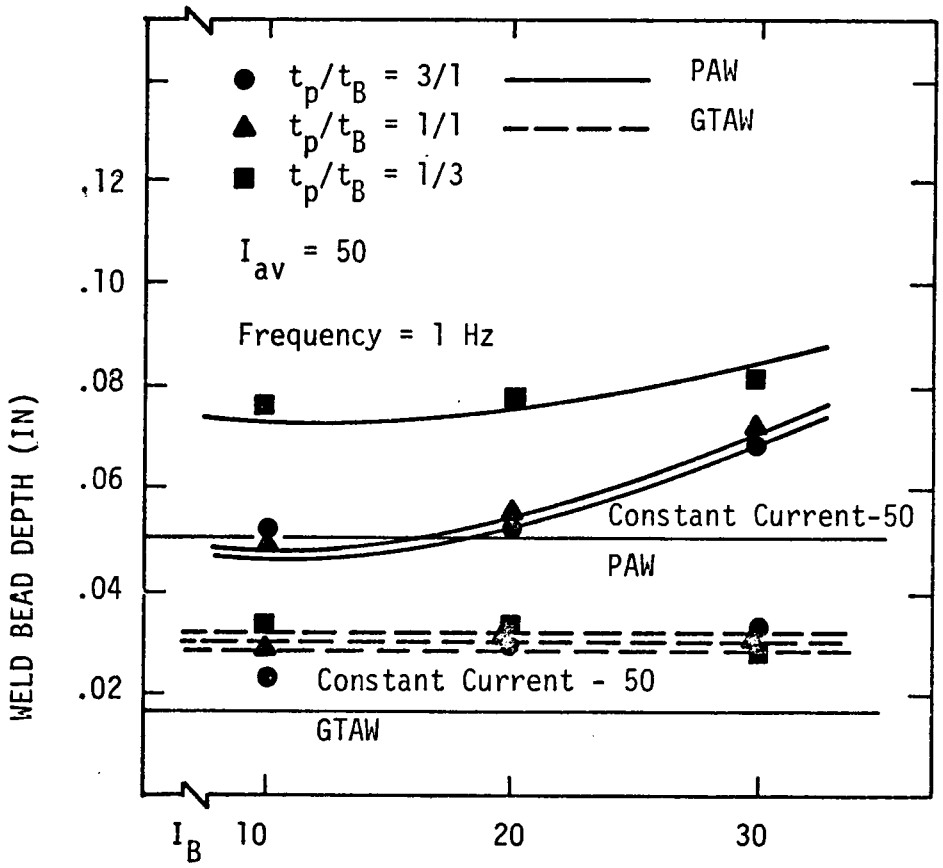
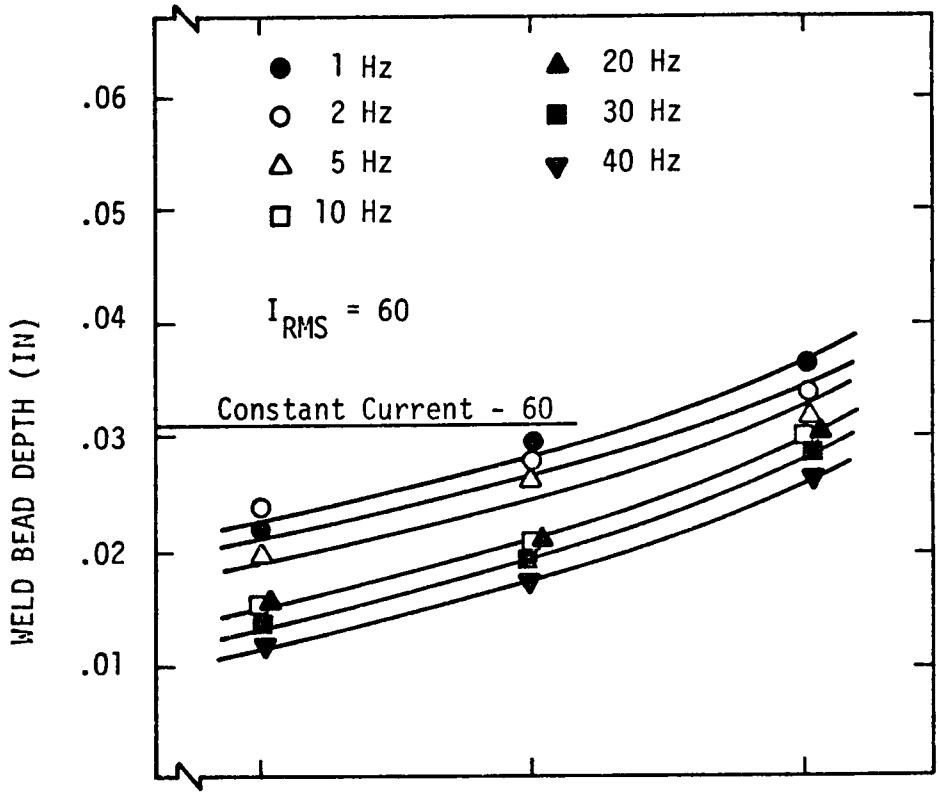
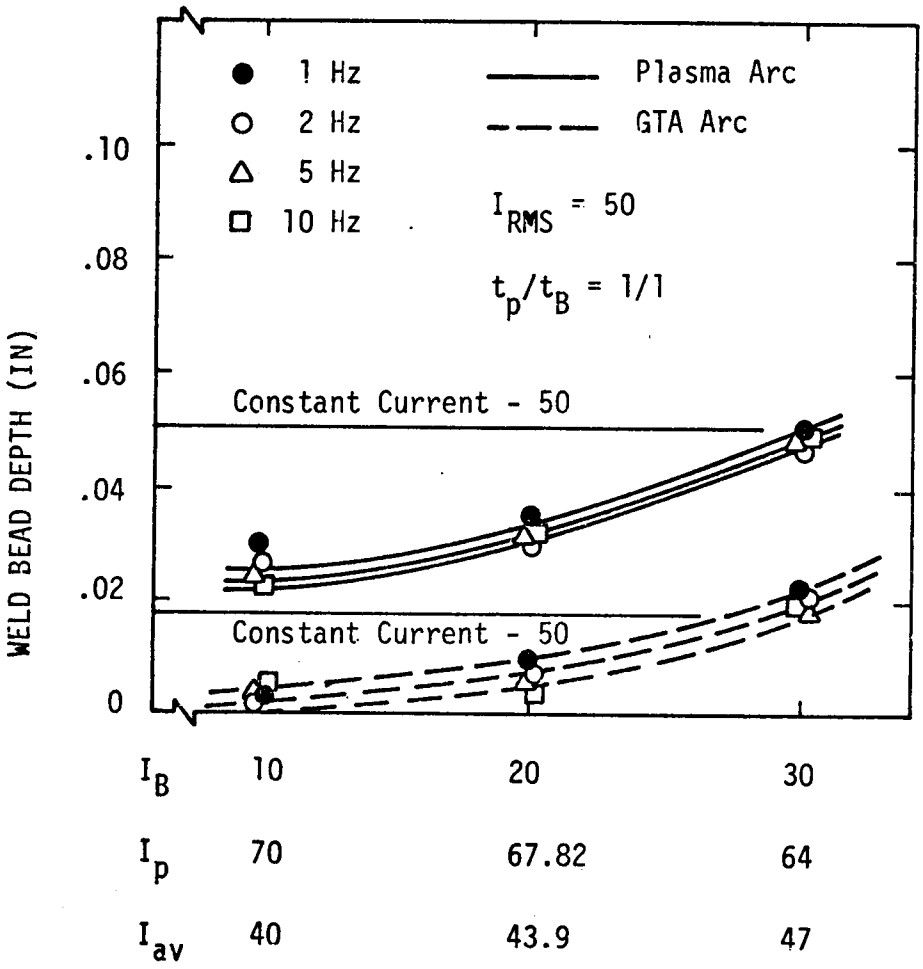


Figure 34. Effect of Varying Pulse Time Ratio (t_p/t_B), Peak and Background Currents on the Weld Bead Penetration for an Average Current of 50 Amperes at a Pulse Frequency of One Hz for the PAW and GTAW Processes



I_B	20	30	40
I_p	100	90	80
I_{av}	46.6	52.5	56.7
t_p/t_B	0.50	0.60	0.72
E.I.(KJ/in)	7.845	8.634	9.253

Figure 35. Effect of Low Frequency Pulsed GTAW on the Weld Penetration for an RMS Current of 60 Amperes at Varying I_B, I_p, I_{av}, and t_p/t_B Values



I_B	10	20	30
I_p	70	67.82	64
I_{av}	40	43.9	47

Figure 36. Effect of Low Frequency Pulsed PAW and GTAW on the Weld Penetration (LSC-300 Supply) Under the Same Conditions of an RMS Current of 50 Amperes at t_p/t_B = 1/1 and Varying I_B, I_p and I_{av} Current Values

TABLE IX

NOMINAL AND ACTUAL CURRENT VALUES FOR THE PULSED HIGH FREQUENCY WELDING CONDITIONS LISTED IN TABLE VI

Frequency (KHz)	Time Ratio t_p/t_B	Shape of Wave Form	I_B (Amps)		I_p (Amps)		I_{av} (Amps)	
			Nominal	Actual	Nominal	Actual	Nominal	Actual
2	2/1	Square	20	0	---	95	60	64
2	1/1	Square	20	0	---	132	60	64
2	1/2	Square	20	0	---	190	60	63
10	2/1	Sloping Square	20	10	---	115	60	62
10	1/1	Sloping Square	20	10	---	140	60	62
10	1/2	Sloping Square	20	10	---	175	60	62
20	2/1	Sine	20	15	---	110	60	63
20	1/1	Sine	20	15	---	120	60	63
20	1/2	Sine	20	15	---	150	60	63
2	2/1	Square	30	10	---	90	60	63
2	1/1	Square	30	10	---	115	60	63
2	1/2	Square	30	15	---	165	60	63

TABLE IX (continued)

Frequency (KHz)	Time Ratio t_p/t_B	Shape of Wave Form	I_B (Amps)		I_p (Amps)		I_{av} (Amps)	
			Nominal	Actual	Nominal	Actual	Nominal	Actual
10	2/1	Sloping Square	30	20	---	100	60	65
10	1/1	Sloping Square	30	20	---	115	60	65
10	1/2	Sloping Square	30	20	---	160	60	65
20	2/1	Sine	30	25	---	100	60	65
20	1/1	Sine	30	25	---	105	60	65
20	1/2	Sine	30	25	---	120	60	65
2	2/1	Square	40	22	---	85	60	64
2	1/1	Square	40	22	---	106	60	64
2	1/2	Square	40	20	---	150	60	63
10	2/1	Sloping Square	40	30	---	90	60	65
10	1/1	Sloping Square	40	30	---	102	60	65
10	1/2	Sloping Square	40	30	---	135	60	65
20	2/1	Sine	40	40	---	90	60	65
20	1/1	Sine	40	35	---	95	60	65
20	1/2	Sine	40	35	---	100	60	65

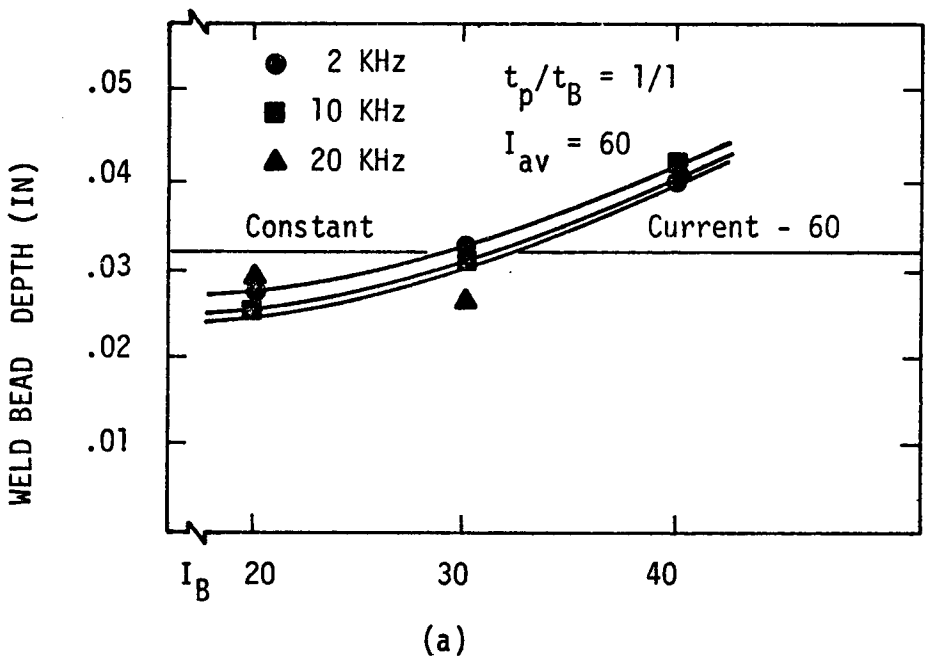


Figure 37. Effect of High Frequency Pulsing on (a) Weld Penetration and (b) Weld Fused Area of the Pulsed GTAW Process for an Average Current of 60 Amperes at t_p/t_B = 1/1 and Varying Pulse Frequency and Background Current Values

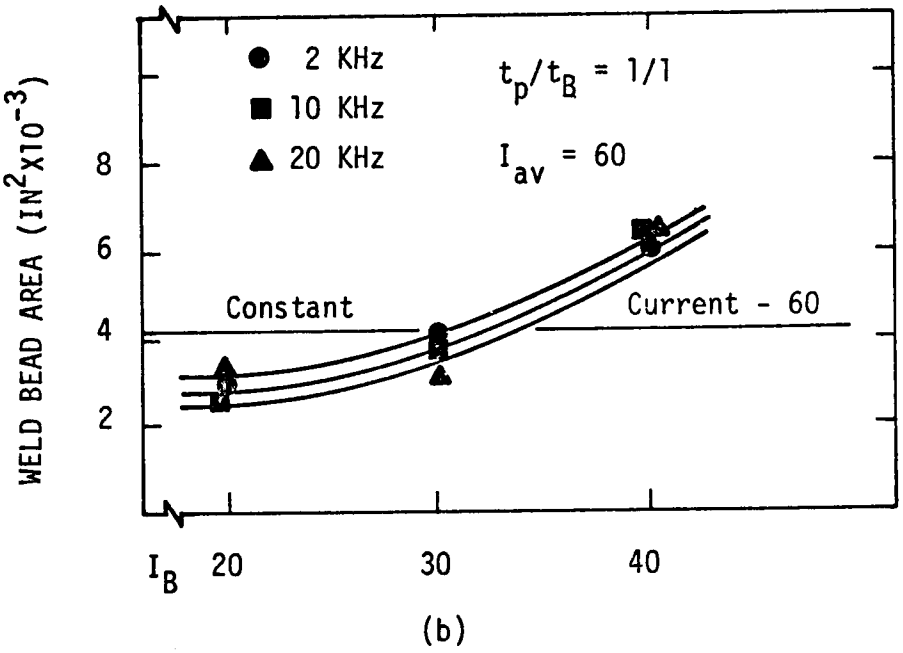


Figure 37. (continued)

steady state constant current mode of welding. Furthermore, it should be noted that a pulse frequency of two KHz appears to have the greatest influence on the weld bead depth and area as compared to the higher frequencies of ten and twenty KHz. There was no significant change in energy input when welding was accomplished at frequencies of two, ten and twenty KHz. At two KHz, the wave form was essentially square but at ten and twenty KHz the wave form degenerated into a saw-tooth. Similar results are seen by examination of Figure 38 which shows the influence of varying pulse time ratio on the weld bead depth for the three frequencies evaluated. The two KHz operation appears to be the optimum regardless of the pulse time ratio chosen.

As was experienced for the low frequency pulsed plasma operation, the background current level was influential in increasing the penetration at a given average current. This is shown in Figure 39 for a ten KHz weld. Similar behavior was exhibited at two and ten KHz also. The data obtained for the two KHz operation is shown in a different form in Figure 40. The influence of peak current and background current can be seen by inspection of this figure.

The increase in penetration achieved with the high frequency operation may be outweighed, however, by the rather unpleasant audible vibration produced during the arc pulsing. In general the higher the frequency, the lower the noise level, but at the same time the penetration increase is not realized. The noise level in reality reflects the current excursion levels as well as the frequency of operation and for the condition described the wave form amplitude degenerated at the higher frequency.

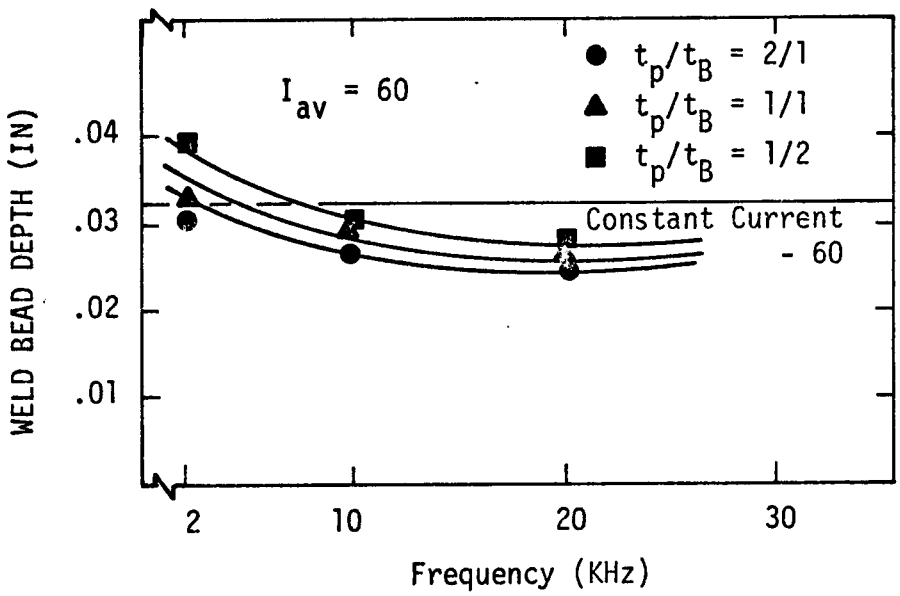


Figure 38. Effect of High Frequency Pulsed GTAW on the Weld Penetration for an Average Current of 60 Amperes and Varying t_p/t_B and Pulse Frequency

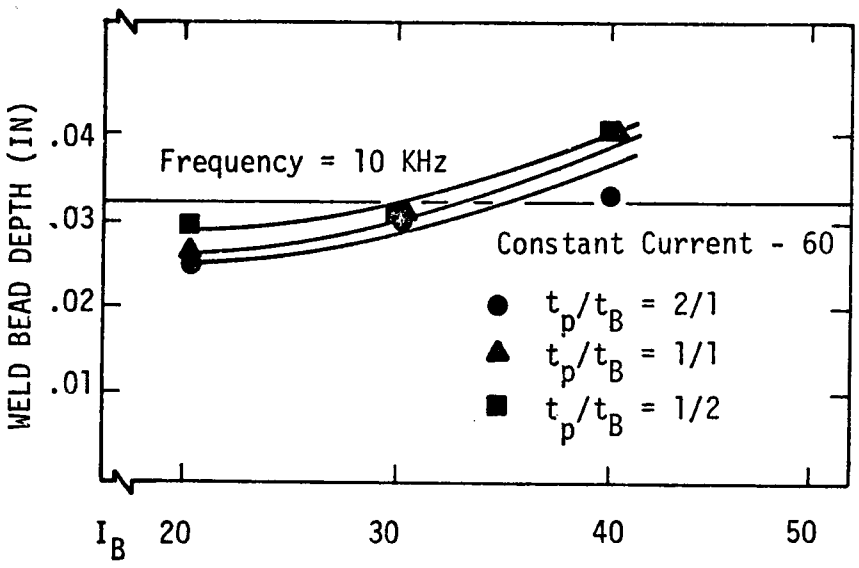


Figure 39. Effect of High Frequency (10 KHz) Pulsed GTAW on the Weld Penetration for an Average Current of 60 Amperes at Varying I_B and t_p/t_B Values

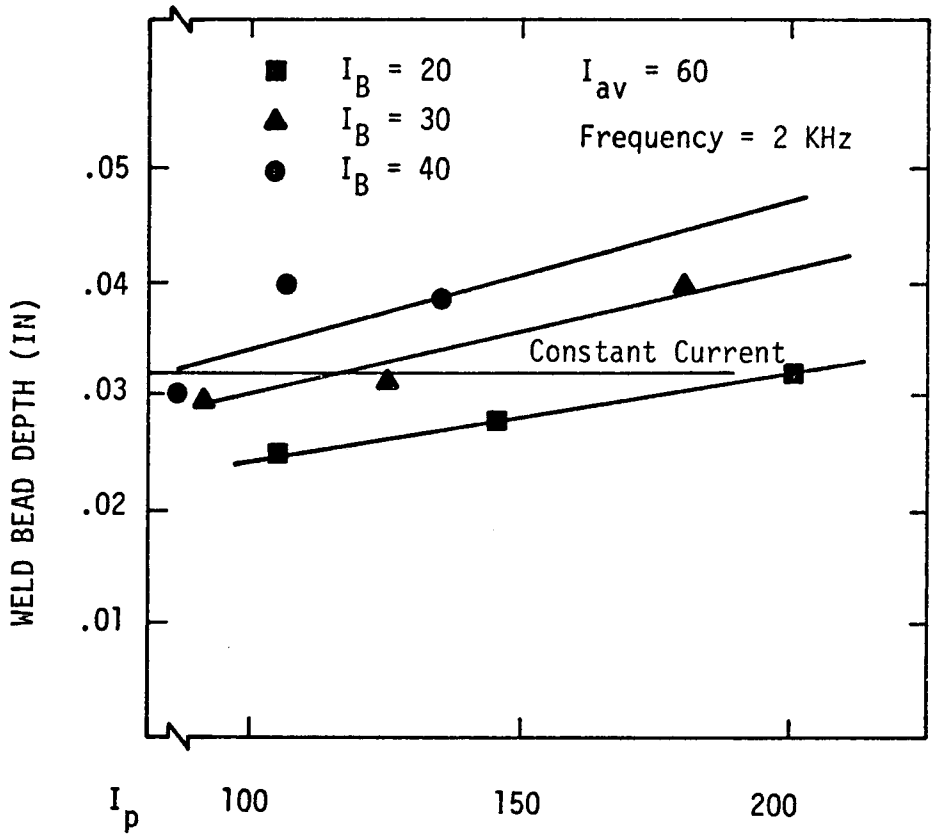


Figure 40. Effect of High Frequency (2 KHz) Pulsed GTAW on the Weld Penetration for an Average Current of 60 Amperes at Varying I_B, I_p and t_p/t_B Values

In general, the following conclusions could be made regarding the pulsed GTAW process:

1. Unlike the pulsed plasma process, the high GTA peak current at short pulse duration for a given average current leads to no enhancement of the weld bead penetration, but it does increase the weld bead width.

2. Pulsing the GTA current does enhance the weld bead depth and area over the constant current value when the optimum welding conditions are used.

3. An optimum welding condition for the low frequency pulsed GTA welding process is one with a low background current and long pulse duration or high pulse time ratio for a given average current.

4. Similar to the pulsed plasma arc process, the average current is the controlling pulse parameter in the GTA pulsed welding process.

5. The optimum low pulse frequency for the GTAW process appears to lie between one and twenty Hz.

6. No marked advantage is observed when the high frequency GTA pulsing operation is utilized. The audible noise generated by the arc during high frequency excursions in current could be harmful to the operator and in any instance is objectionable to individuals working in the area immediately adjacent to the welding operation.

F. SUPERIMPOSED PULSED HIGH FREQUENCY ON PULSED LOW FREQUENCY GTA WELDING PROCESS

General

The primary purpose in superimposing pulsed high frequency on

pulsed low frequency welding mode of operation is to determine what influence such a combinated operation would have on the weld penetration and microstructure. The welding conditions for this evaluation are shown in Table VII. An average current of 60 amperes was used in this segment of the investigation so that the results could be directly compared to those previously presented for separate low frequency and high frequency operation. The average current of 60 amperes is obtained from the algebraic sum of the high frequency current levels and that of the low frequency current levels.

The frequencies, the peak and background currents and high frequency current amplitudes were varied as shown in Table VII to produce a composite average current of 60 amperes. The pulse time ratio of t_p/t_B = 1/1 was held constant for all weld settings evaluated in this segment of investigation.

Results

Figure 41 shows the influence of the superimposition of the high frequency pulsed mode (2KHz) and the low frequency operation on weld penetration. The values selected for low frequency peak and background currents when combined with the high frequency amplitude yield a 60 ampere average current as indicated previously. The weld penetration remains below that of the constant current value of 60 ampere except at the one Hz low frequency level. Thus no beneficial effect on this basis is evident.

Figure 42 allows the comparison of the range of high frequency and low frequency pulsing evaluated. Note that only when a one Hz low

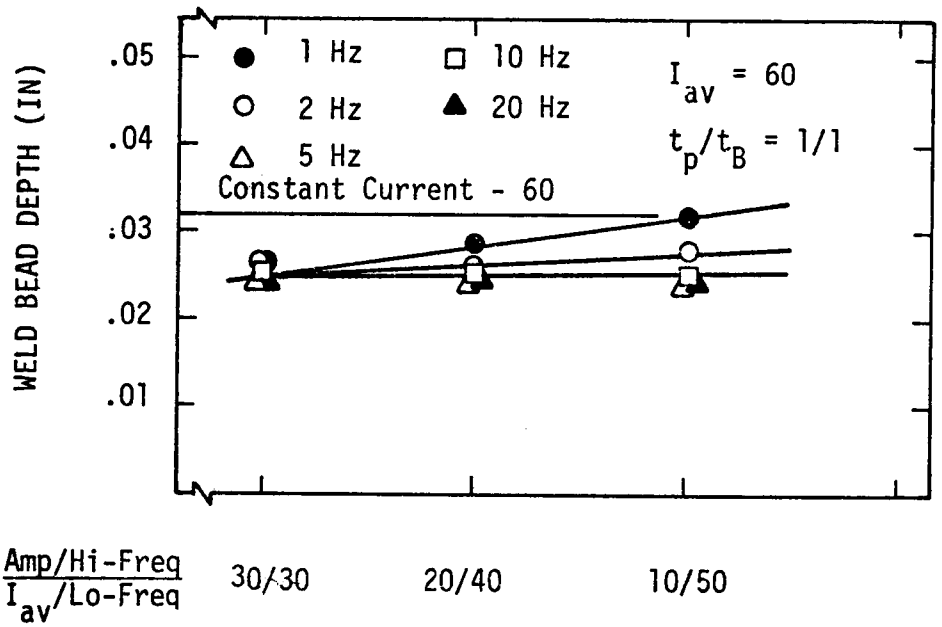


Figure 41. Effect of Superimposed High Frequency (2 KHz) on Varying Low Frequency Pulsed GTAW on the Weld Penetration for a Composite Average Current of 60 Amperes

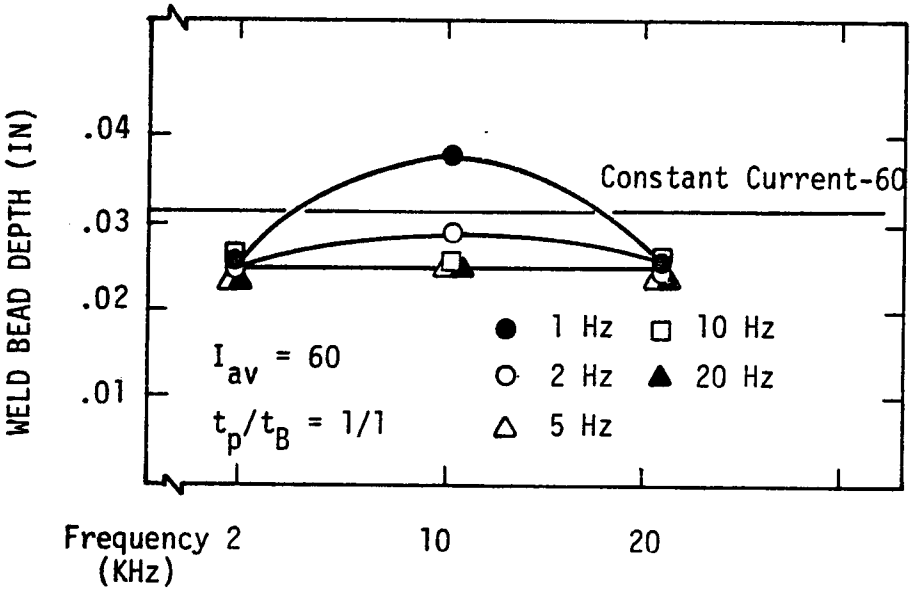


Figure 42. Effect of Superimposed High Frequency on Low Frequency Pulsed GTAW on the Weld Penetration for a Composite Average Current of 60 Amperes at t_p/t_B = 1/1 and Varying High and Low Pulse Frequency

frequency pulse was combined with ten KHz high frequency mode of pulsing did the penetration show a value exceeding the constant current value. Thus it appears that the one Hz low frequency pulse combined with the ten KHz high frequency mode is the optimum in producing enhanced penetration.

G. METALLOGRAPHIC OBSERVATIONS

General

A metallographic study of the fusion and the heat-affected zones was performed to determine the effect of the welding variables on the weld microstructure. Welds examined were those made with average currents of 50 and 60 amperes for the constant and pulsed current modes of the PAW and GTAW processes. The evaluation covered all of the low, high and superimposed pulse frequencies and all of the pulse time ratios that were investigated.

The microstructural observations were made by examining the weld bead transverse, longitudinal top surface and longitudinal centerline sections. Marble's reagent was used to delineate the microstructural features of both the fusion zone and the HAZ. The composition of this etchant is 4g $CuSO_4$, 20 ml HCl and 20 ml H_2O.

Results

Pulsed Plasma-Arc Welds. Upon examining the microstructural features of the constant and pulsed current modes of the plasma arc welds, the following observations were made:

1. No major difference in the grain size or the size of solidification substructure of welds of both current modes was observed.

2. The pulsed current weld bead showed the formation of papillary at high peak currents at a pulse frequency of one Hz. This resulted in an uneven root due to the lack of overlapping of the penetration fingers.

3. The keyhole mode welds showed no difference in grain size or the size of solidification substructure when compared to the full penetration welds of the constant and pulsed current modes. However, the keyhole mode welds showed a higher weld depth-to-width ratio than those of the constant and pulsed current full penetration welds.

4. In general, the lower the pulse frequency, the narrower the HAZ and the wider the fused zone. The narrowest HAZ was found to be at a pulse frequency of one Hz for high peak currents and short pulse duration time ratio, t_p/t_B.

Pulsed GTA Welds. To contrast with the plasma welds, similar microstructural examination of the GTA welds was made with the following observations:

1. No significant difference in the grain size or the solidification substructure of the fusion zone of the low frequency (1-40 Hz) pulsed GTA welds was observed compared to those of the constant current welds.

2. At higher pulse frequency, the fusion zone decreased in size and the HAZ increased. This is an indication of decreasing

melting efficiency of the process at higher pulse frequencies. This behavior was also noted by Edmonds (8).

3. High frequency pulsing of the GTA arc had no enhancing effect on the weld microstructure when compared to that of the constant current.

4. Superimposed high frequency on low frequency pulsing of the GTA arc also had no enhancing effect on the weld microstructure when compared to that of the constant current welds.

5. Similar to the PAW, the narrowest HAZ and the largest fusion zone of the GTAW weld bead was achieved at a pulse frequency of one Hz.

6. Compared to the plasma welds of the same welding conditions, the plasma welds had greater penetration than that of the GTA welds.

Discussion

In general, the structure of the fusion zone is controlled by the size and shape of the weld pool, the temperature gradients in the molten pool, the rate of solidification of the weld pool, and the size and orientation of the grains in the unmelted base metal adjacent to the solid-liquid interface (19, 20). The weld substructure is dependent to a significant degree upon the temperature gradient in the weld pool, the solidification rate, and solute redistribution. The individual grains in the weld metal are generally composed of many elongated cellular-shaped subgrains resulting from a cellular-dendritic/columnar-dendritic mode of solidification. Thus, the metallographic section of the weld intersects the microstructure to produce various apparent shapes of subgrains depending upon the orientation of the

long axis of the cells relative to the plane of observation. The shape of the intersection varied from elongated striations when the long axis of the subgrains is parallel to the surface, to small roughly hexagonal cells when the axis is normal to the surface.

Lundin (20) indicates that grains in the weld metal grow expitaxially from the partially melted grains in the base material at the fusion boundary. Growth occurs in the direction of the maximum temperature gradient, which is perpendicular to a line tangent to the interface. Lundin further indicates that grains in the weld metal exhibit a preferred growth direction paralleling a particular crystallographic direction; for face centered cubic Inconel 600 the preferred direction would be <100>. Thus, the shape of the grains can be used to determine the growth direction of the grains in the fusion zone relative to the welding direction. Lundin (20) further indicates that the properties of the fused zone are dependent upon the fusion zone grain size, grain orientation and solidification substructure size. For a particular welding process the solidification substructure size is restricted to a relatively small range controlled by the process parameters and often further dictated by the economics of producing the welded product. For this reason a significant amount of research has been directed toward reducing the fusion zone grain size and thus gaining enhanced properties by the grain size reduction. The expitaxi inherent in the welding solidification process produces grains the size of which is directly related to the HAZ grain size at the fusion interface. This grain size is controlled by the grain growth characteristics of the alloy in question and the thermal

excursion next to the weld interface. By controlling the thermal cycles next to weld interface, a measure of control of the initial grain size can be affected. This, however, usually requires a change in process to create a significant alteration of the grain size (e.g., arc welds versus electron beam welds). For these reasons the attempts at reducing grain size in welds has been directed toward inducing nucleation ahead of the solidifying interface thus creating randomly oriented and refined grains. This can be accomplished by injection of high melting temperature nuclei into the weld pool but perturbation of the process and weld metal composition cannot often be tolerated.

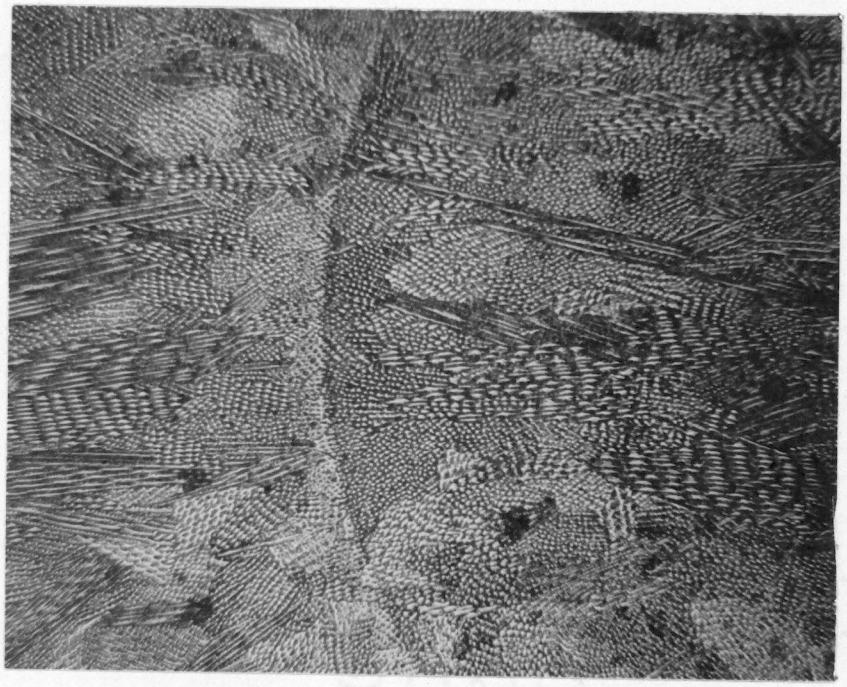
The other avenue of approach has been to introduce vibrations into the pool to help stimulate nucleation. These vibrations have been introduced by arc current pulsing, mechanically and ultrasonically. As discussed previously the arc current pulsation methods employed in this study 1 Hz-20 kHz did not show the validity of this approach either at the fusion zone-HAZ interface or in the overlapping fused regions in the weld fusion zone itself.

The essentially perfect epitaxi is illustrated in the micrographs shown in Figure 43. Figure 43a is a longitudinal top view along the fusion line. The one-to-one grain correspondence across the fusion line is clearly evident. The epitaxi within the fused zone from pulse-to-pulse is also visually evident. This phenomena is also clearly seen in the micrograph showing the longitudinal-top view centerline Figure 43b. Occasionally a slight reorientation of the substructure is noted but the one-to-one grain correspondence is maintained. The full gamut of frequencies studied produced similar



(a) Longitudinal-Top View Along the Fusion Line

Figure 43. Fusion Zone Microstructure of a 60 Amperes Average Current Pulsed GTA Weld Bead at t_p/t_B = 1/1, I_B = 40 Amperes and I_p = 80 Amperes, Marble Reagent, 50X



(b) Longitudinal-Top View Centerline

Figure 43. (continued)



(c) Transverse Cross-Section

Figure 43. (continued)

microstructure. As indicated previously the grain and substructure orientation are influenced by weld pool size and shape, growth rate and HAZ grain size. Investigators must be extremely careful in their assessment of "grain refinement" because the plane of microstructural examination often prejudices the conclusions.

The microstructural investigation conducted during this study does emphasize an important aspect of the solidification process in welds. The partially melting region (liquidus-solidus region) immediately adjacent to the fusion line often exhibits a grain size smaller than that of the HAZ region adjacent to it but slightly further away from the fusion line. The reduced grain size is due to liquid films surrounding the grains in the partially melted region and restricting their growth. Those grains further away from the fusion line where the temperature is less than the solidus do not experience the liquid film pinning effect (except for constitutionally liquated particles in some alloys). This phenomena is clearly illustrated in Figure 43c a transverse cross section of a weld in Inconel. Note that the grain size away from the fusion line is larger than the grain size in the partially melted region adjacent to the fusion line.

The phenomena of partial melting and the observations concerning the microstructure made in this study suggest that a grain refinement effect can be produced if:

1. The partially melted grains can be controlled in extent and magnitude along the fusion line.

2. The application of vibrational energy whether from arc pulsation, mechanical induction or by ultrasonic techniques, may be

influential if it can cause rotation of the grains in the partially melted region and thus alter or randomize their orientation (recrystallization and grain growth induces its own orientation in the HAZ and will tend to control to a certain extent the fusion zone grain orientation). This effect would be enhanced as the extent (temperature range) of partial melting increases. Thus for the same set of thermal conditions the alloy with the larger liquidus-solidus range should be more amenable to initial or starting grain size control. This in essence may be the reason why some investigators report that current pulsation produces a readily observable effect while others report no effect.

Unfortunately, the partial melting phenomena would not be effective in the fused zone where overlapping pulses will produce a series of partially melted regions whose spacing is related to the travel speed, pulse frequency and pulse amplitude. The reason why this effect would not be pronounced is that the competitive grain growth during the interval of solidification between pulses produces a larger grain size than that which existed adjacent to the weld in the HAZ. Careful study of the pulse overlap regions in this investigation revealed only a small influence on grain size and shape between pulses. This is probably due to the small melting range of Inconel 600 alloy ($\sim$ 105°F). An alloy with a larger melting range may be expected to have a more pronounced effect. In addition the higher conductivity materials with their shallower temperature gradients would appear as likely candidates for fusion zone microstructure enhancement. This

area of study deserves more effect in the understanding and possible utilization of the partial melting-vibration interaction potential.

CHAPTER V

CONCLUSIONS AND RECOMMENDATIONS

The results of this investigation permit the following conclusions to be made:

1. In general, the average current is the controlling pulse welding parameter that determines the degree of melting efficiency for both the PAW and GTAW processes.

2. There is an optimum background current setting which when used in the pulsed plasma arc welding process leads to an enhanced weld penetration and melting efficiency coupled with a tangible reduction in energy consumption. It was found that the background current is optimized when it is chosen to produce and maintain a molten pool at all times. This, however, was not experienced in the GTAW process pulsed at comparable welding conditions.

3. For a given pulse average current at a constant background current and constant pulse frequency, the higher the peak current and concurrently the higher the RMS current and the I_p/I_B ratio, the deeper and wider the plasma weld bead becomes. Thus, the optimum weld setting for a given average current would be at high peak current and short pulse duration. This, however, is not the case for the pulsed GTAW process where the higher peak current at short pulse duration resulted in wider weld bead but no enhancement in penetration.

4. The low frequency pulsing of PAW and GTAW processes does enhance the weld bead penetration and melting efficiency when the

optimum pulse parameters settings are used.

5. An optimum welding condition for the GTAW process with a given average current appears to be a long pulse duration or a high pulse time ratio (t_p/t_B) coupled with a low background current.

6. The optimum low pulse frequency appears to lie between one and five Hz for the PAW process and between one and twenty Hz for the GTAW process.

7. No reduction in the energy consumption of the pulsed plasma arc welding was experienced when compared to that of the constant current mode of welding of the same average current value.

8. No marked advantage is observed when the high frequency GTA pulsing operation is utilized. The audible noise generated by the arc during high frequency excursions in current could be harmful to the operator and in any instance is objectionable to individuals working in the area immediately adjacent to the welding operation.

9. Superimposed high frequency on low frequency pulse mode of welding showed no improvement in the resulting metallurgical structure and geometrical configuration of the weld bead.

10. For both the pulsed PAW and GTAW processes, no major difference in the grain size or the size of solidification substructure of welds of both pulsed and constant current modes was observed.

11. Compared to the plasma welds of the same welding conditions, the plasma welds had greater penetration than that of the GTA welds.

12. For the pulsed PAW process, the narrowest HAZ was found to be at a pulse frequency of one Hz for high peak currents and short pulse duration.

13. In general, for both the pulsed PAW and pulsed GTAW processes, the lower the pulse frequency, the narrower the HAZ and the wider the fused zone. At higher pulse frequencies, however, the HAZ becomes wider but the fusion zone becomes narrower, an indication of decreased melting efficiency.

14. It is postulated that weld grain refinement can be achieved if the partially melted grains could be controlled in extent and magnitude along the fusion line and if a technique to cause the rotation and randomization of the grains in the partially melted region can be devised.

During the course of this investigation, some observations of potential importance were made. The surface condition of the weld specimen and the surface cleaning technique or method used (i.e., the orientation continuity of the grinding, milling or scraping marks) was found to have marked influence on the weld bead geometry and the melting efficiency. A necking effect in the weld bead width and depth was observed when the welding arc travelled from a roughly cleaned section to a smoother section of the weld specimen surface. The average current was found to be the controlling welding parameter for both the pulsed PAW and pulsed GTAW processes with a hyporbalic relationship to the weld bead depth and area. Thus, it is the author's recommendations that the following investigations be carried out:

1. A study to determine the optimum surface cleaning technique that will enhance the weld geometrical configurations.

2. A study to establish a relationship between the average current, the welding speed and the material thermal and physical

properties. This could enhance the process control and save the operator the time and material that would otherwise be extended to determining the welding conditions.

LIST OF REFERENCES

LIST OF REFERENCES

1. Ashauer, R. C. and Goodman, S., "Automatic Plasma Arc Welding of Square Butt Pipe Joints," Welding Journal, Vol. 46, No. 5, May (1967), pp. 405-415.

2. Barabokhin, N. S., et al., "Pulsed Arc Welding of Alloy AMg6 in Large Thicknesses with a Consumable Electrode," Welding Production, No. 3 (1973), pp. 30-34.

3. Boughton, P. and Males, B. O., "Penetration Characteristics of Pulse TIG Welding," Welding Research International, Vol. 3, No. 1 (1973), pp. 47-71.

4. Boughton, P., "High Precision Pulsed TIG-Welding," Proceeding of the Conference on Advances in Welding Processes, April (1970), The Welding Institute (1971), pp. 95-98.

5. Cooper, G., Palermo, J. and Browning, J. A., "Recent Developments in Plasma Welding," Welding Journal, Vol. 44, No. 4, April (1965), pp. 268-276.

6. Danilov, V. A. and Chernyshov, G. G., "On the Mechanism of Action of a Pulse of Current on the Weld Pool," Welding Production, No. 1 (1974), pp. 90-93.

7. Dickens, R. G. and Pinfold, B. E., "Investigations in Pulsed Tungsten Inert-Gas Welding," Paper II, Proceedings of the Conference on Advances in Welding Processes, April (1970), The Welding Institute (1971), pp. 63-67.

8. Edmonds, D. P., "The Effect of Shield Gas Composition and Pulsed-Current on the Weld Pool of Plasma-Arc Welds," B.S. Thesis, Department of Chemical and Metallurgical Engineering, The University of Tennessee, June (1973).

9. Esibyan, E. M. and Shnaider, B. I., "The Thermal Balance for Welding with Pulsed Low Power Arcs," Automatic Welding, Vol. 20, No. 4 (1967), pp. 16-19.

10. Grist, F. J., "Improved, Lower Cost Aluminum Welding with Solid State Power Source," Welding Journal, Vol. 54, No. 5, May (1975), pp. 348-357.

11. Gruzder, B. L. and Nikiforov, G. D., "Some Aspects of the Crystal Structure of Weld Metlas Deposited by the Pulsed-Arc Process with Non-Consumable Electrodes," Welding Production, Vol. 18, No. 6, June (1971), pp. 77-80.

12. Hasui, A., Kasaharu, E., Taguchi, H. and Yamamto, S., "Development of Plasma Arc Spot Welding," Transactions of National Research Institute for Metals, Vol. 12, No. 1, (1970), Welding Research Abroad, October (1970), pp. 48-56.

13. Hasui, A., Kasahara, E. and Taguchi, H., "Studies on Plasma Arc Welding," Transactions of National Research Institute for Metals, Vol. 10, No. 6, (1968), Welding Research Abroad, December (1969), pp. 14-21.

14. Jackson, C. E. and Niles, R. W., "Weld Thermal Efficiency of the GTAW Process," Welding Journal, Vol. 54, No. 1, January (1975), Welding Research Supplement, pp. 25S-32S.

15. Kattamis, T. Z. and Juers, R. H., "Structure and Fatigue Strength of 5456 Aluminum Alloy GTA Welds," Welding Journal, Vol. 52, No. 6, June (1973), Welding Research Supplement, pp. 240S-246S.

16. Lawrence, B. D. and Jackson, C. E., "Variable Frequency Gas Shielded Pulsed Current Arc Welding," Welding Journal, Welding Research Supplement, March (1969), pp. 97S-104S.

17. Leitner, R. E., McElhinney, G. H., and Pruitt, E. L., "An Investigation of Pulsed GTA Welding Variables," Welding Journal, Welding Research Supplement, Vol. 52, No. 9, September (1973), pp. 405S-410S.

18. Lenivkin, V. A., et al., "Features of Weld Formation in Pulsed-Arc Welding with a Consumable Electrode," Welding Production, No. 2, (1973), pp. 29-31.

19. Lundin, C. D. and Ruprecht, W. J., "Pulsed-Current Plasma-Arc Welding," Welding Journal, Vol. 53, No. 1, January (1974), pp. 11-19.

20. Lundin, C. D., Chemical and Metallurgical Engineering Department, University of Tennessee, Knoxville, Personal Communication.

21. Malakhovskii, V. A., Stikhin, V. A. and Popkov, A. M., "Effect of Torch Geometry on the Penetration Capacity of a Constricted Arc in Bead Deposition, Welding Production, No. 8 (1973), pp. 16-17.

22. Matthews, L. B., "The Effect of Slow and Rapid Current Pulsation on the Metallurgical Structure and Geometrical Properties of GTA Welds," B. S. Thesis, Department of Chemical and Metallurgical Engineering, University of Tennessee, Knoxville, June (1972).

23. Metals Handbook, Vo. 6, Welding and Brazing, American Society for Metals (ASM), Metals Park, Ohio, (1971), pp. 113-140.

24. Metcalfe, J. C. and Quigley, M. B. C., "Heat Transfer in Plasma Arc Welding," Welding Journal, Welding Research Supplement, Vol. 54, No. 3, March (1975), pp. 99S-103S.

25. Mirlin, G. A. and Denisov, P. V., "Heating in Pulsed-Arc Welding of Sheet Steel," Welding Production, No. 4 (1968), pp. 7-12.

26. Normando, N. J., "Manual Pulsed GTA Welding," Welding Journal, Vol. 52, No. 9, September (1973), pp. 566-573.

27. Norrish, J., "Plasma Welding Developments," Paper 12, Proceedings of the Conference on Advances in Welding Processes, The Welding Institute, April (1970), pp. 5-9.

28. O'Brien, R. L., "Arc Plasma for Joining, Cutting, and Surfacing," Bulletin, No. 131, Welding Research Council (WRC), July (1968), pp. 1-2.

29. Petrov, A. V. and Slavin, G. A., "An Investigation into the Technological Possibilities of the Pulsed Arc," Welding Production, Vol. 13, No. 2, February (1966), pp. 1-6.

30. Prokhorov, N. M. and Mastryukova, A. A., "Primary Structures and Their Importance When Estimating the Strength of Weld Metal," Automatic Welding, No. 8, August (1965), pp. 15-21.

31. Savage, W. F., Strunk, S. S. and Ishikawa, Y., "The Effect of Electrode Geometry on GTA Welding," Welding Journal, Welding Research Supplement, Vol. 44, No. 11, November (1965), pp. 489S-496S.

32. Shnayder, B. I., "TIG Butt Welding of Copper Sheet," Welding Production, Vol. 20, No. 5, (1967), pp. 77-78.

33. Shaw, C. B., Jr., "Diagnostic Studies of the GTAW Arc," Part 2, The Welding Journal, Welding Research Supplement, Vol. 54, No. 3, March (1975), pp. 81S-86S.

34. Slavin, G. A., Petrov, A. V., Smirnova, S. V., and Korotkova, G. M., "The Automatic Pulsed-Arc Welding of Aluminum Sheet with a Non-Consumable Electrode," Welding Production, No. 2 (1965), pp. 18-20.

35. Slavin, G. A. and Morozova, T. V., "Some Special Features of Solidification of Liquid Pool Metal in Pulsed Arc Welding Using a Tungsten Electrode," Welding Production, No. 6 (1973), pp. 10-14.

36. Smart, M. D. and Pinfold, B. E., "Comparison of Modulated and Unmodulated Current Plasma-Arc Welding," Welding and Metal Fabrication, Vol. 39, September (1971), pp. 332-340.

37. Spiller, K. R. and MacGregor, G. J., "Effect of Electrode Vertex Angle on Fused Weld Geometry in TIG-Welding," Paper 9, Proceedings of the Conference of Advances in Welding Processes, April (1970), The Welding Institute (1971), pp. 83-88.

38. Stockinger, G. R., "Pulsed DC High Frequency GTA Welding of Aluminum Plate," Welding Journal, Welding Research Supplement, Vol. 52, No. 12, December (1973), pp. 558S-567S.

39. Tomsic, M. J. and Jackson, C. E., "Energy Deistribution in Keyhole Mode Plasma Arc Welds," Welding Journal, Welding Research Supplement, Vol. 53, No. 3 (1974), pp. 109S-115S.

40. Tret'yakov, F. E., Backs, I. A. and Prokhorova, K. A., "Pulsed Argon Arc Welding of Thin Titanium Alloys," Welding Production, Vol. 14, No. 3 (1967), pp. 51-55.

41. Tuthill, R. W., "Plasma Welding," Airco Welding Products, Union, New Jersey, July (1970), pp. 1-8.

42. Vagi, J. J., Mishler, H. W., and Randall, M. D., "Pulsed-Current Arc Welding Processes," D.M.I.C. Memorandum No. 250, Battle Memorial Institute, September (1970), pp. 1-21.

43. Vagner, F. A., "Method of Producing a Pulsating Alternating Current Arc for Welding with a Tungsten Electrode," Welding Production, Vol. 20, No. 1, January (1973), pp. 34-35.

44. Vilkas, E. P., "Pulsed Current and Its Applications," Welding Journal, Vol. 49, No. 4, April (1970), pp. 225-262.

45. Vilkas, E. P., "New Weld Current Pulsation Methods," Welding Journal, Vol. 47, No. 7, July (1968).

46. Vilkas, E. P., "Square-Wave Welding," IEEE Transactions on Industry and General Applications, Vol. IGA-3, No. 6, November/December (1967), pp. 525-530.

47. Stout, R. D. and Doty, W. D. (Editors), Weldability of Steels, Welding Research Council (WRC), 2nd Edition (1971), pp. 23-24.

VITA

Ahmed A. Omar was born in Tulkarm, Palestine, on November 10, 1944. He graduated from Al Fadiliya High School in 1963. In July 1965, he came to the United States to pursue his college education where he entered Indiana Institute of Technology and received a Bachelor of Science degree in Mechanical Engineering in June 1969. After graduation he was employed by Sylvania Electric Products Corporation and in June of 1971 he joined General Electric Company in Milwaukee, Wisconsin as a design and development engineer. In September 1973, he accepted a teaching assistantship at the University of Tennessee, Knoxville and began a study toward a Master's degree in Metallurgical Engineering.